APPENDIX E
BIOGENIC SILICA ASSESSMENT OF SEDIMENT SAMPLES FROM THE SOIL PROFILE AND SELECT CULTURAL FEATURES AT 41TV2161

Prepared for:

TRC Environmental Corporation
505 East Huntland Drive, Suite 250
Austin, Texas 78752

Prepared by:
J. Byron Sudbury, Ph.D.
J. S. Enterprises, Inc.
P. O. Box 2282
Ponca City, Oklahoma, 74602 USA

This page intentionally left blank

BIOGENIC SILICA ASSESSMENT OF SEDIMENT SAMPLES FROM THE SOIL PROFILE AND SELECT CULTURAL FEATURES AT 41TV2161

J. Byron Sudbury[1] Ph.D.

E.1 SUMMARY

The Big Hole Site (41TV2161) is located on a floodplain in Travis County, Texas, on a relict paleochannel near Onion Creek above its juncture with the Colorado River. As reported in the Interim Report (Quigg et al. 2007) preliminary laboratory evaluation showed that phytolith preservation at the site was variable with significant weathering, but that data potential was present and additional study was recommended (Bozarth 2007). Thirty-six soil samples collected from 41TV2161 were received for phytolith analysis (Table E-1). Although some phytoliths are present in these current samples, this new study suggests that selective dissolution of portions of the phytolith assemblage occurred due to chemical conditions in the soil environment; mechanisms potentially contributing to this loss are detailed. Some larger phytoliths remained (specifically the bulliform cells—which showed variable degrees of weathering as reported in 2007—and some cucurbit phytoliths, as well as larger Pooid phytoliths [aka, the "crenate" form]). However, the samples' short cell phytolith content appears to be skewed and only partially preserved. Beyond the short cell Poaceae climatic indicators, phytoliths with evidence of being burned were present, phytoliths indicative of trees and cucurbits were present, and charcoal was abundant.

When phytoliths are extracted from the soil, other biogenic silica residues are also recovered as they have the same particle density. Of these other forms, diatoms were essentially absent from these soil samples as were Chrysophycean Cysts (except in both surface control samples). However, sponge spicules were recovered from numerous samples suggesting that they are more resilient in this particular soil environment.

Beyond the phytolith data, the sample soil texture data for the Block C profile samples is suggestive of periods of higher water flow (increased sand deposition) and aeolian activity (increased silt deposition). The sand fraction contained a very rich snail community which has been recovered and documented; the species have not been identified. Several snail fragments show evidence of being burned. Trace bone fragments were also noted in many sand samples, and ranged from being unburned to calcined. Charcoal is also abundant in many of the samples; ultimately, charcoal may have contributed to selective dissolution of portions of the biogenic silica signature. This study resulted in a wealth of data—just not the anticipated data.

E.2 PHYTOLITHS AND BIOGENIC SILICA

Phytoliths form when silica (as monosilicic acid dissolved in soil pore water) is taken up by plant roots, and then trapped in the plants when the water is lost through transpiration. As water is lost, the silica in the plant cells forms a gel and gradually forms an amorphous solid silica deposit (Iler 1979:741)—thus, the name "plant stones" or phytoliths. Upon plants' senescence their organic components degrade; however, the solid inorganic silica particles—the phytoliths—become part of the soil silt fraction (nominally 2-50 microns) and thus record the local vegetative signature present at that point in time.

[1] JSEConsulting.com; JSE c/o J. Byron Sudbury, P. O. Box 2282, Ponca City, OK 74602-2282 USA (jschemistry@hotmail.com).

Table E-1. Big Hole Site (41TV2161) Sediment Samples.

Sample ID	Subarea	AU	Unit N	Unit E	Level	Depth (cmbs)	Feature No.	PNUM	Comments
MQ13'-1	Block C	CN	66	95	29	281-283	18	2026	-
MQ13'-2	Block	-	Profile		-	360	-	2411	#11
MQ13'-3	Block	-	Profile		-	350	-	2410	#10
MQ13'-4	Block	-	Profile		-	340	-	2409	#9
MQ13'-5	Block	-	Profile		-	330	-	2408	#8
MQ13'-6	Block	-	Profile		-	320	-	2407	#7
MQ13'-7	Block	-	Profile		-	310	-	2406	#6
MQ13'-8	Block	-	Profile		-	300	-	2405	#5
MQ13'-9	Block	-	Profile		-	290	-	2404	#4
MQ13'-10	Block	-	Profile		-	280	-	2403	#3
MQ13'-11	Block	-	Profile		-	260	-	2401	#1
MQ13'-12	Block	-	Profile		-	248	-	2400	#0
MQ13'-13	Block B	CN	72	83	28	270-273	-	2143	grey lens
MQ13'-14	Block D	CN	81	91	28	275-278	-	2261	from cultural zone SE
MQ13'-15	Block D	CN	80	95	26	270-272	-	2257	lithic concentration
MQ13'-16	Block B	CN	71	83	27	260-270	26	2110	from below grey zone
MQ13'-17	Block B	CN	71	83	28	268-277	26	2112	-
MQ13'-18	Block B	BA	74	86	22	212-220	27	2197	-
MQ13'-19	Block B	BA	74 75	86	23	218-231	28	2200	-
MQ13'-20	Block B	BA	76	86	24	230-235	29	2424	-
MQ13'-21	Block B	BA	70	80	24	230-240	32	2078	-
MQ13'-22	Block B	BA	71	80	24	235-240	30	2092	-
MQ13'-23	Block B	BA	77	82	24	236	-	2224	from near Big Sandy Point
MQ13'-24	Block D	CN	79	93	27	256-258	-	2246	-
MQ13'-25	Block A	CN	95	96	28	270-280	19	2367	-
MQ13'-26	Block B	BA	72	84	23	216-230	22	2146	-
MQ13'-27	Block B	BA	72	85	23	218-230	22	2149	-
MQ13'-28	Block B	BA	73	85	23	218-230	24	2176	-
MQ13'-29	Block C	-	N69	E95	26	251-253	21	2060	-
MQ13'-30	Block B	BA	73	86	23	223-230	24	2179	-
MQ13'-31	Block D	CN	78	93	27	266	25	2239	-
MQ13'-32	Block D	CN	82	91	28	270-280	33	2280	-
MQ13'-33	Block C	BA	67	95	29	281-283	18	2044	
MQ13'-34	Block D	BA	82	28	28	270-280	33	2275	
MQ13'-35	-	-	-	-	-	Surface	-	2450	Hilltop
MQ13'-36	-	-	-	-	-	Surface	-	2451	Flood Plain

Figure E-1. Representative short cell Poaceae phytoliths from floodplain surface A horizon soil control sample (4TV2161, PNUM 2451). A-L, N (lower), and Q (left) are various forms of Panicoideae short cell phytoliths. L, M (lower), P, Q (right), and rare Chloridoideae short cell phytoliths. N (upper) and S-AC are Pooideae short cell phytoliths ("crenate" morphology; the smaller Pooid forms were essentially absent in these samples). The Panicoid phytoliths in G and H have been burned—the discoloration is due to carbon embedded in the silica matrix. The white bar scales are 10 microns.

Variations in cell metabolism among the Poaceae are visible in the phytolith record because their cell morphology varies among subfamilies. The three most useful climatic indicator grass subfamilies are the Pooideae, Panicoideae, and Chloridoideae (Figure E-1). The differences in cell morphology between subfamilies are reflective of their climatic preference for temperature and moisture—the environmental niche for their optimal growth. Thus the pooids thrive in a cool moist environment, whereas optimal chloridoid growth occurs in a hot dry environment; the panicoids are intermediate between these two extremes. For example, the chloridoids are well represented in dry arid shortgrass prairies whereas the panicoids are the dominant species of tallgrass prairies which—although hot—have more moisture than the shortgrass prairie. Pooids are the first plants to grow in the late winter/early spring, and the last to go dormant in the fall. Riparian settings provide a different mix of species than a prairie environment due to increased water availability. Other specific phytolith forms found during this study include cucurbits (wild gourds), sedges (a moist environment indicator), and generic tree indicators.

Neumann divides plants into two broad categories based on propensity for silica uptake—the

> "-Si accumulators - members of the Cyperaceae and wetland Gramineae (10-15% Si on

a dry wt. basis), dryland grasses, most of the other cereals and some members of the dicots (1-3% Si on a dry wt. basis).

-Si nonaccumulators - many of the dicots (<0.5% Si on a dry wt. basis)." (2003:149).

Neumann's classification verbiage is clearly adopted from the relatively new field of phytoremediation in which plants are used to sequester and remove heavy metals during soil cleanup at hazardous waste sites (c.f. Anderson et al. 2005). More recently, plants have been proffered as a mechanism for mining precious metals (Wilson-Corral et al. 2011). Many of the plants in the central swath of the United States including the Great Plains fall in the "Si accumulator" class including the botanical phytolith sources addressed in this current study.

In addition to phytoliths, there are other forms of biogenic silica including diatoms, sponge spicules, and Chrysophycean Cysts ("statospores"). Since these particles all have the same chemical composition and specific gravity range, when present in a soil sample that is fractionated by particle density they are recovered together. Thus, rather than obtaining a phytolith isolate—one actually ends up recovering a "biogenic silica isolate" which contains phytoliths along with other biogenic particle types. At 41TV2161 well-preserved fresh water sponge spicules were recovered with the phytoliths in a number of samples and are illustrated and discussed in this report. The small number of statospores (all specimens were illustrated) were recovered from the two surface samples—and are presumably absent from the other samples because they dissolved along with many of the smaller short cell phytoliths. Diatoms, incredibly sensitive environmental indicators, are addressed elsewhere in this volume (Winsborough 2015).

E.3 LABORATORY PROCESSING

Good detailed procedures for laboratory processing and subsequent phytolith analysis are available, as presented by Piperno (1988, 2006), Pearsall (2000), and others. A number of methodological improvements from a chemist's point of view have been made since those publications (c.f., Sudbury 2011a, 2011b, 2013) and are ongoing.

The as received soil samples were transferred to pre-weighed 250 ml graduated glass jars with Teflon®-lined lids, oven-dried, cooled in a desiccator, and reweighed to obtain the dry soil sample weights.

The soil samples were then shaken vigorously in Calgon® solution for 24 hours on an Eberbach® Shaker. Due to shaker space limitations, the samples were processed as three sets of twelve samples in numerical order. Once disaggregated, the soil samples were fractionated into the three soil textural components based on settling times calculated by Stoke's Law. For the initial step, to separate the sand from the clay and silt mixture, the particles were resuspended by shaking, and then allowed to sit long enough for the sand fraction (particles > 50 microns, with settling time based on a particle density of 2.65 g/cm^3) to settle out. After this brief settling interval (~40 seconds depending on temperature), the upper ~80% of the liquid phase containing the suspended silt and clay was decanted into a 2-liter container. DI water was added to the sand and remaining liquid component to a total depth of 10 cm, and the above steps repeated with the decants from a given sample being pooled for further processing. The above steps were repeated until the liquid phase being decanted from above the sand was clear. This procedure results in the collection of 2-4 liters of silt/clay mixture for each sample while leaving behind a clean sand fraction. The sand fractions are oven-dried, weighed, particles of interest photographed during examination via stereomicroscopy, and then transferred to storage containers.

The combined silt and clay fraction for each sample was initially allowed to settle for three days (30 cm settling distance); this prolonged first settling interval significantly speeds up subsequent decants and helps to minimize loss of silt to the clay fraction. The upper 80-85% of the clay-bearing liquid phase was aspirated off from above the silt sediment into another bottle and retained until all sample analyses were completed. The bottom component of the mixture—primarily silt (2-50 microns) with some residual liquid and suspended clay (< 2 microns)—was then transferred to a 250 ml glass container (Figures E-2 and E-3). Again, Stokes Law was used to determine the silt settling time (~7.5-8 hours depending on temperature), and the upper 80% of the clay solution which remained suspended after that time was aspirated into a separate container and pooled for curation [all components of each sample were saved until the final analysis was completed]. The above steps were repeated until the liquid phase above the silt fraction was free of residual clay. The silt fractions were then oven-dried, weighed, and quantitatively transferred to porcelain crucibles for the next step--removal of organics.

Figure E-2. Silt clay fraction solutions prior to first aspiration from 250 ml sample bottles. Note incomplete settling visible in the middle two bottles in the top row. Also note the drastic difference in appearance of the two surface control samples (bottom row, last two bottles). The above samples are in the same order as listed in Table E-1.

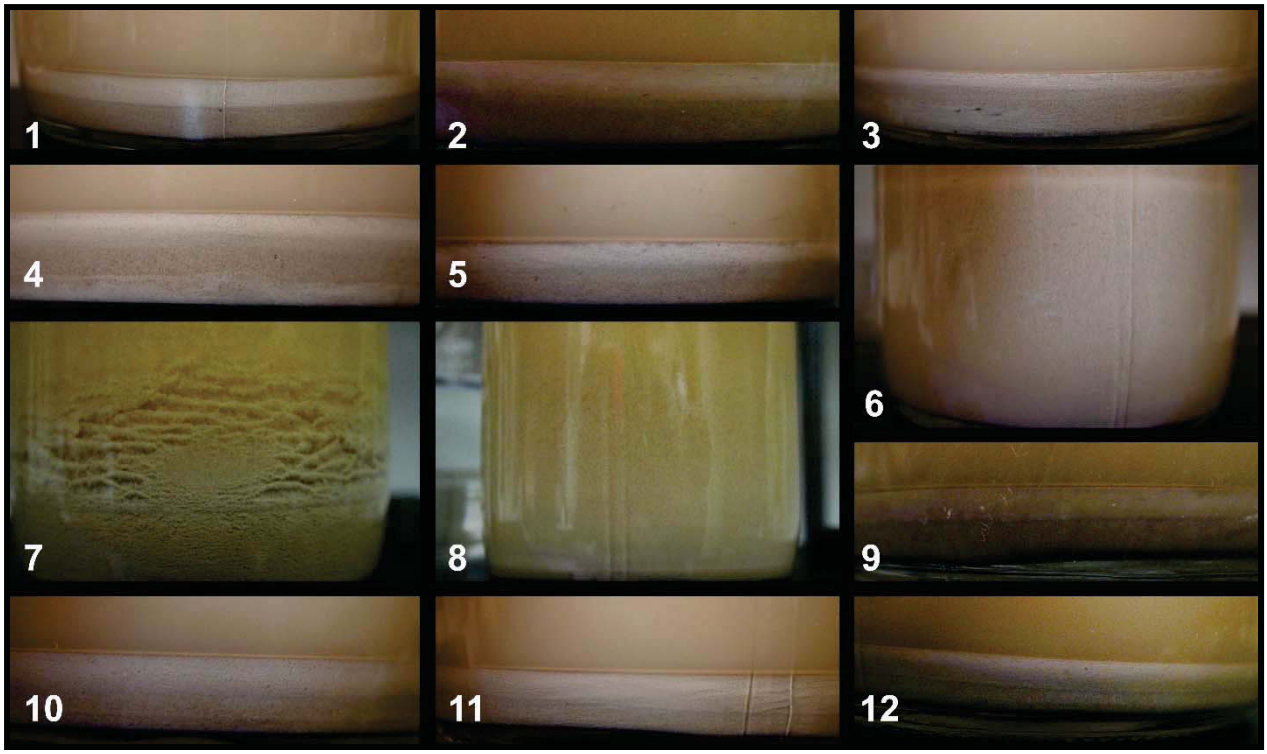

Figure E-3. Close-up view of the lower portion of the twelve silt samples in the top row of Figure E-2. Samples F-H did not settle well—and at this point required acid pretreatment and a much longer time to settle. The other 9 samples show the tan/brown silica-based silt layer at the bottom of each sample jar below a whitish sediment layer. This thick white layer is not normally observed in the silt fraction at other sites, and was subsequently found to consist of a combination of carbonates and low density soil minerals. A fine intermediate grey layer(s) is also visible in some of these sample sediments. The white layer was significantly thinner in the hill top surface control sample, and nearly absent in the flood plain surface control sample.

After transfer, the wet silt fractions were allowed to settle in the crucibles, and the excess water was removed via pipette. The silt samples were oven dried at 105ºC, and then ashed in a muffle furnace to burn off the organics. The muffle furnace temperature ramp was from room temperature to 530ºC, with 4-6 hour intermediate plateaus at 110ºC and 350ºC to allow temperature equilibration. The final temperature was held at 530ºC for a minimum of 8 hours. The furnace was then turned off and allowed to cool to room temperature.

For the next processing step—silica flotation—the ashed samples were transferred to 50 ml plastic centrifuge tubes. Rather than rinsing the crucibles with water to effect the quantitative transfer, 10% HCl was used which also neutralized any carbonates that were present. The effervescent response was incredibly strong for this sample suite—so strong that a normal few hours to rinse and transfer 12 samples turned out to last for weeks. Following slow acid addition and the decline of the vigorous effervescence, the neutralized HCl solution was removed following centrifugation, and fresh HCl added to the silt fraction; this procedure was repeated many times for each sample. The first two sets of twelve samples were processed in this manner—so much time was required the third set of samples was transferred with water and not neutralized. [The phytoliths from the final twelve samples were recovered without acid treatment--and then the isolated phytolith fractions were acid treated to remove any carbonate that carried over following flotation. This processing change turned out to be much more time effective for samples with a carbonate problem. The down side is that the expensive heavy liquid solution used for flotation was contaminated with high carbonate levels, and will either will have to be discarded or a method developed to recover the zinc bromide via recrystallization to remove the carbonate. In the end, there was no visible difference in state of preservation between the biogenic isolates prepared by these two different acid treatment protocols.]

When no effervescence following acid addition was observed upon gentle mixing, the silts in the centrifuge tubes were repeatedly washed with aliquots of deionized water by mixing and centrifuging to dilute the acid adjusting the sample fraction pH back to neutrality. Once neutralized, the silt fractions were oven dried and weighed. The heavy liquid for floatation—zinc bromide solution at a density of 2.35 g/cm^3—was then added to each tube and the mixture stirred thoroughly via a vortex mixer. The tubes were examined and remixed daily while checking for phytolith release from the silt matrix. Once phytoliths were observed floating on the surface, the samples were centrifuged and the upper liquid containing the phytoliths transferred to new tubes. More heavy liquid was added to the remaining silt pellets, and these flotation steps continued until no more phytoliths were released. The phytolith decants were evaluated for matrix carryover, and cleaned by additional centrifugation and transfers if necessary. Once the phytolith fractions were clean, water was added to the tubes containing the phytoliths to lower the liquid density so that the phytoliths would sink. The phytolith tubes were centrifuged, the liquid decanted, and fresh deionized water added; these steps were repeated until the heavy liquid was diluted and removed and the phytoliths remained in water. The isolated phytolith fractions were then quantitatively transferred to preweighed 4 dram glass vials, oven dried, and weighed.

A representative 1-2 mg sample of each biogenic isolate was placed on a cleaned labeled microscope slide, one or two drops of warm Canada Balsam added, the mixture gently stirred to distribute the particles, and a cover slip placed on top of the sample. The prepared slides were placed in an incubator at 35ºC until the Canada balsam around the edges of the cover slips set up—which required several weeks. At this point, some 5-6 months after starting the isolation procedure, the slides were

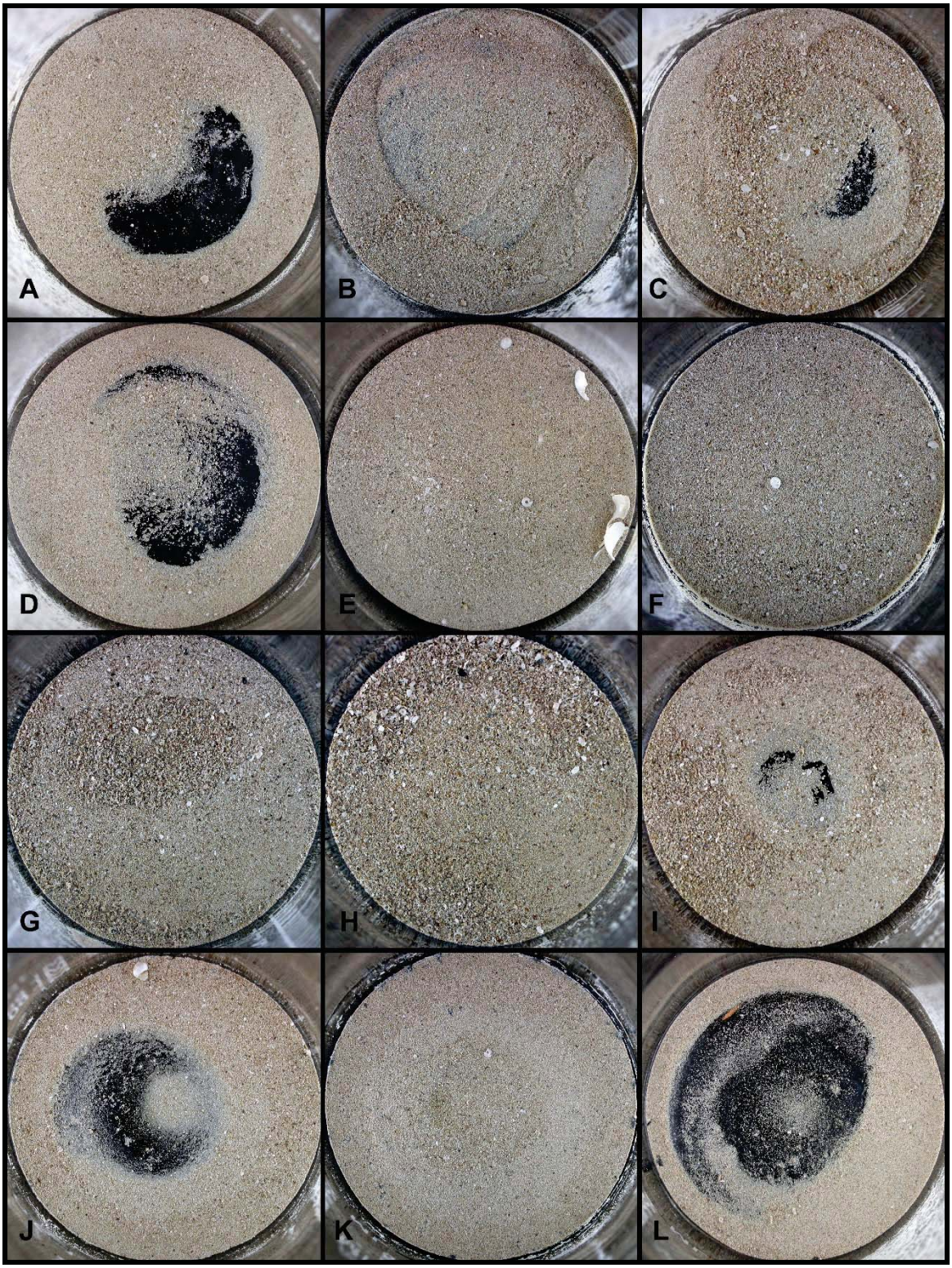

Figure E-4. Sand fractions from Block C soil profile, Big Hole site (41TV2161). A: PNUM 2026; B: PNUM 2411; C: PNUM 2410; D: PNUM 2409; E: PNUM 2408; F: PNUM 2407; G: PNUM 2406; H: PNUM 2405; I: PNUM 2404; J: PNUM 2403; K: PNUM 2401; and L: PNUM 2400. Complete snails are readily visible in E, F, H, J and L.

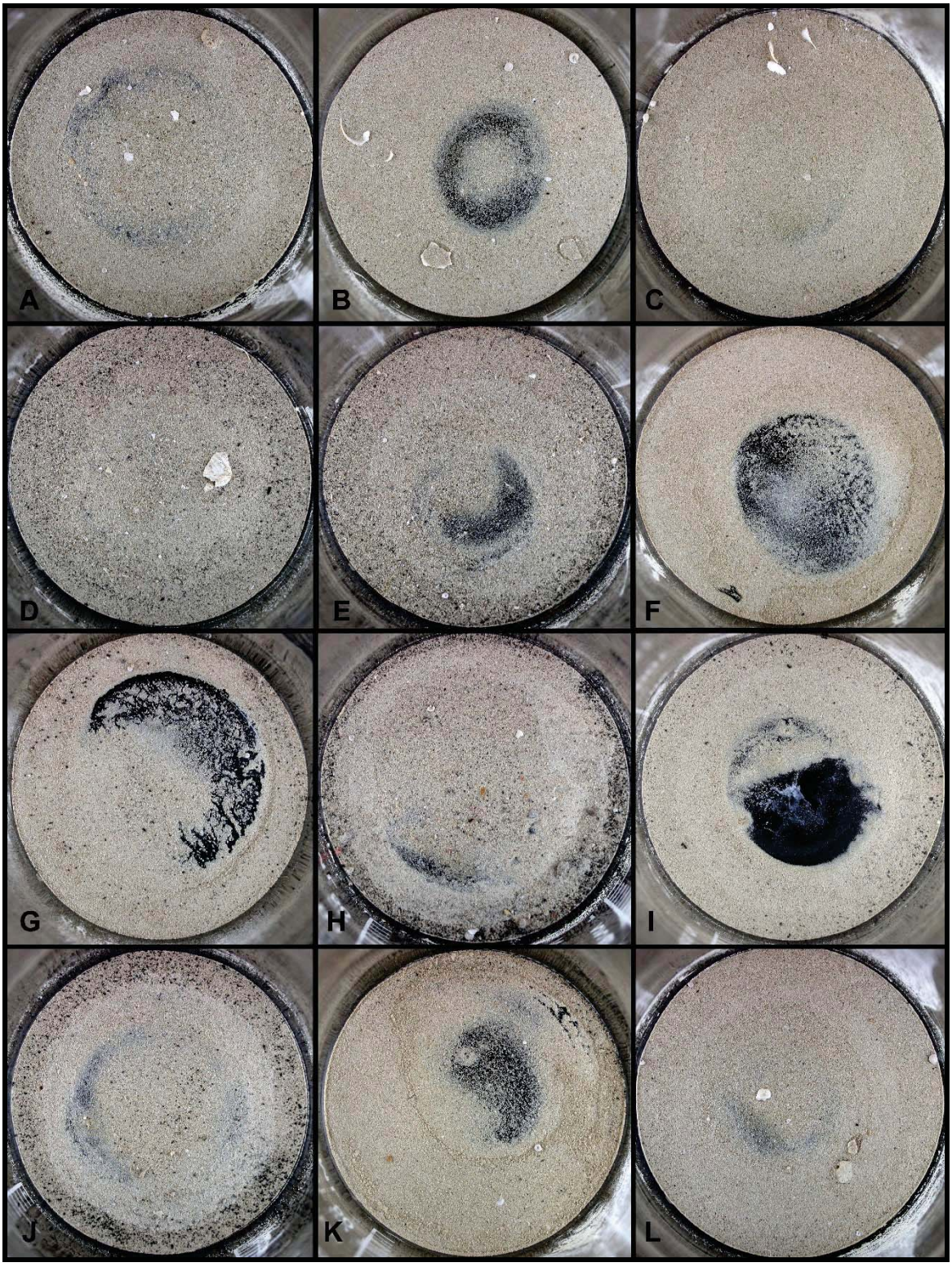

Figure E-5. Sand fractions from Block B and D samples, Big Hole site (41TV2161). A: PNUM 2143; B: PNUM 2261; C: PNUM 2257; D: PNUM 2110; E: PNUM 2112; F: PNUM 2197; G: PNUM 2200; H: PNUM 2424; I: PNUM 2078; J: PNUM 2092; K: PNUM 2224; and L: PNUM 2246. Complete snails are visible in A-C, E, G-H, J, and L.

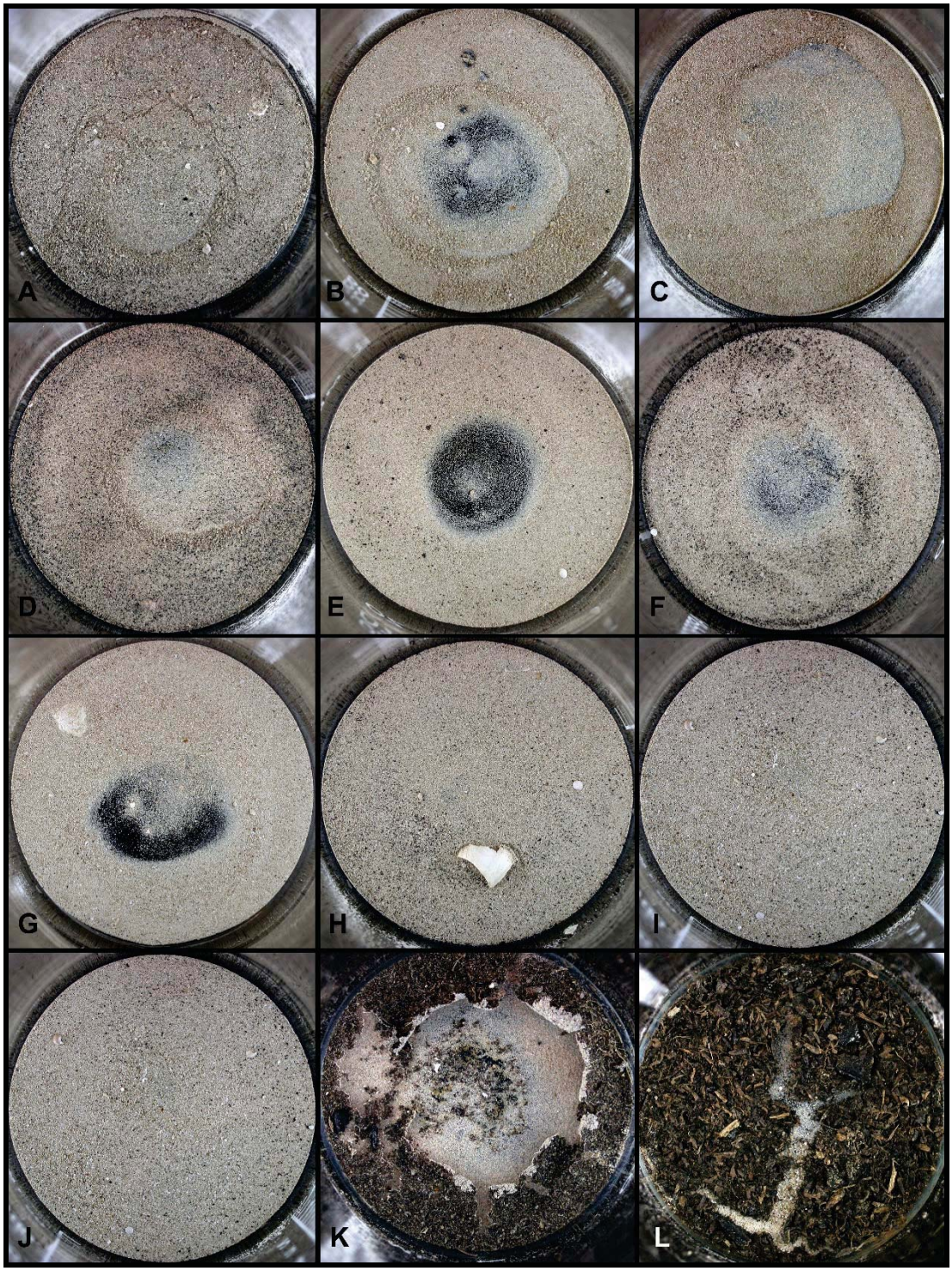

Figure E-6. Sand fractions from miscellaneous Blocks A-D samples, and surface control samples, Big Hole site (41TV2161). A: PNUM 2367; B: PNUM 2146; C: PNUM 2149; D: PNUM 2176; E: PNUM 2060; F: PNUM 2179; G: PNUM 2239; H: PNUM 2280; I: PNUM 2044; J: PNUM 2275; K: PNUM 2450; and L: PNUM 2451. Complete snails are visible in A, E, and H-J.

[Sample PNUM 2275 ["G"] overheated during initial sample drying when an oven heating element burned out baking part of the clay in the sample. The free sand, silt, and clay remaining on the side of the jar away from the heating element were processed.]

ready for examination and scanning. Many of the steps in this laboratory protocol have been illustrated in prior publications (Sudbury 2013; 2011a, 2011b). All isolated fractions (sand, silt, clay, and biogenic isolates) have been archived.

E.4 DATA - SAND FRACTIONS

The clean dry sand fractions were photographed in the 250 ml extraction jars prior to microscopic examination (see Figures E-4 through E-6). These as-dried fractions show an incredible amount of detail, including the relative amount of sands present (the jar bottoms are domed in the center), different matrix color tints, the presence of charcoal, and also visible non-quartz debris—such as snails and shell fragments. The sands were transferred to Petri dishes, and examined via stereo microscopy. Photographs were taken of the fields of view during scanning the material (magnification varied from 3.5-25x; most images were taken at 25x). Representative images of sample PNUM 2406 are shown in Figures E-7 and E-8. Although the entire sand fraction was examined, gently swirling the Petri dish tended to concentrate the larger particles in the center; the photographs in these two figures were taken in this concentrated area of larger particles.

The images in Figures E-7 and E-8 show the incredible amount of shell debris present in many of these samples—most of it likely from snails. Equally striking is the amount of carbonate conglomerates present in the sand (granular off white particles; some of the carbonate conglomerates in 8A and 8B are denoted by arrows). Carbonate and snail shell fragments are the major portion of the large sand fraction non-quartz particles. Whole snails are also visible (7B) as well as hollow ellipsoid particles with a spiral pattern (7C-F, 8B). These later particles have been identified as calcareous oogonia of Charophytes (Chad Yost, personal communication, 5-30-14) and were previously noted in sands at 41LM51 (Sudbury 2014b: Figure 15). Charophytes "are obligate water plants, growing submerged in calcareous fresh water.... The water must be still, or only slow-flowing." (Wikipedia)

The common opaque off-white rods in the images (c.f. 7F, lower right corner; 8C center) are sponge spicules. These large spicule sections in the sand fraction dissolved when tested with hydrochloric acid [whereas the siliceous spicules later observed in the silt fraction were insoluble in HCl]. The reaction with HCl indicates that the spicules in the sand are made of carbonate rather than silica, which means that they are marine sponge spicules (i.e., in this case, fossiliferous—likely originating from an area geological deposit). Rather than being plain like the sponge spicules, the central specimen in 8D has a pattern on the surface; this is another fossil—likely a section from a fossil echinoid spine. A number of fossil foraminifera were also noted (c.f. 8F). The Central Texas Cretaceous Foraminifera volume illustrates nine species present of the general form in Figure E-8F (Carsey 1926); several different species are present in the 41TV2161 samples, but the species were not identified. A number of foraminifera species were noted in the samples, but by far the most abundant were the form illustrated in 8F.

A total of 137 probable bone fragments were also found in 20 samples (Table E-2). The fragments are tabulated, along with their apparent degree of heat exposure (58% unburned). Several fragments are illustrated in Figure E-9. The polish on some specimens may be a result of the vigorous mixing for a day in the suspended detergent-laced soil matrix.

Micro flakes were noted in the sand fractions from samples PNUM 2261, PNUM 2257, PNUM 2110, PNUM 2112, PNUM 2197, PNUM 2367, and PNUM 2450. An amorphous fragment showing conchoidal fracture from PNUM 2367 could either be lithic material, or a piece of melted tree phytolith that had been spalled off.

Table E-2. Bone Fragments Observed in the Sand Fractions.

PNUM	Feature No.	Depth (cmbs)	Total No.	Original	Partly Burned	Burned	Calcined
2403	-	280	3	3			
2143	-	270-273	2			2	
2261	-	275-278	10	10			
2110	26	260-270	9	3		6	
2112	26	268-277	7		5	2	
2197	27	212-220	3	1	1	1	
2200	28	218-231	5	4		1	
2424	29	230-235	9	6	2	1	
2078	32	230-240	2	1	1		
2092	30	235-240	14	2	2		10
2224	-	236	19	19			
2246	-	256-258	5	5			
2367	19	270-280	7	2		3	2
2146	22	216-230	14	6		7	1
2176	24	218-230	1	1			
2060	21	251-253	10	3		6	1
2179	24	223-230	1		1		
2239	25	266	7	4		1	2
2280	33	270-280	8	8			
2450	-	Surface	1	1			
Total			137	79	12	30	16

The snails from the Block C profile samples were photographed during sand examination (the dry sand fractions shown in Figure E-4). Images of the rather large variety of snail species present in these twelve samples are recorded in Figures E-10 through E-20. Species identifications were not made. All of the samples processed contained snails except PNUM 2275 and 2451; the specimens in the other 22 samples were photographed, but illustrations were not prepared.

Distinctive but unidentified charcoal fragments were observed in sample PNUM 2060 (Figure E-21). Inquiries to several archeologists who routinely study excavated botanical remains did not provide identification of these fragments. Hackberry seed fragments, some burned, were observed in PNUM 2367.

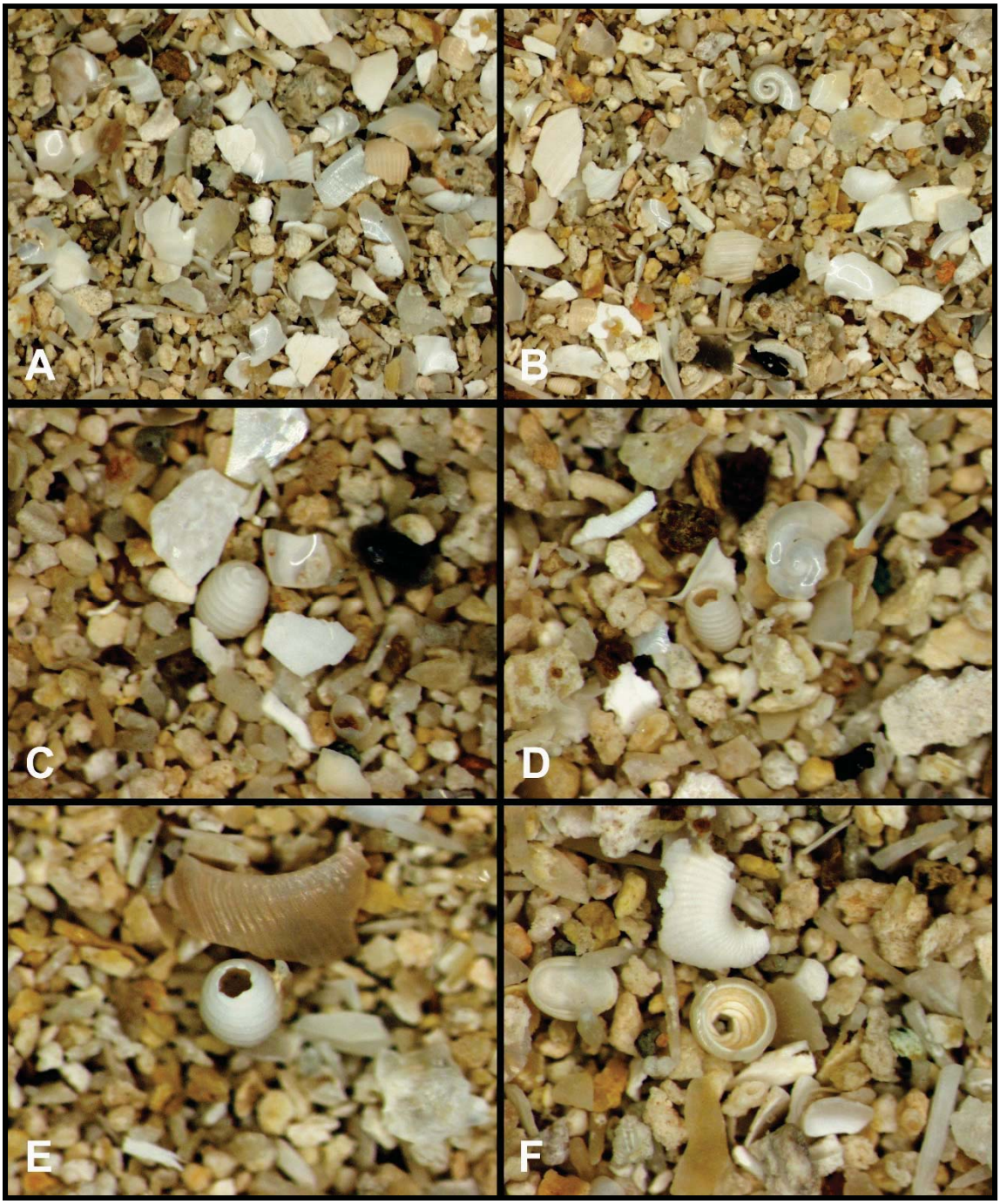

Figure E-7. Representative sand fraction images 1 (PNUM 2406, 41TV2161). Larger particles present in sand fraction. A: Predominantly shell fragments and carbonates. B: Charcoal and snail in addition to other debris. C-F: Four specimens of egg-shaped ornamented particles which are calcareous oogonia of Charophytes (specimen in F is broken in half showing interior detail). The coiled white wire-like piece in Figure E-17H is a fragment of oogonia; the fragments were much more abundant than whole particles—possibly broken during laboratory shaking and particle size separations. Carbonate, fossil marine spicules, charcoal, snails, shell fragments, and miscellaneous items are present.

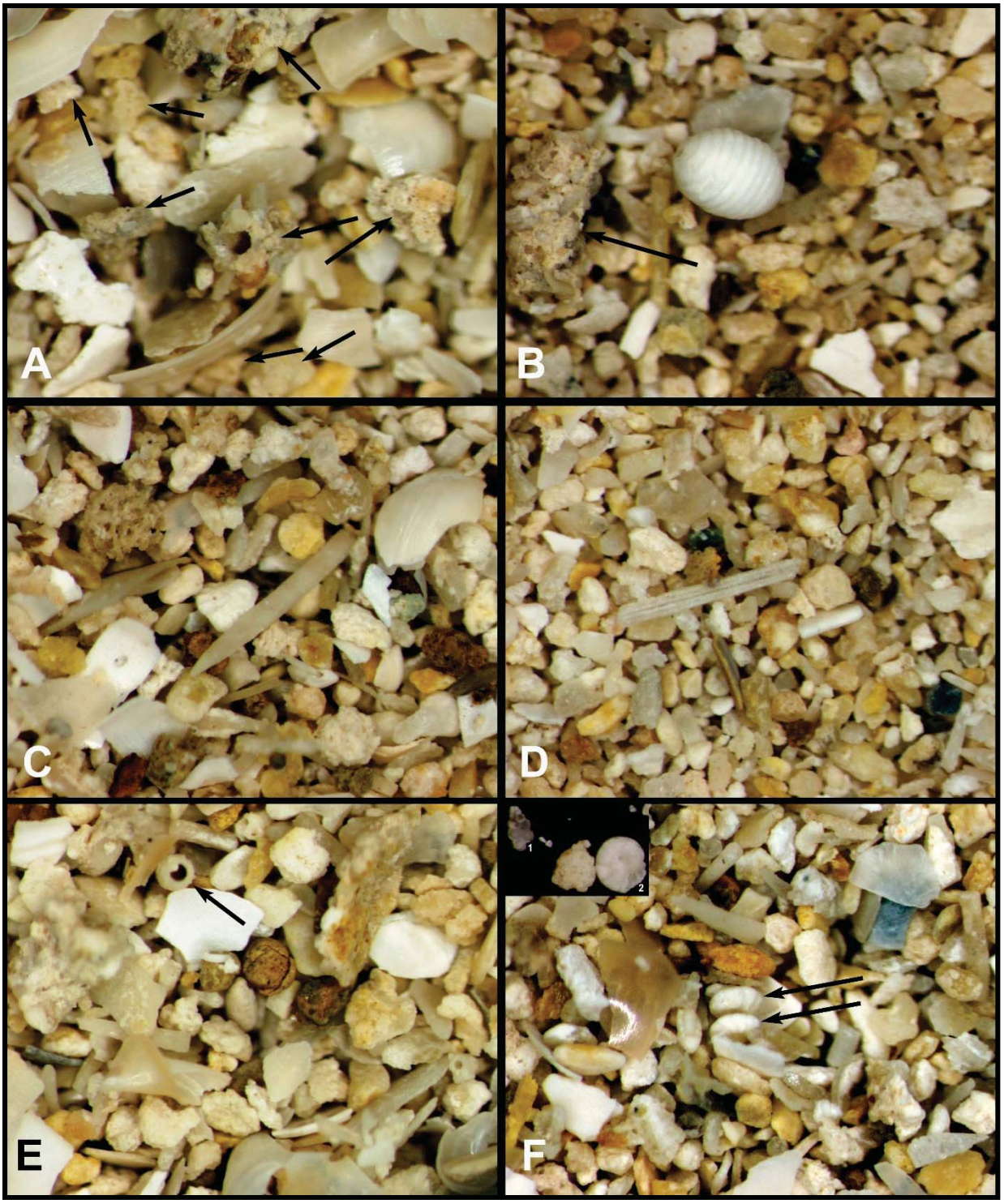

Figure E-8. Representative sand fraction images 2 (PNUM 2406, 41TV2161). A: Arrows highlight some of the many carbonate fragments some of which contain embedded quartz sand. B: Carbonate concretion highlighted. C: Carbonate sponge spicule in center (marine fossil). D: Possible echinoid spine in center (marine fossil). E: Arrow denotes a sheaf of carbonate that had encrusted a root. F: Arrows denote two foraminifera standing on edge (#2 on the insert shows one of these forams in planar view).

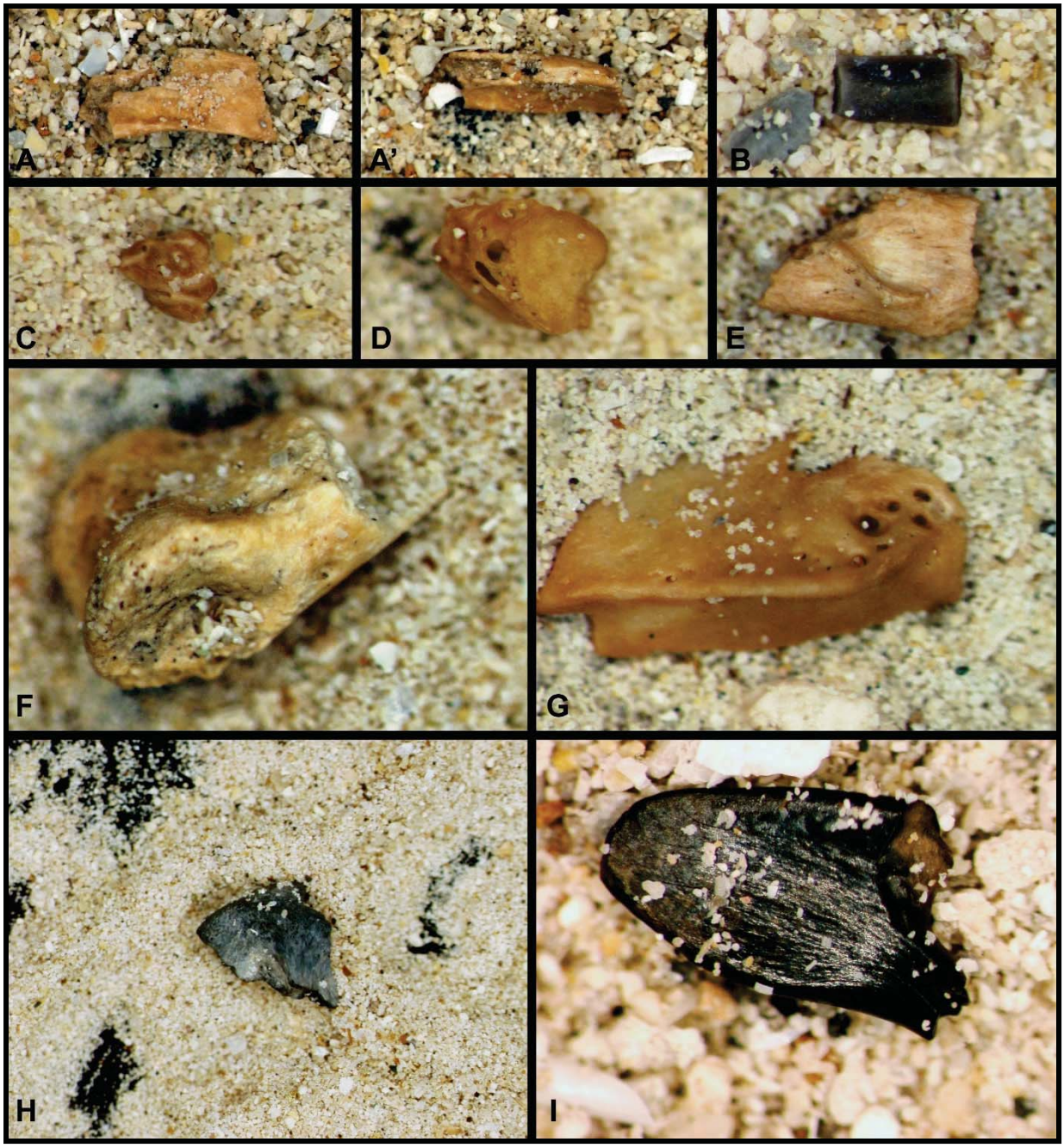

Figure E-9. Significant bone fragments observed in the sand fractions. A: PNUM 2403; B, E: PNUM 2224; C, D: PNUM 2261; F, G: PNUM 31; H: PNUM 2146; and I: PNUM 2112. Scales at 3.5x, 10x, and 25x. The specimens in F and H appear to be ends of long bones; the specimen in I may be the tip of a tool.

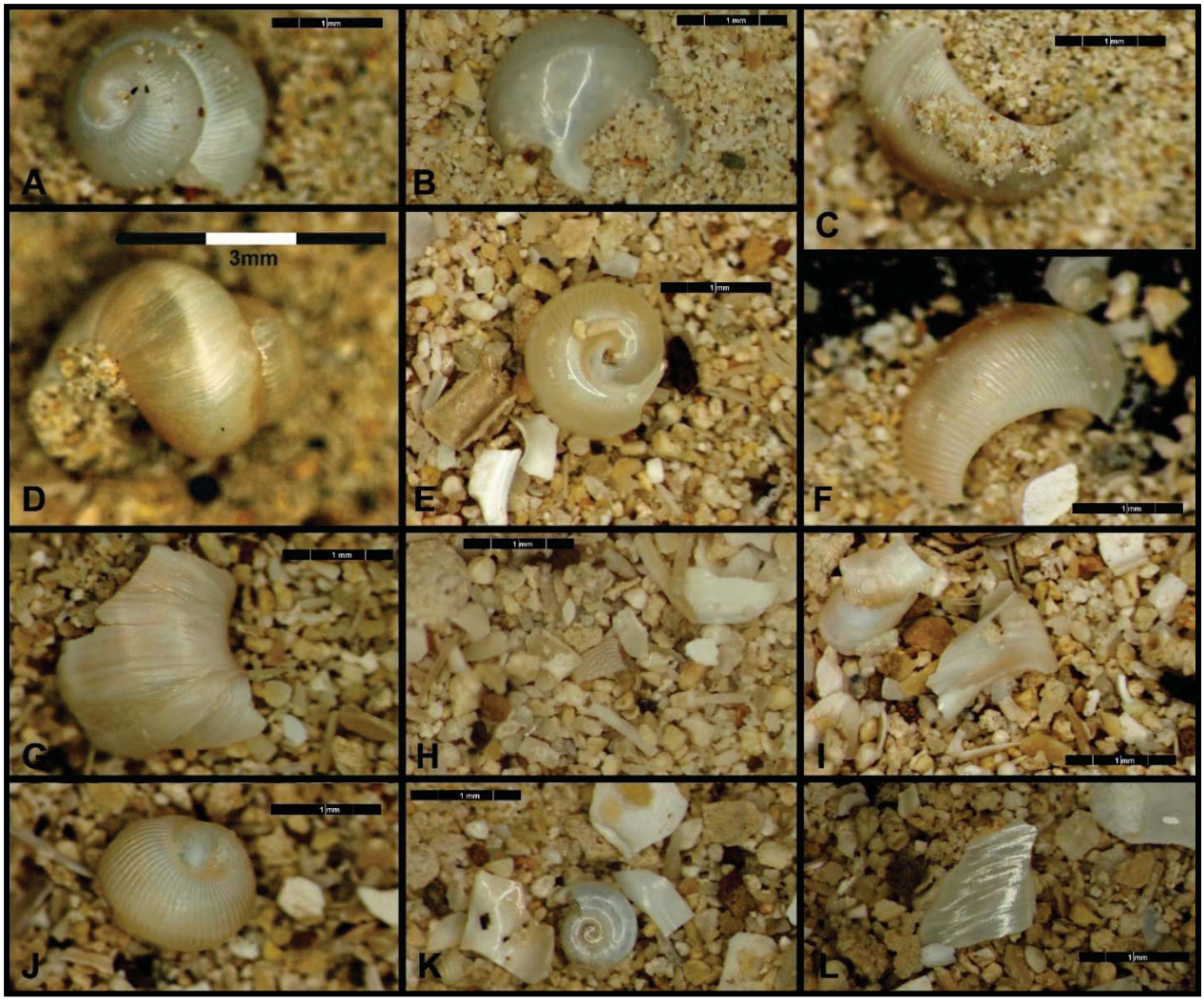

Figure E-10. Snails and fragments from Big Hole site (41TV2161) Block C Profile. PNUM 2026 specimens A-L.

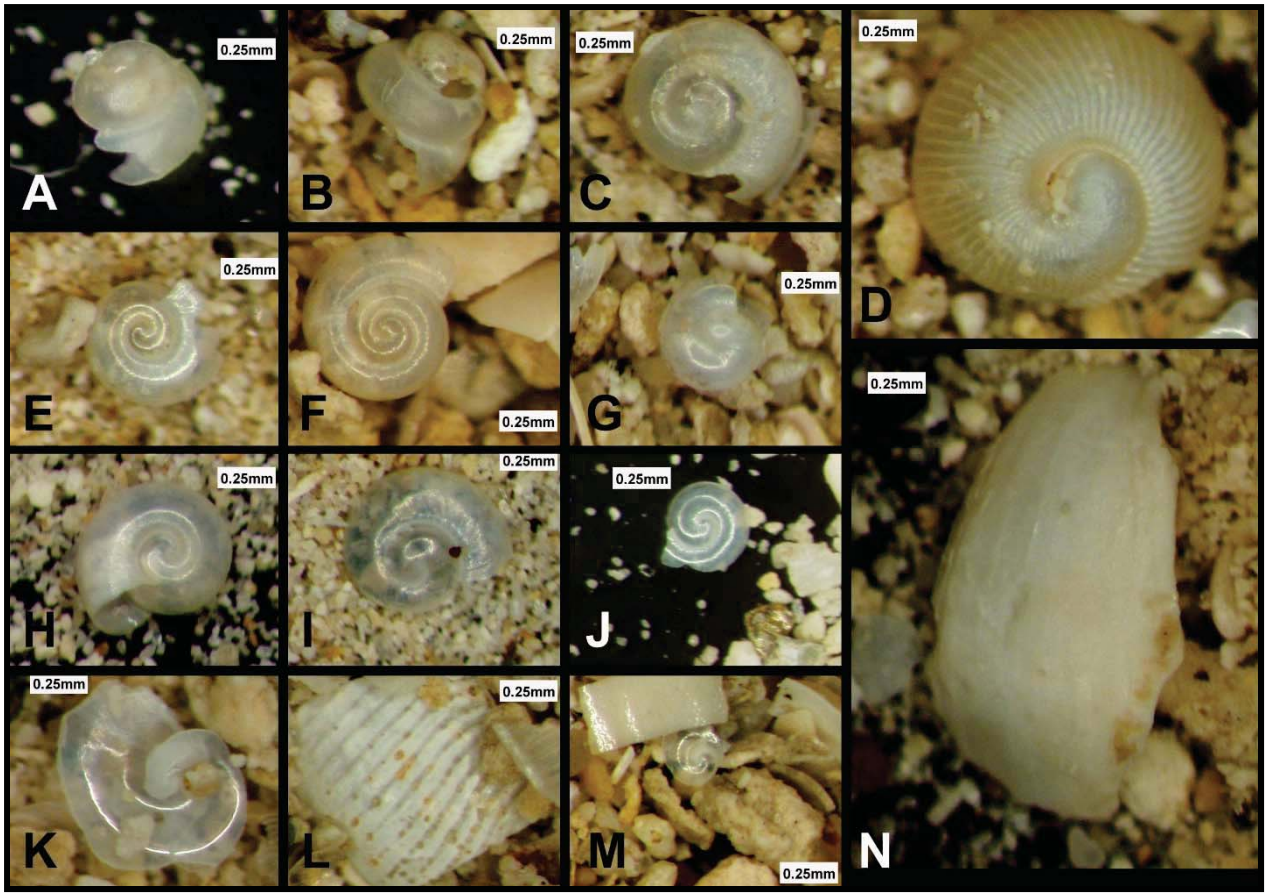

Figure E-11. Snails and fragments from Big Hole site (41TV2161) Block C Profile. PNUM 2026 specimens A-N.

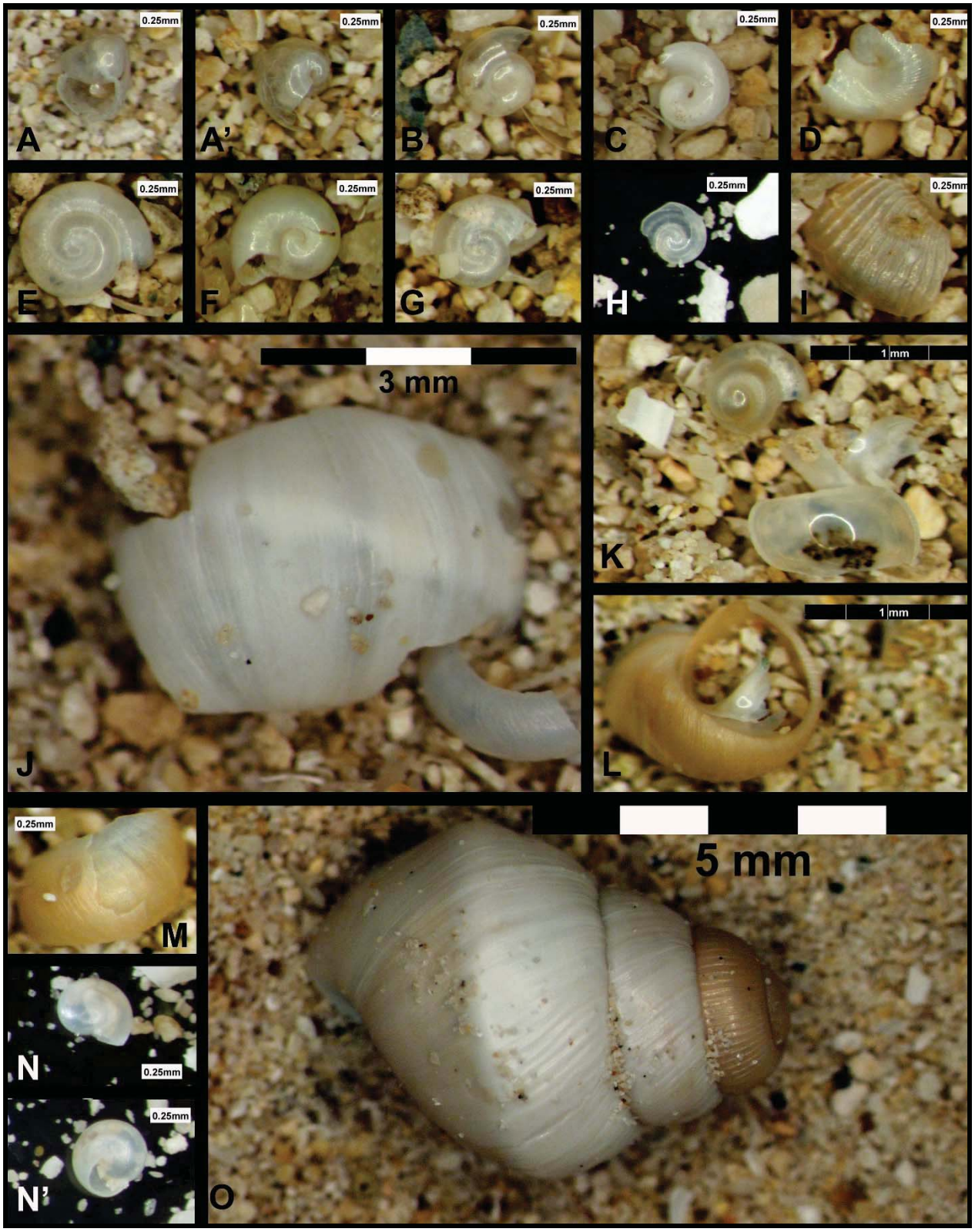

Figure E-12. Snails and fragments from Big Hole site (41TV2161) Block C Profile. PNUM 2411 specimens A-M, and PNUM 2410 specimens N-O.

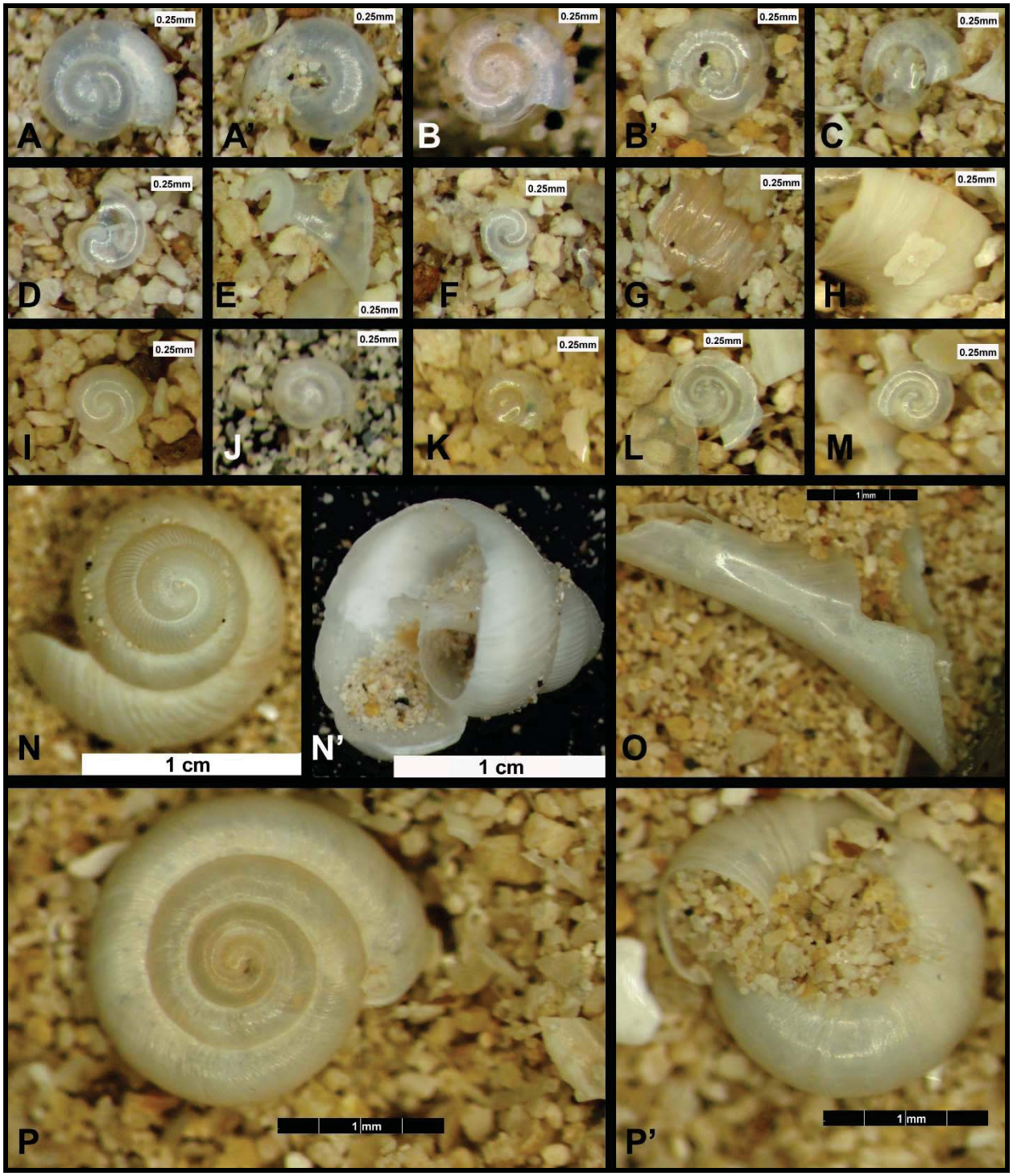

Figure E-13. Snails and fragments from Big Hole site (41TV2161) Block C Profile. PNUM 2409 specimens (A-G), and PNUM 2408 specimens (H-P).

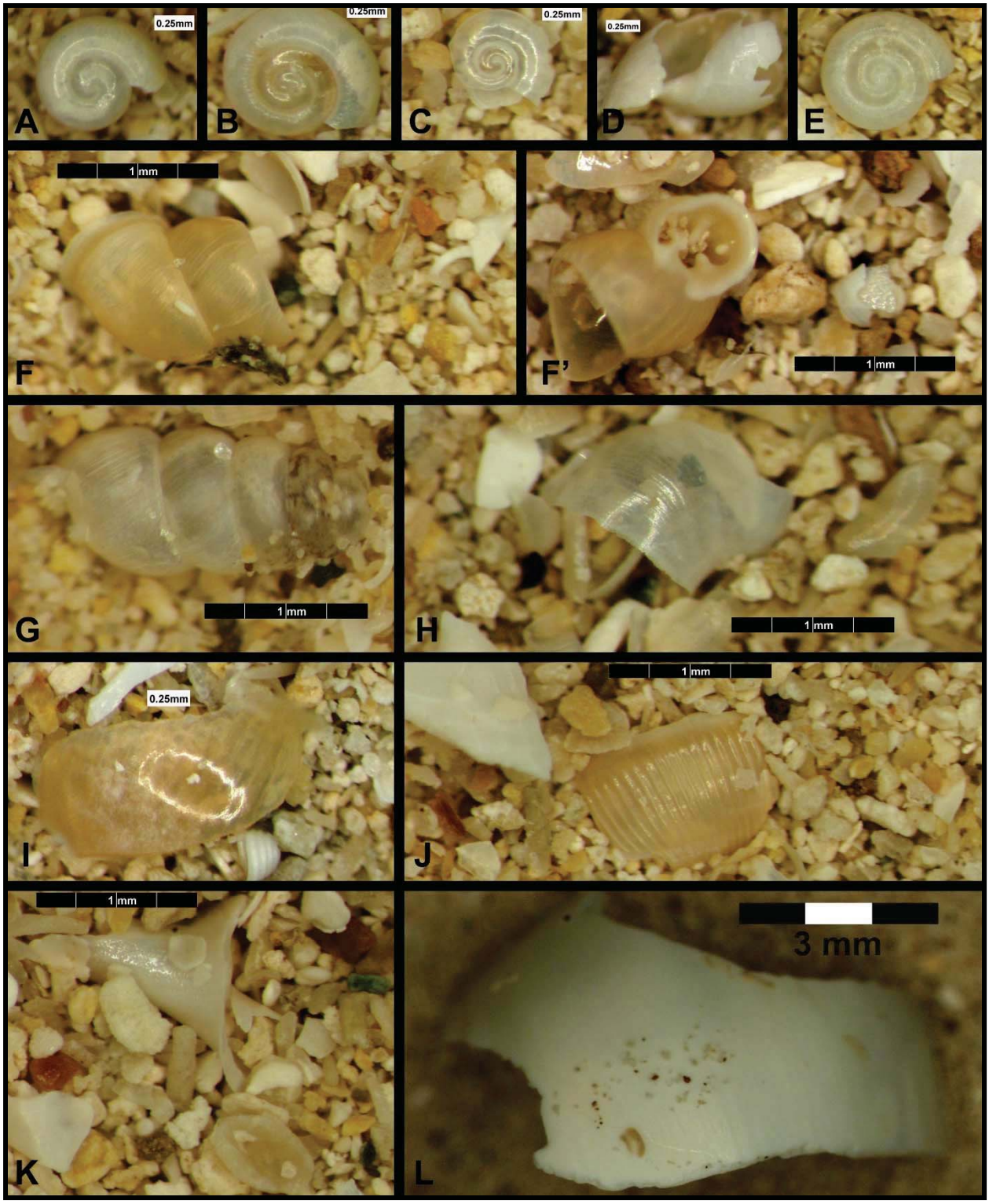

Figure E-14. Snails and fragments from Big Hole site (41TV2161) Block C Profile. PNUM 2408 specimens A-L.

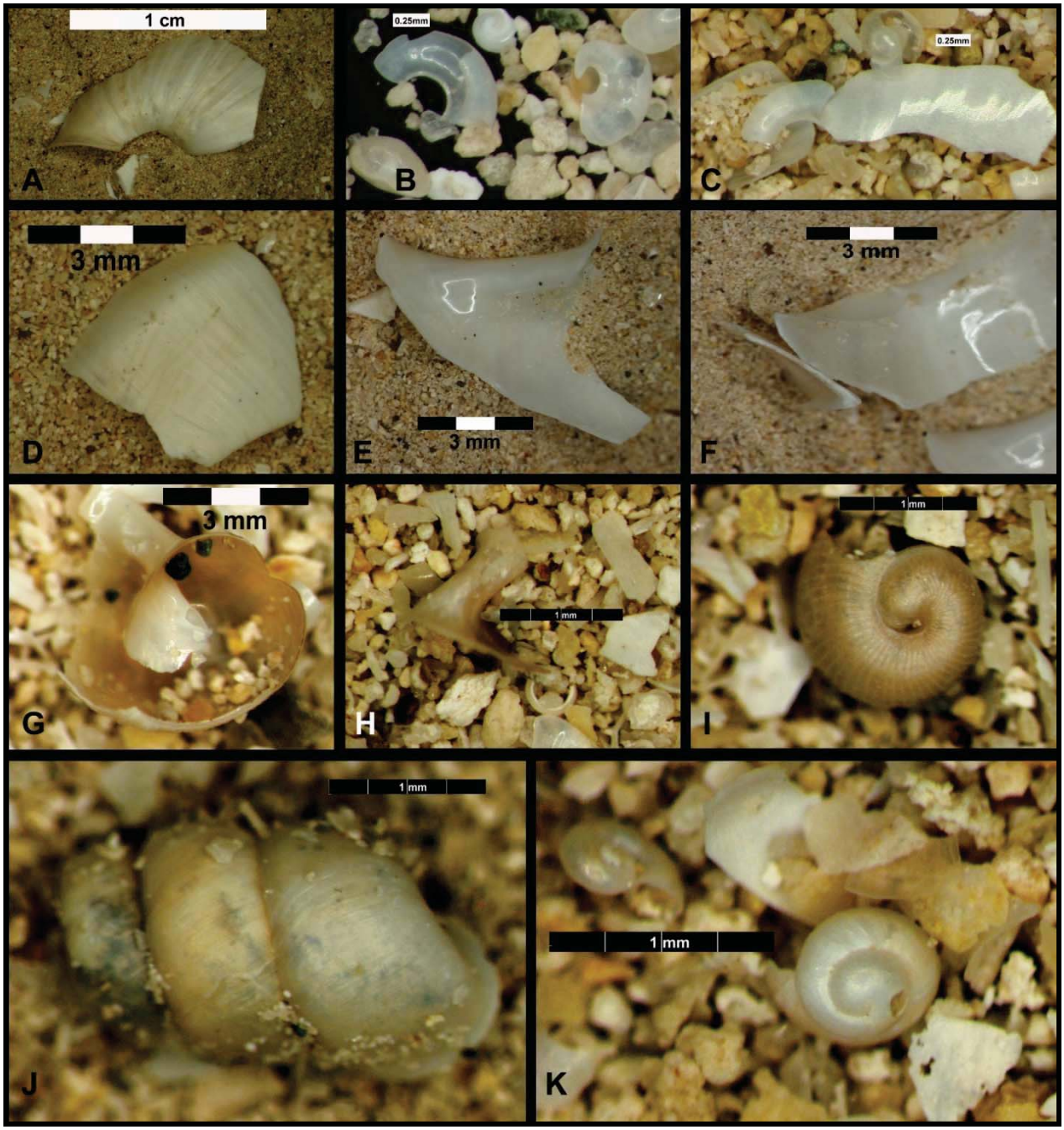

Figure E-15. Snails and fragments from Big Hole site (41TV2161) Block C Profile. PNUM 2408 specimens A-F, and PNUM 2407 specimens G-K.

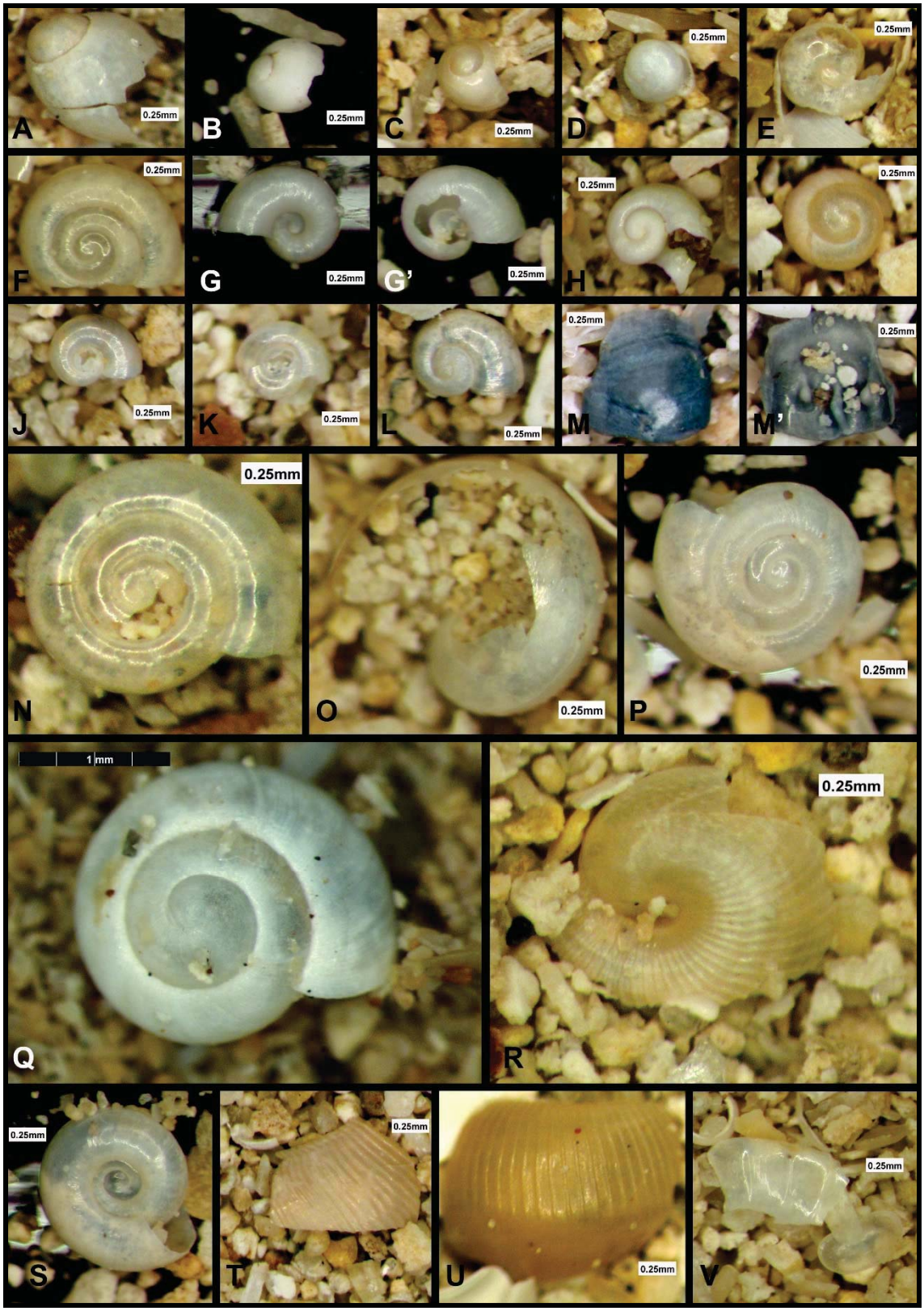

Figure E-16. Snails and fragments from Big Hole site (41TV2161) Block C Profile. PNUM 2407 specimens A-V. Specimen M is burned.

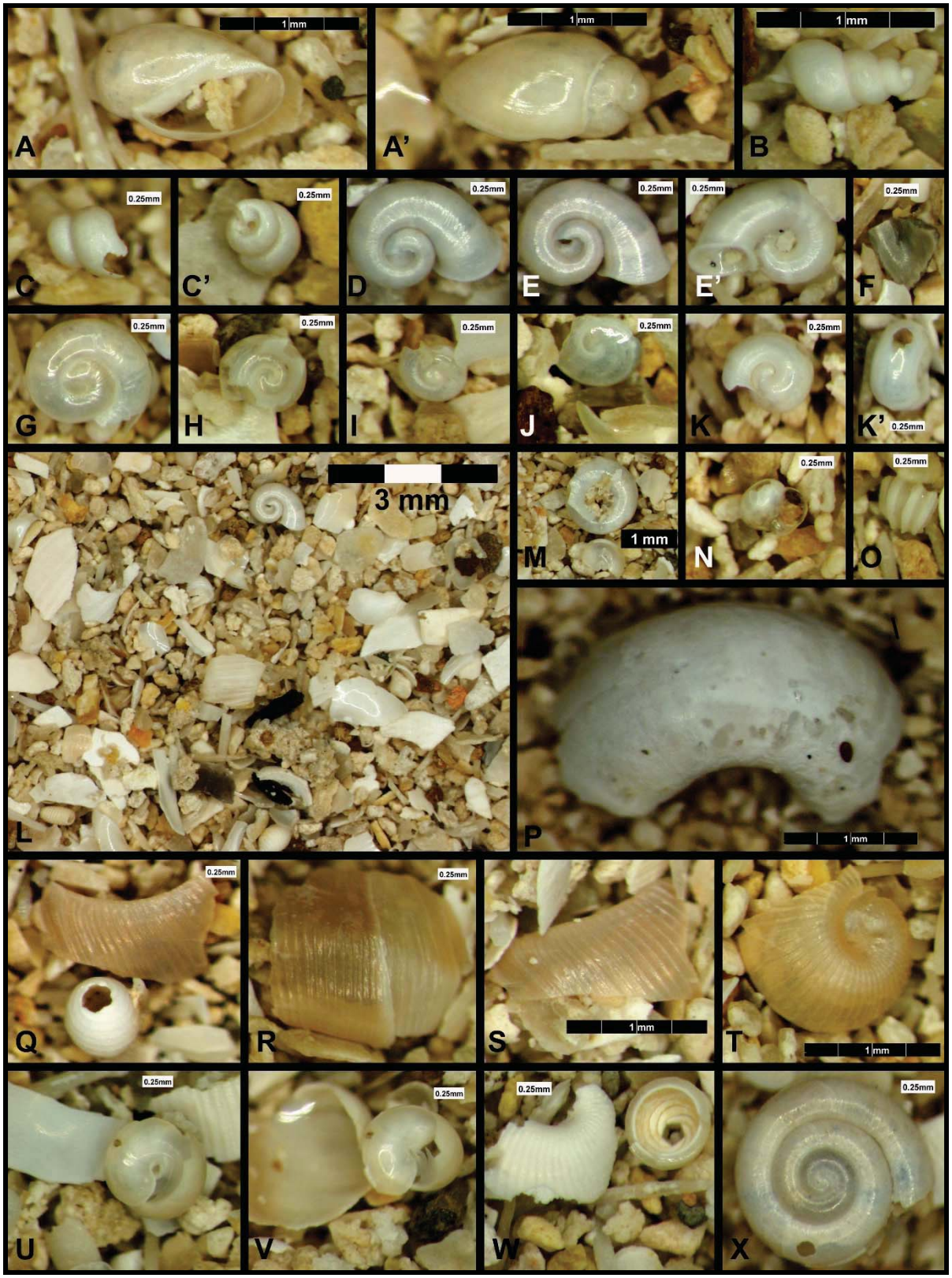

Figure E-17. Snails and fragments from Big Hole site (41TV2161) Block C Profile. PNUM 2406 specimens A-X.

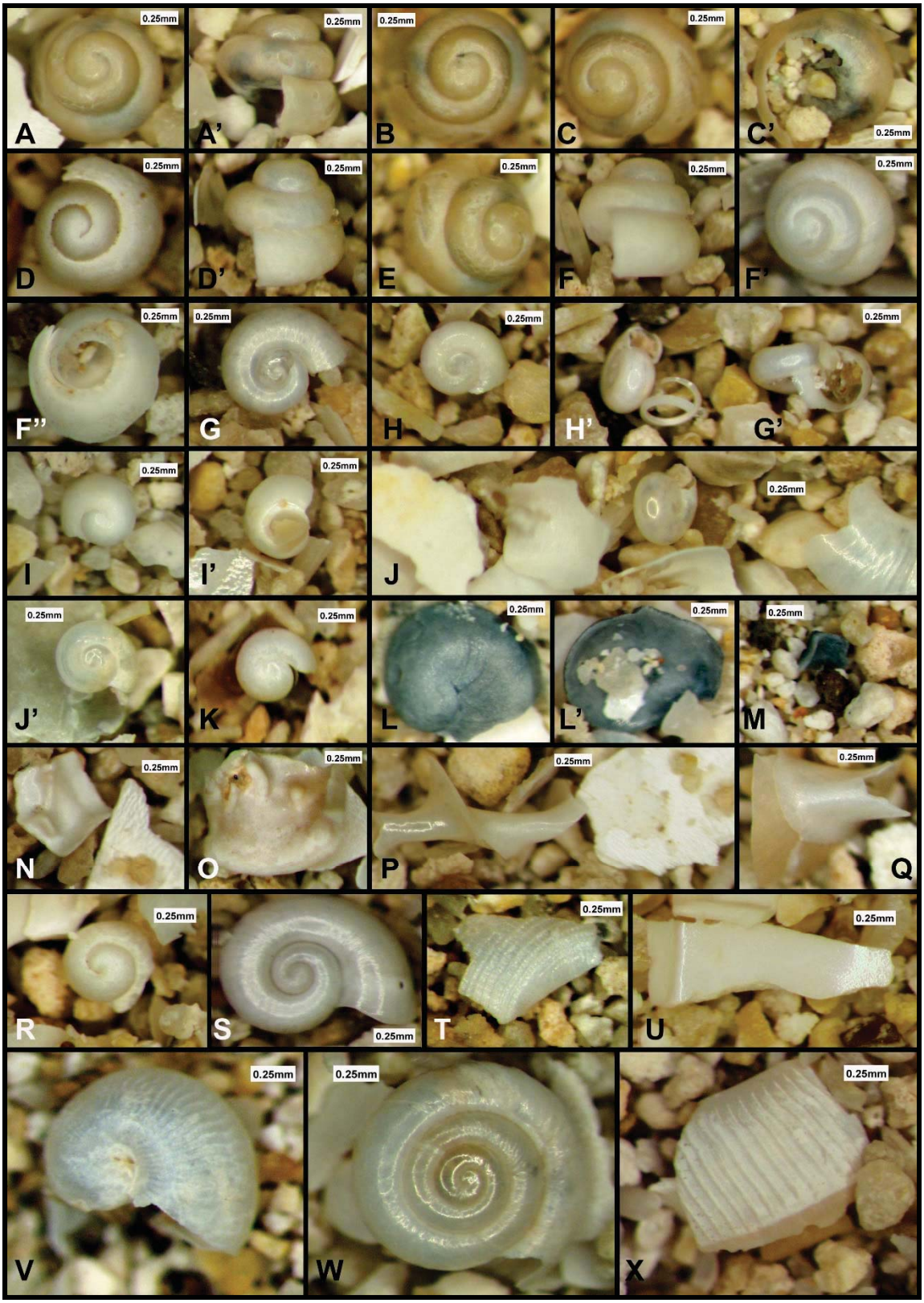

Figure E-18. Snails and fragments from Big Hole site (41TV2161) Block C Profile. PNUM 2405 specimens A-X. Specimen L is burned.

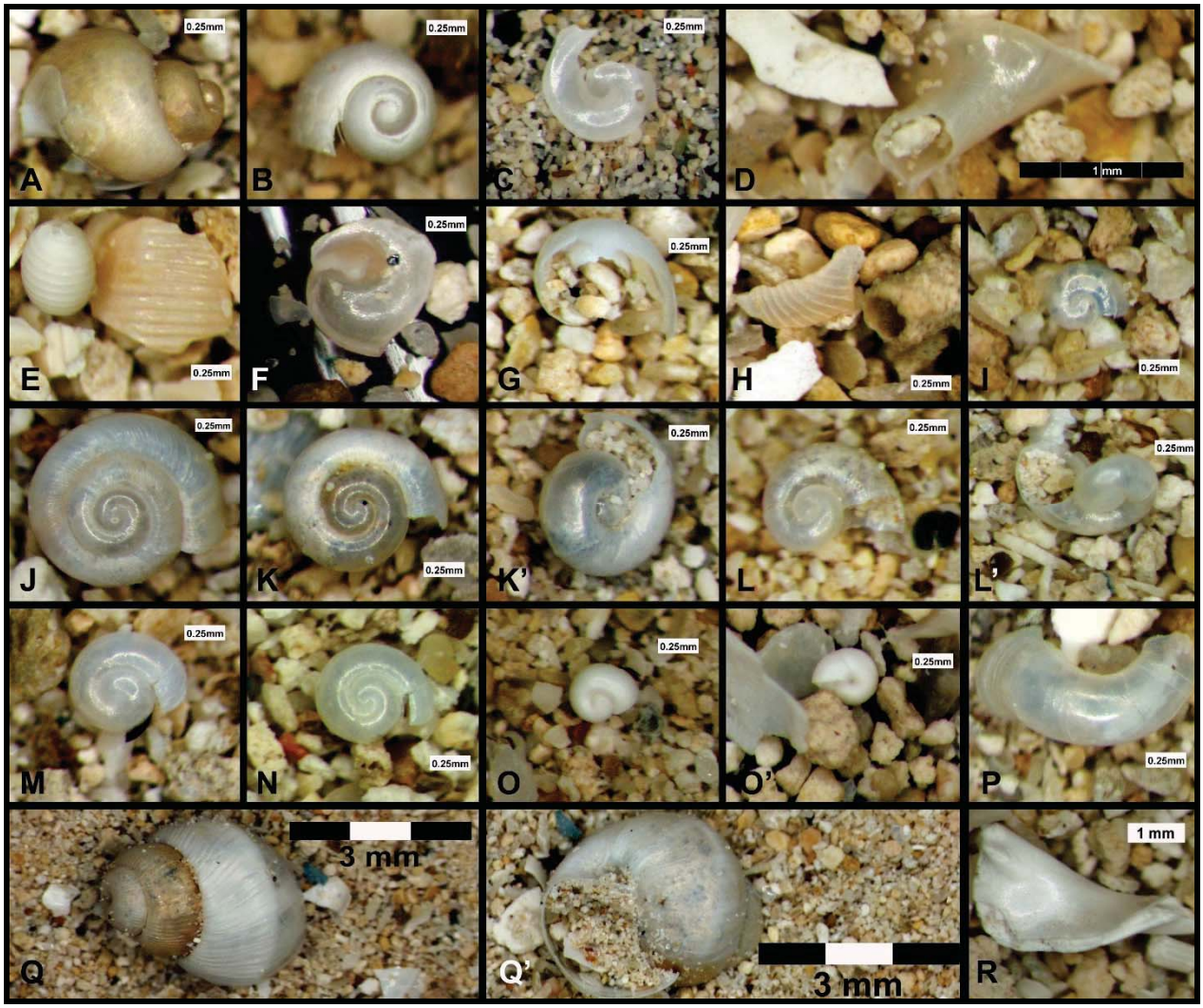

Figure E-19. Snails and fragments from Big Hole site (41TV2161) Block C Profile. PNUM 2404 specimens A-H, and PNUM 2403 specimens I-R.

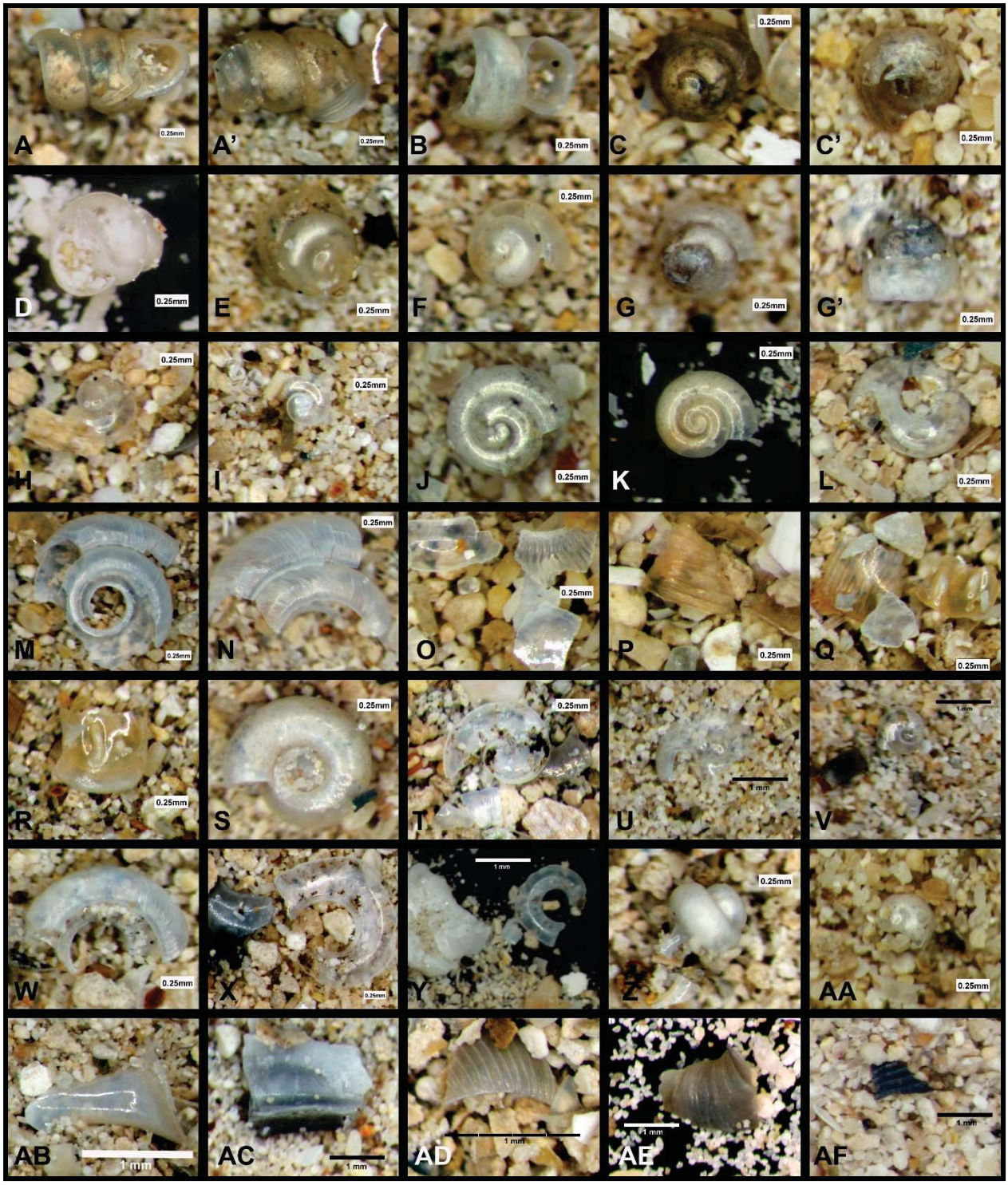

Figure E-20. Snails and fragments from Big Hole site (41TV2161) Block C Profile. PNUM 2401 specimens A-R, and PNUM 2400 specimens S-AF. Specimens X and AC-AF are burned.

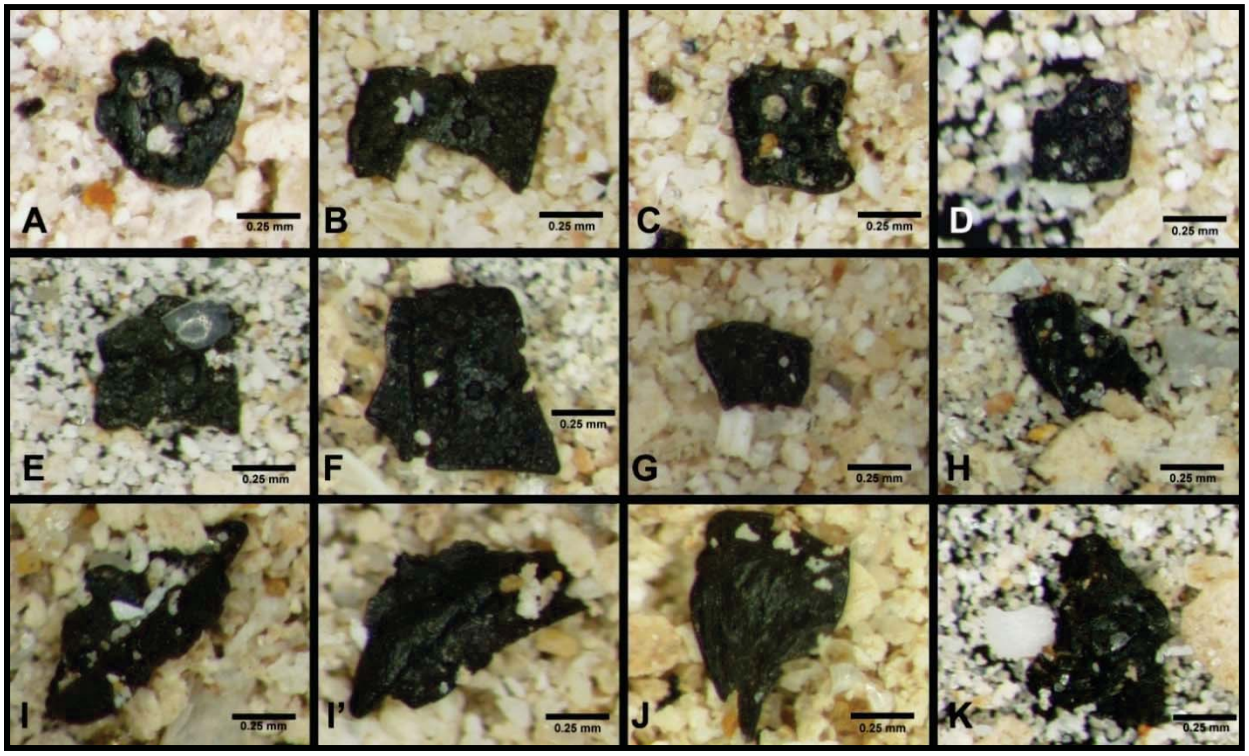

Figure E-21. Distinctive charcoal fragments from PNUM 2060. Specimens A-H all have the same distinctive circular "divots" in the surface. I-K also have distinctive traits. All specimens remain unidentified as to botanical origin(s). A piece of burned shell is on top of specimen in E.

E.5 DATA - SOILS AND SOIL TEXTURE

The site soil profile and environmental history have previously been addressed in some detail (Frederick et al. 2007); the sampled soil column is illustrated by Frederick in Figures 3.1 and 3.2. The site soil type is Lewisville silty clay, with large areas of Altoga and Houston Black soils within 100 meters of the excavation. According to the USDA soils data, the calcium carbonate equivalent of these three soils, in the order listed, is 20-40%, 40-75%, and 2-35%, which identifies all three soils as containing calcic horizons.

With the sand and silt weights for each sample, the soil textures were determined (Figure E-22). Carbonate content of the sand fraction was very high; it was not neutralized in order to preserve snail and spicule data. Later removal of carbonates from the silt fractions—present in amounts as high as six weight per cent—actually altered the textural classification of several samples. It was decided to plot the texture data for the as received samples (i.e., including the carbonate in the fraction weights). In Figure E-22, significant variation between the two control samples is evident (sample numbers 35-36 [PNUM 2450 and 2451]). It is probable that the control soil from the hilltop (#35) was partially deflated by erosion mixing the lessened modern A horizon with formerly deeper horizons. Excluding the surface control samples and the Block C soil column textures (sample numbers 1-12 [PNUM 2400-2411, 2026]), the other 22 sample textures are generally similar with occasional minor perturbations (sample PNUMs are in Table E-1). The textures of samples 20 (PNUM 2424), 25 (PNUM 2367), and 33 (PNUM 2044) are the most dissimilar of these remaining 22 samples.

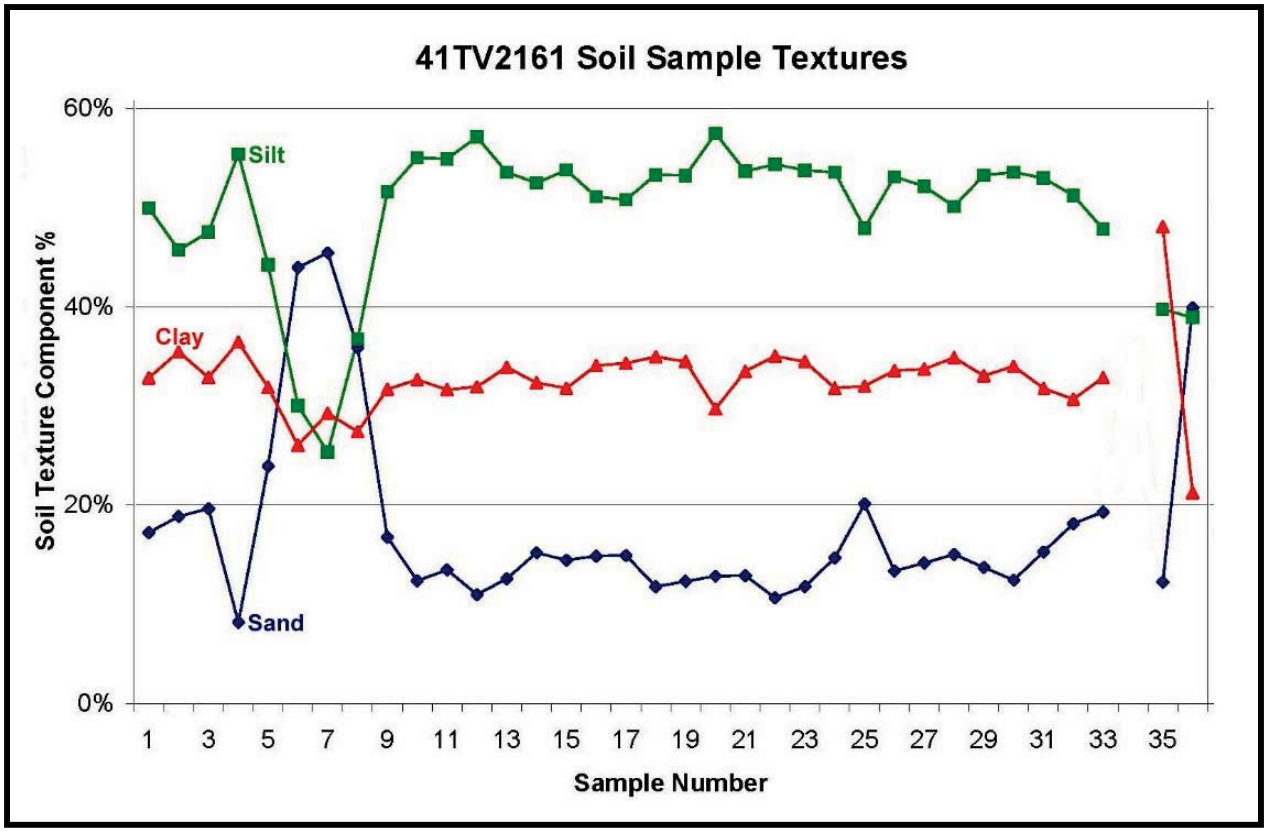

Figure E-22. Soil texture values of the 4TV2161 sample suite. The laboratory sample numbers are on the x-axis, and the PNUM values are in Table E-1. Samples 1-12—showing the greatest variability—are the Block C soil profile column samples. [Sample 34 omitted]

The texture plot containing only the Block C soil column data is in Figure E-23, with the sample depth (cmbs) indicated instead of the sample PNUM (sample key in Table E-1). This data clearly shows that at 320-300 cmbs (sample numbers 6-8, PNUMs 2407, 2406, and 2405) there was a significant increase in sand content at the expense of silt. This supports interpretation of a major wetter interval with more sand deposition via flood episodes along Onion Creek. Prior to that wet interval, the silt deposition rate was higher (340 cmbs; PNUM 2409)—possibly from aeolian deposition during a relatively dry interval. Following the wetter interval, the silt component in the soil again increased to offset the decrease in sand deposition suggesting a drying interval (290-260 cmbs).

E.6 DATA - BIOGENIC SILICA (PHYTOLITHS)

Overall, phytolith preservation in these samples is relatively poor. The examples of short cells from three basic environmental/climatic categories illustrated in Figure E-1—Panicoid, Pooid, and Chloridoid—were photographed while scanning and counting phytoliths in the surface control sample (#36, PNUM 2451). Using Strömberg's recommended particle count criteria (Strömberg 2009) only the flood plain surface control sample in this 36-sample suite provided enough short cells for a reliable particle short cell particle count and climatic interpretation (Table E-3).

Table E-3. Flood Plain Control Sample Phytolith Signature (Normalized %).

PNUM	Panicoid %	Pooid %	Chloridoid %	Saddle Ratio (T:S)
2451	17.2	33.3	49.5	0.68

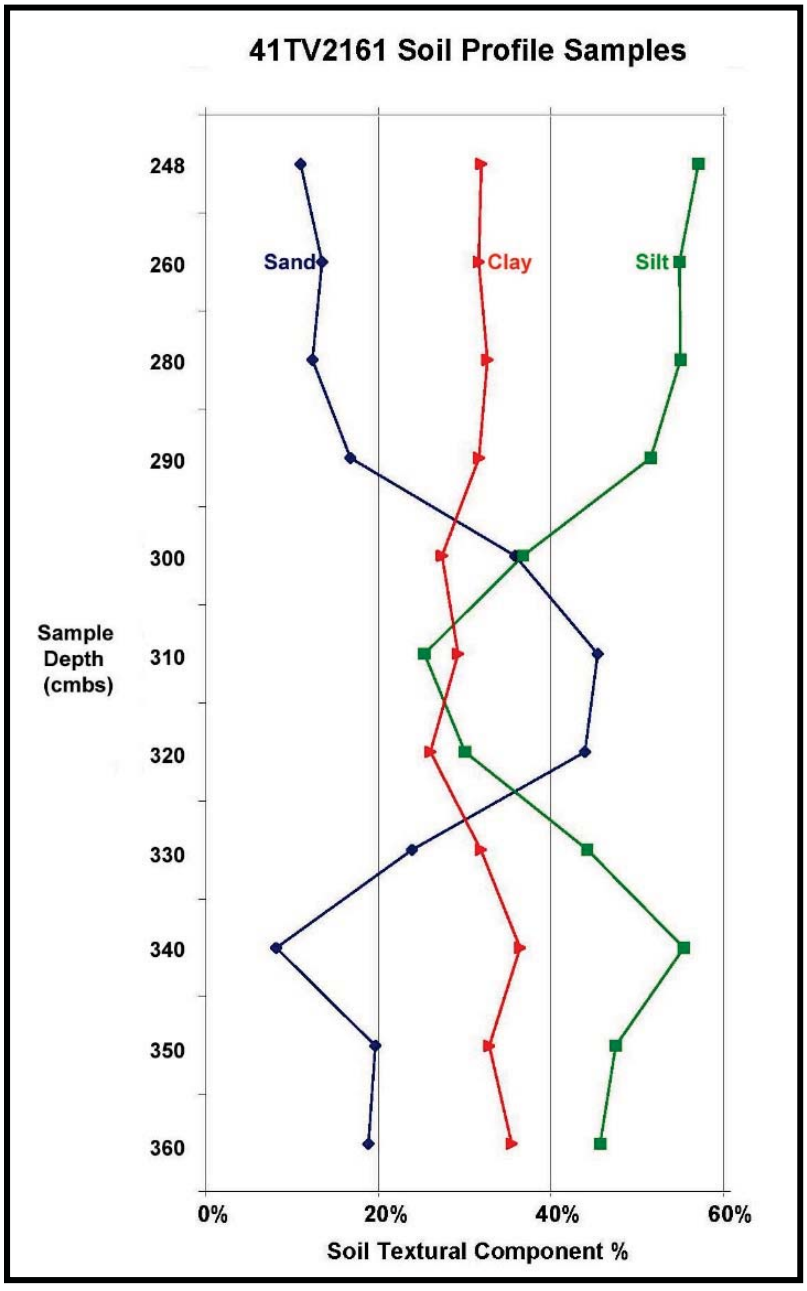

Figure E-23. Block C soil profile and soil texture plot [PNUM 2400-2411] shows a relatively stable clay content and significant variations in the sand and silt fractions over time.

Table E-4. General Biogenic Strew Slide Observations.

Lab Spl #	PNUM	Observations	Charcoal: Bulliform Particle Ratio
MQ13'-1	2026	Charcoal particle count 2x higher than the phytoliths (primarily bulliforms, weathered). Few tree phytoliths (one burned)	2.0
MQ13'-2	2411	Less charcoal than above sample, several tree phytoliths (one burned), primarily bulliforms observed	0.5
MQ13'-3	2410	Similar to previous sample (less total particles on slide)	0.3
MQ13'-4	2409	More tree phytoliths.	0.8
MQ13'-5	2408	No tree phytoliths.	0.9
MQ13'-6	2407	Tree phytoliths present	1.6
MQ13'-7	2406	Few tree phytoliths	1.3
MQ13'-8	2405	Few tree phytoliths	1.2
MQ13'-9	2404	No short cells, poor preservation	0.3
MQ13'-10	2403	Low count, poor preservation	0.3
MQ13'-11	2401	Low count, poor preservation	1.0
MQ13'-12	2400	Tree phytoliths (one burned)	0
MQ13'-13	2143	Tree phytoliths (one burned)	0.5
MQ13'-14	2261	Few tree phytoliths (one burned)	1.0
MQ13'-15	2257	Low count, poor preservation	0
MQ13'-16	2110	Good preservation (but not enough for a formal count). Rare Pooids, mainly Chloridoids (20% were burned); and a few Panicoids (42% were burned)	0.4
MQ13'-17	2112	Few short cells, none burned; tree phytoliths (30% burned); Gemmosclere	0.2
MQ13'-18	2197	Few short cells, none burned	0.7
MQ13'-19	2200	Very few short cells (none burned); few tree phytoliths	0.3
MQ13'-20	2424	Few panicoids (100% burned); few Chloridoids (0% burned). Gemmosclere	0.8
MQ13'-21	2078	Few short cells, few tree phytoliths (some burned)	0.5
MQ13'-22	2092	No short cells, few tree phytoliths (none burned); possible cucurbit	0.3
MQ13'-23	2224	Poor preservation	0.5
MQ13'-24	2246	Poor preservation, few tree phytoliths (some burned)	0.1
MQ13'-25	2367	Few short cells, Chloridoid burned, abundant tree phytoliths (some burned)	0.2
MQ13'-26	2146	No short cells, a few tree phytoliths	0.2
MQ13'-27	2149	Poor phytolith preservation; some complete spicules	0.1
MQ13'-28	2176	Numerous spicules, abundant tree phytoliths; otherwise poor preservation	0.1
MQ13'-29	2060	Numerous spicules, abundant tree phytoliths; otherwise poor preservation	0.2

Table E-4. General Biogenic Strew Slide Observations (continued).

MQ13'-30	2179	Abundant tree phytoliths, possible cucurbit phytolith, possible flake	<0.1
MQ13'-31	2239	Abundant tree phytoliths, no charcoal, possible cucurbits	0
MQ13'-32	2280	Numerous spicules, abundant tree phytoliths; possible cucurbits, poor preservation.	< 0.1
MQ13'-33	2044	Numerous tree phytoliths (some burned), spicules, cucurbit, short cells absent	0
MQ13'-34	2275	Few short cells, abundant tree phytoliths (some burned), possible cucurbits	0
MQ13'-35	2450	Good bulliform load; abundant tree phytoliths. short cells present (too low a #)	0
MQ13'-36	2451	Good slide, "Normal" phytolith strew. Sedge fragment. Counts reported.	<0.1

As will be addressed in detail in the Discussion section, the soil environment (basic pH and high carbonate content) appears likely to have preferentially dissolved the smaller thinner phytoliths (i.e., the majority of the smaller short cell phytoliths critical to climatic interpretation) in nearly all samples. This selective dissolution could be due to a combination of relative particle surface area to volume ratio, variations in particle density (hydration status), loss of surface-protective mechanisms (such as metals), or even extreme repeated variations in soil moisture given the alkaline conditions and floodplain setting. Frequent flood events would tend to regularly flush the soil pore water from the profile more rapidly thus shifting the chemical equilibrium to dissolve more silica into more water than at steady state under drier conditions. The site is located near a paleochannel so at some point it was situated close to Onion Creek.

Numerous sample biogenic isolates contained no short cell phytoliths observed during the slide scans. During the formal sample count scans and the subsequent slide overview scans to evaluate the entire slide and search for other forms, the following observations were made (Table E-4).

Bulliform cells were the predominant phytolith type remaining in the 41TV2161 samples. Other common particles observed were charcoal fragments, phytoliths likely of tree origin, sponge spicules, and weathered elongate cells. All short cell phytolith forms were chronically under-represented or absent in most samples—with the exception of crenate specimens. Some bulliform cells were in a reasonably good state of preservation, but most exhibited evidence of weathering and pitting—likely by surface dissolution due to the soil matrix chemistry. Typical examples are shown in Figure E-24. Some show weathering all over the particle (c.f. Figures E-24D, K, N, S, T, and W), whereas other specimens tend to show more dissolution along one edge (c.f. Figures E-24C, E-J, L, M, R, U, V, X, and Y). Still other specimens show dissolution in the center of the phytolith (c.f. Figures E-24A, B, and O-Q).

Several phytoliths of *Cucurbita* (wild gourd rind phytoliths) were observed in these sample scans (Figure E-24 shows likely cucurbits). These phytoliths were all in a good state of preservation.

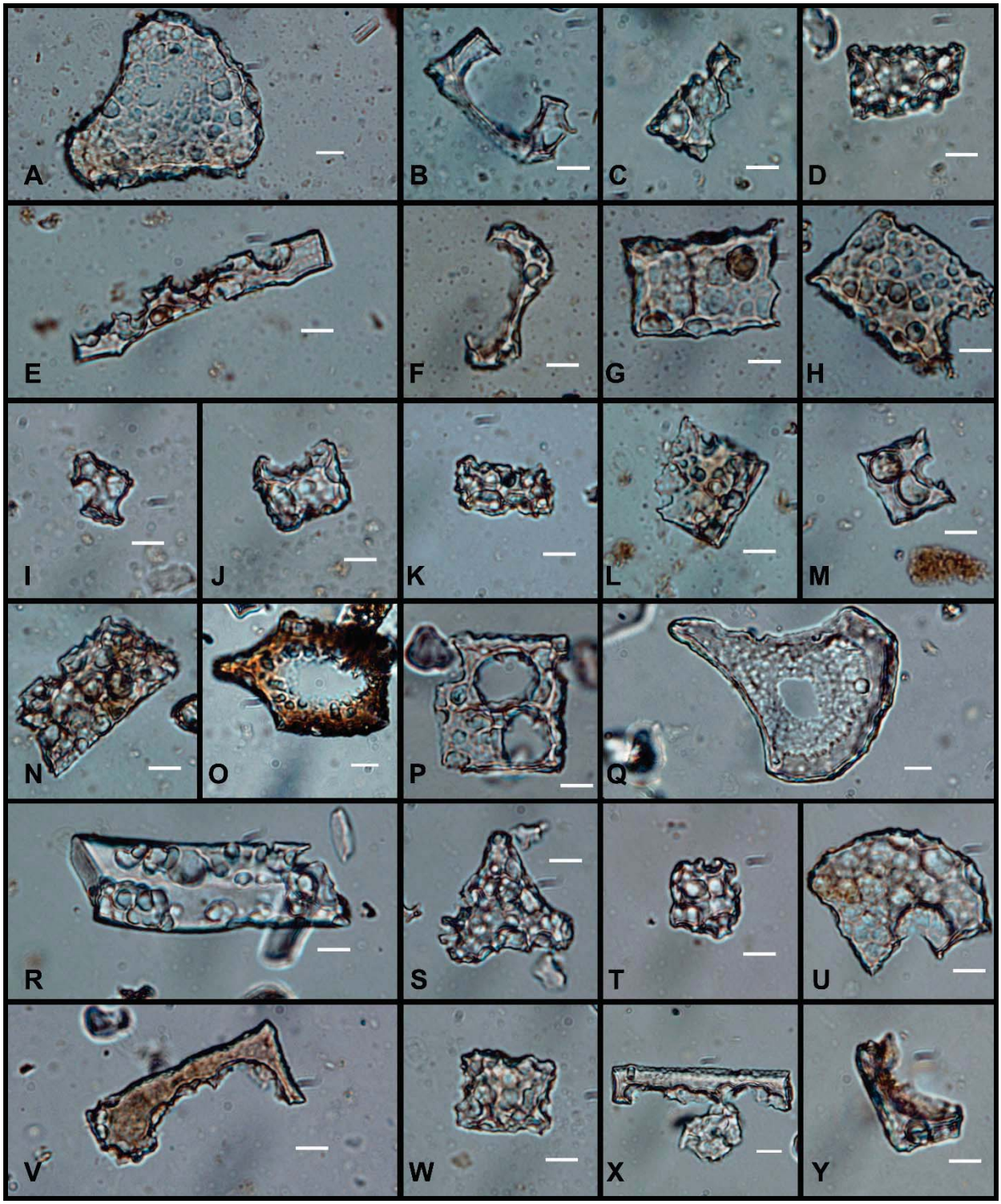

Figure E-24. Representative weathered bulliform specimens from various samples (the specimen in E is likely an elongate or a tree type phytolith; R is amorphous silica, but may not be a bulliform cell). A, B: PNUM 2407; C-D: PNUM 2406; E-N: PNUM 2110; O-Q: PNUM 2176; R-T: PNUM 2060; U, W-X: PNUM 2239; V: PNUM 2179; and Y: PNUM 2280. The white bar scales are 10 microns.

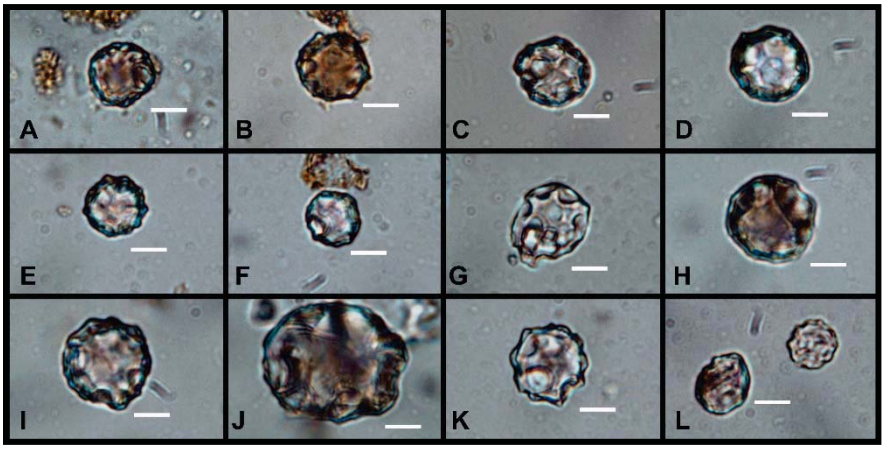

Figure E-25. *Cucurbita* phytoliths. A-B: PNUM 2092; C: PNUM 2179; D-F: PNUM 2239; G-J: PNUM 2280; K: PNUM 2044; and L (left specimen): PNUM 2275. Several specimens may be burned (A, B, H, J, and L (left). Specimen J is atypically large for the period. White bar scales are 10 microns.

E.7 DATA - BIOGENIC SILICA (SPONGE SPICULES)

Freshwater sponges grow in many streams and bodies of water and have spicules made of amorphous silica. Long linear spicules—the megascleres and microscleres—provide a skeleton or framework for sponges, while other spicules—the gemmoscleres–-are part of the reproductive process. An excellent overview from a biological point of view is available, and includes images as well as a summary line drawing of nearly all North American species (Reiswig et al. 2010:91-123). The best detailed environmental summary of sponge habitats remains that by Harrison (1974:29-66). A recent archeological site report including spicule data presented from a paleoenvironmental point of view is also available (Sudbury 2011d:75-101).

Twenty-seven of the soil samples examined contained siliceous sponge spicules (Table E-5). Whereas the large fossiliferous carbonate spicules in the sand fractions were of marine origin (Figure E-8C, center), the smaller spicules recovered in the silt fractions are amorphous biogenic silica and represent area freshwater sponges from the time of soil deposition (Figures E-26 through E-31).

The spicule specimen data for the Block C soil column in Table E-5 (PNUM 2411-PNUM 2400) are the same samples for which the climatic soil texture profile was previously presented (Figure E-23). The highest spicule count in this section (PNUM 2406, the 310 cmbs sample) correlates with the highest sand textural sample at the site suggesting a very wet period. Conversely, this was also smallest silt fraction (from which the spicules were isolated—which means the spicules were really concentrated). While the spike in the sand data suggests high water flow, the two adjacent spicule data counts from samples with high sand content have very low spicule counts (PNUM 2405 and 2407)—at background level for this sample suite. Thus, it is conceivable that the spicule spike observed in PNUM 2406 could represent period of an attractive environmental setting for habitation due to the readily available water supply. The Charophyte concentration seemed to also peak during this same interval, which suggests—even with greatly increased sand deposition—that the flow was not always high volume.

Excluding sample PNUM 2406, the non-surface samples in the assemblage that were not from features averaged 1.1 spicule per sample; this is presumably a reasonable environmental background value (n=16).

Table E-5. Sponge Spicule Counts, 41TV2161.

Sample ID (PNUM)	No. of Spicules	Complete Spicules			Broken Spicules (mid-section / tip)			Germmo-scleres
		Smooth	Spined	Thin-walled	Pristine	Abraded	Chemically weathered	
2026								
2411	2	1				1		
2410	1					/ 1		
2409	1					1		
2408	2				/ 1	1		
2407								
2406	10		1	1	1 / 2	2, 1 / 1	/ 1	
2405	1				1			
2404	1					1		
2403								
2401								
2400								
2143	4	1		1	1 / 1			
2261								
2257	4	1	1	1	/ 1			
2110	65	1	1		4, 9, 1 / 8, 9	3, 7 / 3, 2, 1	8 / 2, 6	
2112	17		2		1, 3 / 2, 1	2, 1 / 1	2 / 1	1
2197								
2200								
2424	2				/ 1			1
2078	1				/ 1			
2092	1						/ 1	
2224	1				/ 1			
2246								
2367	18	2		1	1, 4 / 3, 1	1 / 1	1 / 3	
2146	5				/ 2	1	/ 2	
2149	11	2		1	1 / 1, 1	1, 1 / 2	/ 1	
2176	25	2		1	6 / 7, 1	2 / 4	2	
2060	26	1		2	2, 3 / 6, 2	3, 1 / 3	1, 1 / 1	
2179	4	1			1	1	1	
2239	1					/ 1		
2280	15	2			/ 3	2, 1 / 2, 1	2, 2	
2044	10	1			2, 1 / 3	1	1 / 1	
2275	8				2, 2 / 1		3	
2450	4				1	3		
2451	6			1	1, 1 / 1	1, 1		
Totals	**246**	**15**	**5**	**9**	**109**	**63**	**42**	**2**

(Feature Samples Highlighted in Blue)

This value is elevated due to the inclusion of samples PNUM 2143 and 2257. Excluding these two samples—each with counts of 4 spicules—the average spicule count for the remaining 14 samples of 0.79 spicules per sample may be a more accurate background value. Clearly, some spicule sample counts in Table E-5 are elevated above background level; the nine highest spicule counts (excluding PNUM 2406) occur in cultural features.

Perhaps more important is the causation of elevated spicule counts in some feature samples; seven samples have more than 10 spicules per sample with a range from 11 to 65 spicules observed on the slide. The most obvious explanation for this high spicule concentration is that spicules may be an indicator of water usage associated with the feature—such as cooking with boiling water. If so, the spicule concentration variation between samples could simply be an indication of how long the feature was in use, or how much water was boiled over or otherwise spilled during food processing.

Several alternative explanations come to mind that may explain the lower concentration samples beside shorter duration of feature use. Although historic use of fire for multiple purposes has been documented, it is also possible that a fire would sometimes need to be doused—such as to safely put out a fire during severe wind events, or to quickly put out a fire when enemies were near. Another alternative explanation would be in game processing; it is likely that water imbibed by game would contain some spicules which could be deposited at the site in the offal. Excrement is another possible spicule source.

It seems most probable that features with higher spicule concentration were likely used in food processing and/or cooking. Conversely, it is likely that features with very low spicule counts were used for a shorter period of time or were not used for cooking via boiling water.

Examples of complete and nearly complete smooth sponge spicules are shown in Figure E-26. Relatively complete examples of spined spicules are shown in Figure E-27. Also from freshwater species, the spined form is always less abundant in the Oklahoma (ibid.) and Texas archeological samples reported to date. Spined spicules were only present in nine samples at 41TV2161 (Table E-4) including the modern surface control sample where they comprised 50% of the sample. Sponge species are sensitive to environmental water conditions, so this modern-day presence may indicate that the prehistoric water environment when sponge species with this spicule morphology were present was similar to that of modern times.

The images in the third spicule figure are herein referred to as thin-walled or large diameter axial canal spicules due to their morphology (Figure E-28). Spicules are literally defined as needle-shaped. These specimens are so radically different that it was initially uncertain if these are actually spicules--until finding the specimen with the classic expanded area to house the sclerocyte (Figure E-28K, arrow). This morphology is not described or illustrated in Reiswig (et al. 2010) or other sponge reference works. Spicule images of two species types were not available (ibid. 120) but the descriptions do not match these thin-walled specimens. Reiswig did note some species grow differently based on concentration of available environmental silica by producing smaller outer diameter spicules in response to lower silica concentrations; however, drastic changes in axial canal diameter were not mentioned (ibid. 103). It is conceivable that these specimens represent some abnormal response to an environmental stress; the possibility that these spicules originated from a previously unreported sponge species was also considered. Additional specimens with similar morphology were recently reported from another Texas Holocene site (Sudbury IP). However, Reiswig stated that the "figures of spicules are the most typical representatives of a wider range of

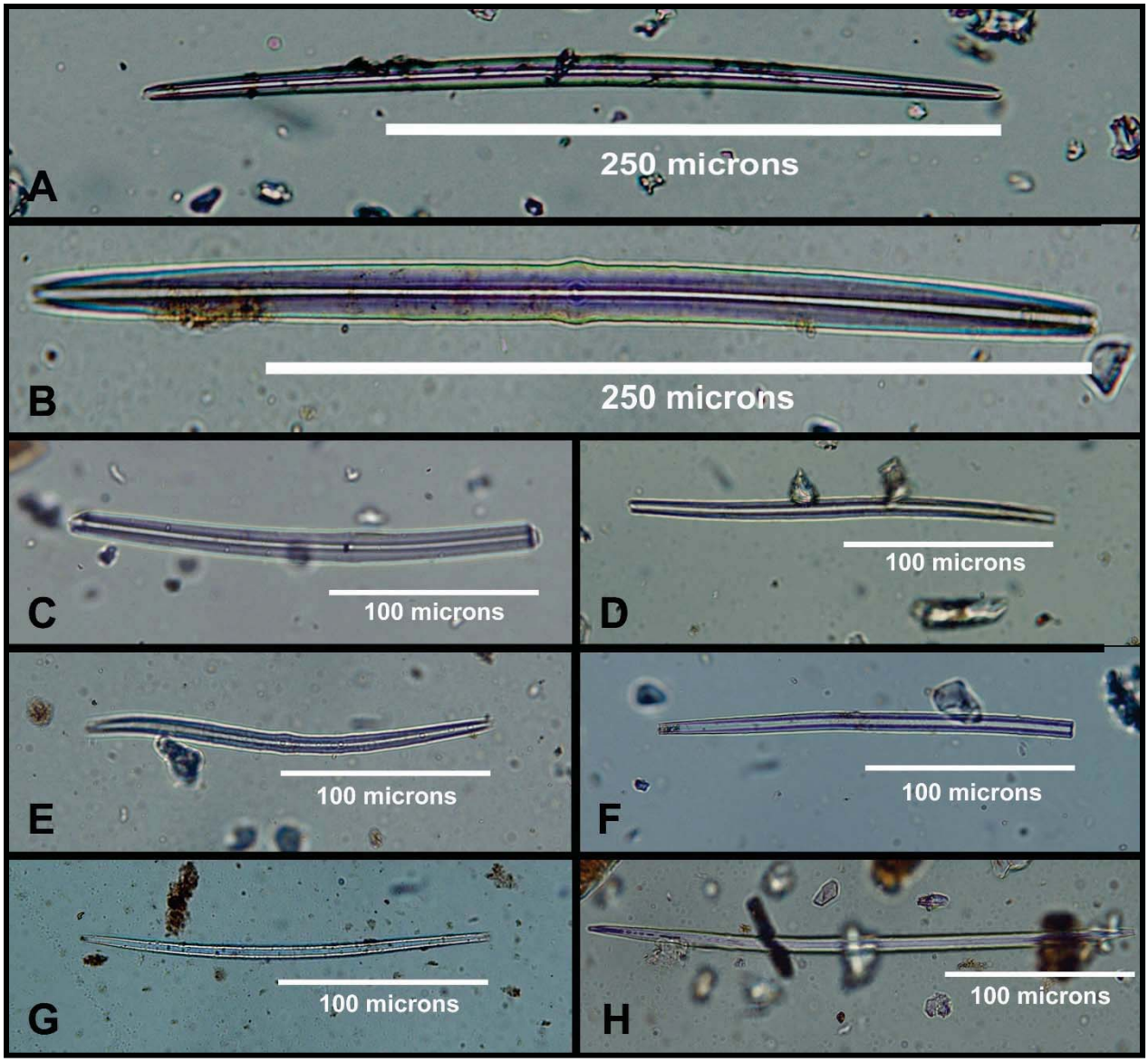

Figure E-26. Smooth surfaced freshwater sponge spicules (megascleres). A & C: PNUM 2280; B: PNUM 2411; D: PNUM 2149; E: PNUM 2143; F & H: PNUM 2367; and G: PNUM 2110. All specimens are complete spicules except C and F (C shows a bending break on the right end). In the center of specimens B, C, and E the enlarged area is where the sclerocyte lived that synthesized the spicule.

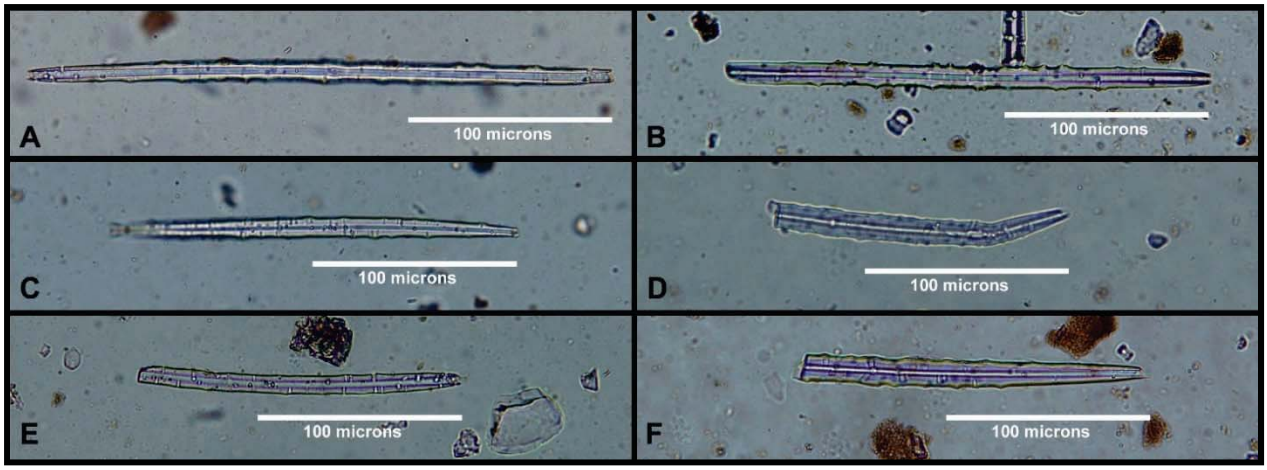

Figure E-27. Spined freshwater sponge spicules. A: PNUM 2112; B, D-F: PNUM 2110, and C: PNUM 2406.

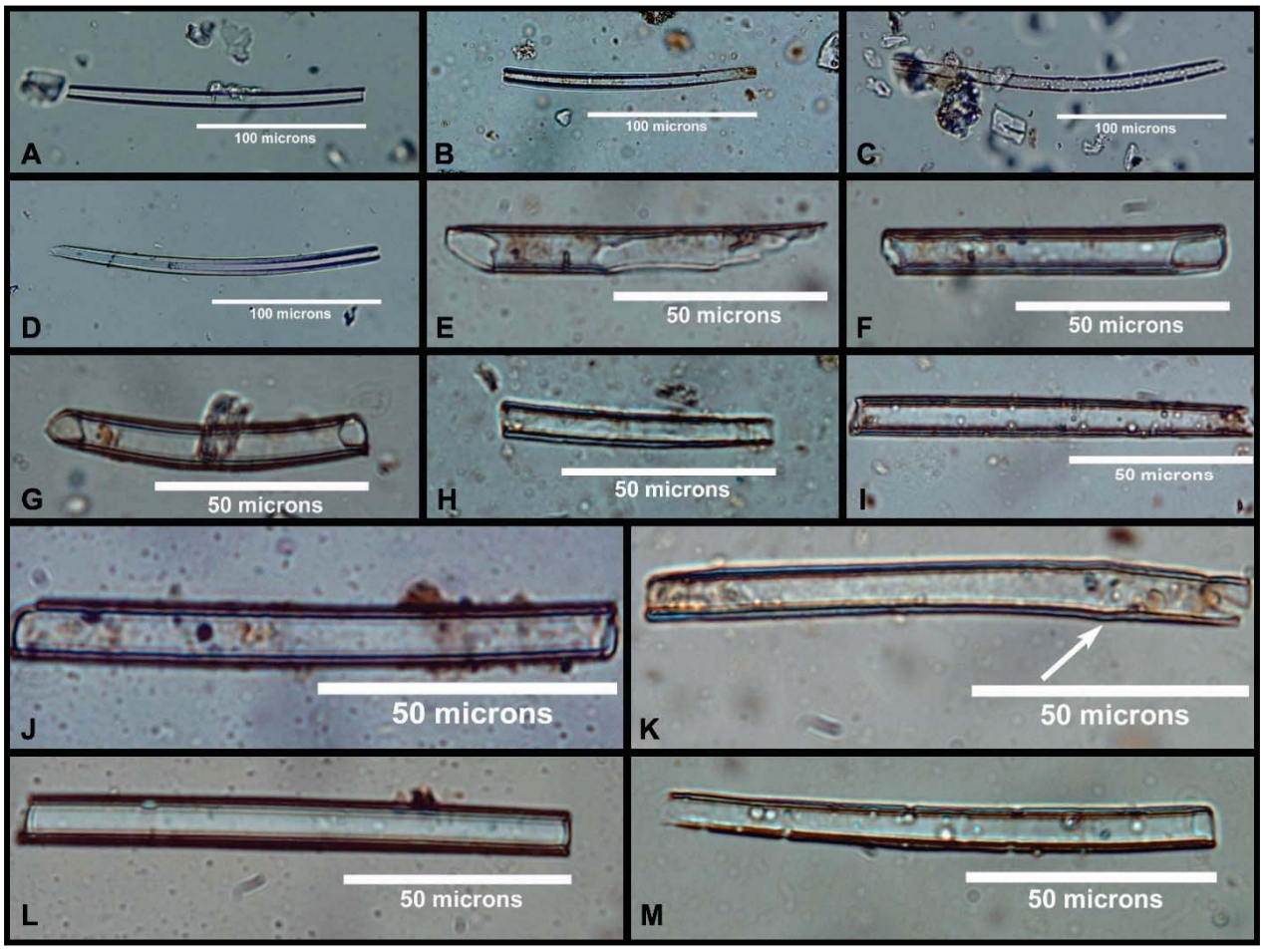

Figure E-28. Freshwater sponge spicules with thin-walls and large diameter axial canals. A and L: PNUM 2149; B: PNUM 2110; C, F-G, M: PNUM 2367; D: PNUM 2179; E: PNUM 2406; G: PNUM 2367; H: PNUM 2424; I and J: PNUM 2110; and K: PNUM 2143.

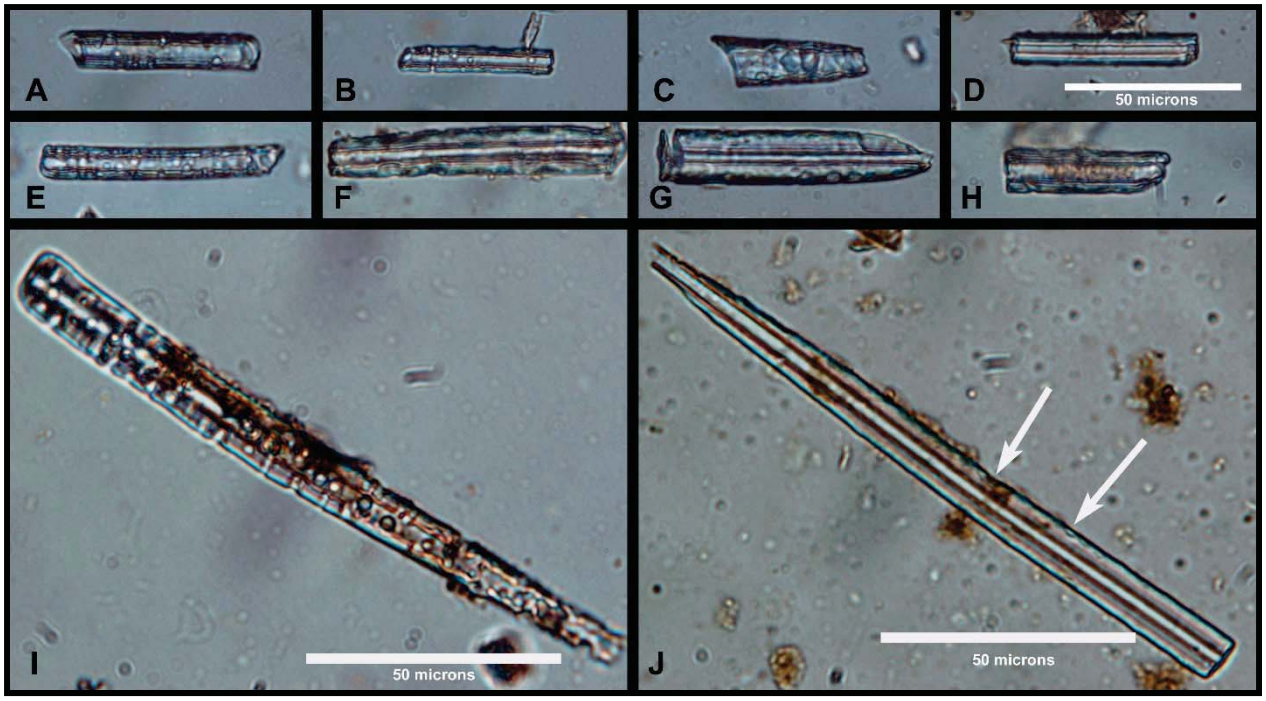

Figure E-29. Examples of weathered (physically abraded) spicules. A-B, E: PNUM 2060; C and I: PNUM 2146; D and J: PNUM 2110; F: PNUM 2112; G: PNUM 2239: and H: PNUM 2450. Specimen I demonstrates signs of both physical abrasion and chemical weathering. The arrows in J indicate localized points of abrasion.

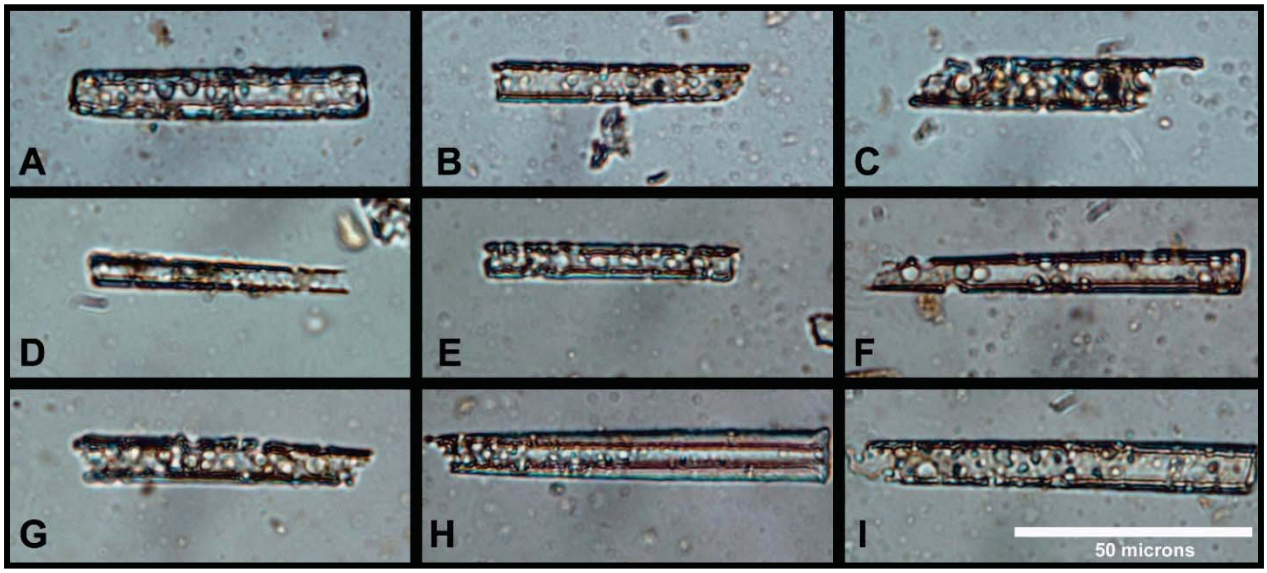

Figure E-30. Examples of chemically weathered spicules. Note that the thinner walls near the tip show more evidence of dissolution than the thicker areas (c.f., left end of F, H, and I; right end of B and D). A: PNUM 2408; B-C, E-F, and H-I: PNUM 2110; D: PNUM 2146; and G: PNUM 2112. Specimen A shows evidence of both physical abrasion and chemical weathering.

morphologies" (personal communication 3-7-15) and that "large axial canals are due to erosion—dissolution…They are not normal and not a species character" (personal communication, 3-8-15).

The specimens in Figure E-29 show surface evidence of physical abrasion and weathering. While tumbling and being sand-blasted while migrating down Onion Creek drainage is the probable cause, aeolian transport cannot be ruled out. The exterior surface is pitted, and the ends are frequently rounded and worn.

The Figure E-30 specimens show evidence of what is referred to here as chemical weathering, meaning partial dissolution by interaction with soil pore water at a basic pH. This chemical weathering is the same process that is suspected to have caused dissolution of many of the short cell phytoliths. The impact on spicule preservation is less, but still clearly visible.

The final spicule figure shows the two gemmoscleres observed in the samples (Figure E-31). Gemmoscleres represent the reproductive phase of the sponge. Gemmoscleres form the wall of gemmules—hollow spheres of radially aligned gemmoscleres that protect the contained amoebocytes during times of environmental stress as well as during normal reproduction. Gemmoscleres are the only spicule type that can be identified to species in isolation from other spicule types, but these particular specimens are not positively identifiable.

Reiswig stated that these two gemmoscleres could be any one "of seven species on the basis of morphology" of which there are three in his reference material reported from Texas: *Heteromeyenia* baileyi, *Racekiela ryderi,* and *Radiospongilla crateriformis.* It was also stated that "the distal parts of the rotules undergo fairly rapid dissolution in sediments so they are respectively widened and lost" (personal communication 3-7-2015).

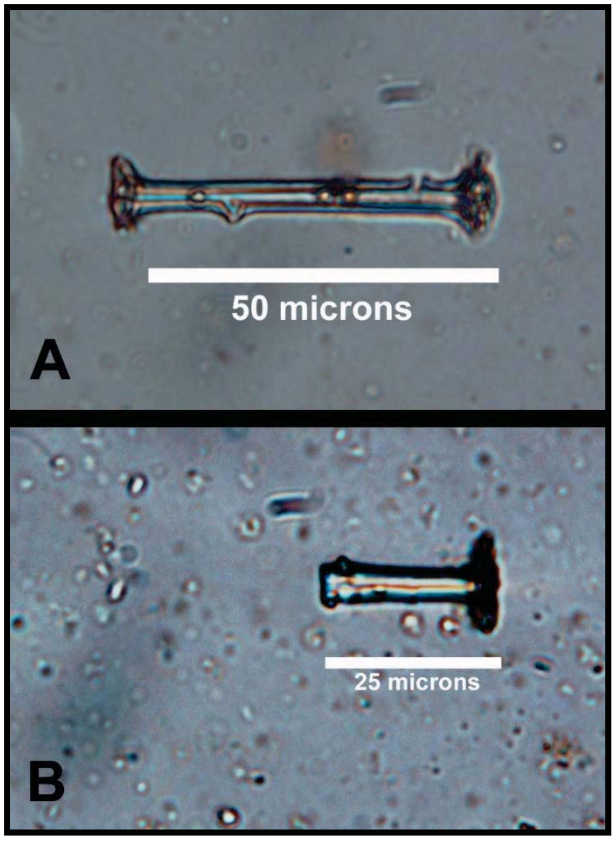

Figure E-31. Gemmoscleres. A: PNUM 2112; and B: PNUM 2424 (broken).

Harrison summarized the habitat information from the literature for these three sponge species in his 1974 Porifera chapter:

Racekiela ryderi, previous referred to as

> "*Anheteromeyenia ryderi* [Reiswig et al. 2010:115] is usually found in lightly shaded locations in swamps, ponds, or slowly moving streams, never in rapids (Old 1932a, b; Neidhoefer, 1940; Hoff, 1943; Eshleman, 1950; Poirrier, 1969). M. A. Poirrier (personal communication) noted that the species grows rapidly in the fastest moving Louisiana streams during fall and winter. It is more common in acid areas of relatively low bicarbonate content (Neidhoefer, 1940; Old, 1932a; Poirrier, 1969). It is somewhat limited by higher temperatures, forming gemmules with the approach of 30°C water temperatures

(Poirrier, 1969) but thrives during winter. It was plentiful throughout winter in lakes and ponds near Cold Spring Harbor, Yew York (Potts, 1987). Local variations are apparently present, however. Old (1932a) found the species limited by both high and low temperatures, with a range for 19°-26.5°C. Jewell (1939) found it to tolerate the entire range of calcium in Wisconsin waters (1.2-22 ppm), but Stephens (1912) never found it on limestone rocks. It is always absent from polluted waters (Old, 1932a) and brackish water (Poirrier, 1969)." (Harrison 1974:38)

A table of water conditions drawn from the cited sources for *Racekiela ryderi* was also provided. (ibid. 39)

"*Heteromeyenia baileyi*…[exhibits] a widely scattered distribution throughout eastern North America (Penney and Racek, 1968), [and] tolerates a wide range of environmental conditions. It is a quiet water form, not occurring in rapids (Old, 1932a). In temporary habitats, gemmulation occurs in late spring (Poirrier, 1969). It is adversely affected by the combination of rising temperatures and falling water levels (W. G. Moore, personal communication). In permanent habitats it may be found throughout the year. Its toleration of extremely low dissolved oxygen levels (0.80 ppm) and high free CO_2 levels (26.5 ppm) is very likely related to the presence of zoochlorellae in this bright green (Moore, 1953; Penney and Racek, 1968) species. Old (1932a) noted that the optimum habitat of *H. baileyi* is pollution free. It has been collected once in slightly brackish water, conductivity 3000 micromhos/cm chloride 1.1 ppt (Poirrier, 1969)." (Harrison 1974:47).

A table of water conditions drawn from the cited sources for *Heteromeyenia baileyi* was also provided. (ibid. 48)

"*Radiospongilla crateriformis*, a species preferring alkaline waters high in bicarbonates and conductivity (Wurtz, 1950; Poirrier, 1969), is unusual in its ability to tolerate very stagnant or very turbid waters (Smith, 1921; Eshleman, 1950; Cheatum and Harris, 1953; Poirrier, 1969). Its tolerance of siltation is related to some extent by its preference for colonizing undersurfaces of supports (Hoff, 1943; Cheatum and Harris, 1953). However,…in view of collections of healthy colonies buried in the mud (Cheatum and Harris,1953), other factors must also be involved.

"*Radiospongilla crateriformis* is seasonal, at least in some areas, with gemmulation usually occurring in fall and active colonies present May through September (Poirrier, 1969). Considering the widely discontinuous distribution of this species (Penny and Racek, 1968), life histories may vary in distant populations." (Harrison 1974:49-50).

Of these three candidate species, *Racekiela ryderi* can likely be excluded due to its preference of slightly acidic waters. Based on the current range of modern species, these specimens are likely *Heteromeyenia baileyi* and/or *Radiospongilla crateriformis.*

Follow-up field work along the Onion Creek drainage to collect extant sponges and identify the species present in the drainage would be informative. Species identification of a living sponge is based on the total spicule assemblage (i.e., all three spicule types)—information which cannot be obtained from individual spicules recovered from soils. The relatively uncommon gemmoscleres are the only spicule type which can potentially be individually identified to species of origin from soil samples.

E.8 DATA - BIOGENIC SILICA (CHRYSOPHYCEAN CYSTS)

Chrysophycean cysts, sometimes called "stomatospores" or "statospores", is the final biogenic silica category recovered. These cysts are the resting phase of Chrysophycean algae made of biogenic silica which form during times of environmental stress (i.e., drying out). Thus, they would form if a stream or pools dried out, or possibly following a flood as overbank deposits dried. In a lake environment, Wetzel notes that the common Chrysophycean algae prefer "neutral to slightly alkaline [water; either..] nutrient-poor lakes or more productive lakes at seasons of nutrient reduction." (1983:Table 15.2) The recovered examples observed in the biogenic silica strews were all recovered in the surface samples (Figure E-32A-J). It is probable any statospores present in the 34 subsurface samples may have dissolved in the same manner as the missing short cell phytoliths. Although these cysts can be identified to species and provide specific environmental information, that assessment generally requires SEM imagery. Several particle atlases are available that illustrate and summarize the known cysts (Duff et al. 1995, Wilkinson et al. 2001).

E.9 DISCUSSION - BIOGENIC SILICA STABILITY IN SOILS

The biogenic silica that comprises most phytoliths and all siliceous sponge spicules, diatoms, and Chrysophycean cysts is amorphous (i.e., non-crystalline [versus crystalline forms of silica such as quartz sand]). The solubility of amorphous silica varies with temperature and with pH. A plot of amorphous silica solubility vs. solution pH from multiple literature sources, copied from Iler (1979:Figure 1.6) is reproduced in Figure E-33, and shows the basic effect of these variables in an aqueous system. Baumann's data clearly shows that temperature affects solubility (Figure E-33). However, as the temperature of non-surface soils is relatively constant, the primary environmental variable to be considered when evaluating the biogenic silica stability data at 41TV2161 is soil pH. The soil pH is reflected in the soil pore water which, if basic enough, dissolves biogenic silica. Silica dissolution occurs naturally at a low rate; dissolved silica is always present at low concentrations in soil pore water. It is this soluble silica—in the form of monosilicic acid—that enables plants to absorb dissolved silica with the soil pore water which subsequently forms phytoliths as a byproduct of transpiration. However, excessive silica dissolution into soil pore water—such as that caused by high soil pH—can have the negative effect of selectively altering or even eliminating the soil phytolith record.

Although all forms of silica are covered, Iler's chapter titled "The Occurrence, Dissolution, and Deposition of Silica" contains a number of comments and observations regarding biogenic silica which will be briefly noted here (Iler 1979:3-115). Although performed in aqueous solutions in the laboratory, these observations are directly relevant to the biogenic silica sample recovered from the Big Hole Site. As the Iler volume is very difficult to obtain, a number of quotes follow to make this information available to the archeological research community [key concepts are highlighted in bold; emphasis mine]. Regarding surface area,

"Essentially all biogenic silica is amorphous. It often has a substructure of extremely small particles less than 50 Å̄ in diameter which have surface of SiOH groups. These are joined together in close-packed three-dimensional structures, some of which are isolated microscopic masses; others are solids permeated by holes like Swiss cheese; and still others are like an interconnected mass of rods. The ultimate particles in this size range can coalesce into denser structures as the intervening pores become finer. Further deposition of silica can obliterate the particulate appearance and lead to an impervious solid. Thus **specific surface areas observed in biogenic silicas vary widely** from

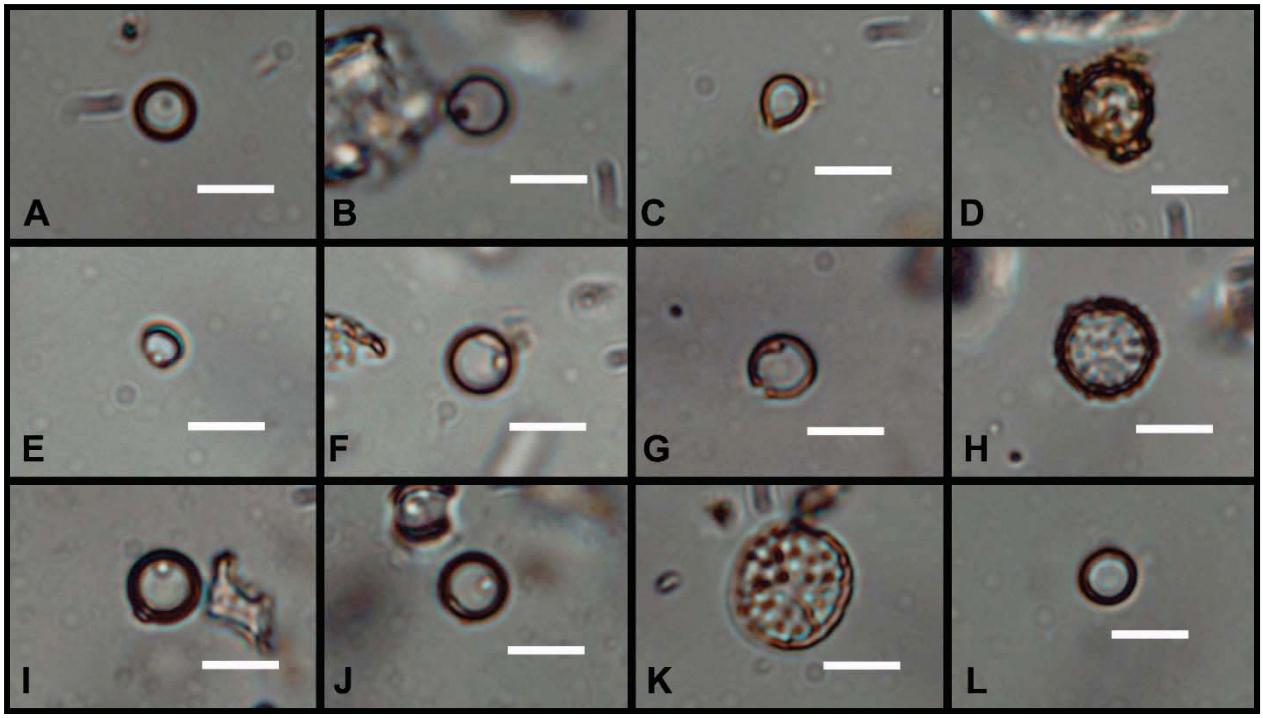

Figure E-32. Chrysophycean Cysts. A-D: PNUM 2450; and E-J: PNUM 2451. Additional images from PNUM 2451: K (unidentified particle), and L (air bubble for comparison). The bar scales are 10 microns.

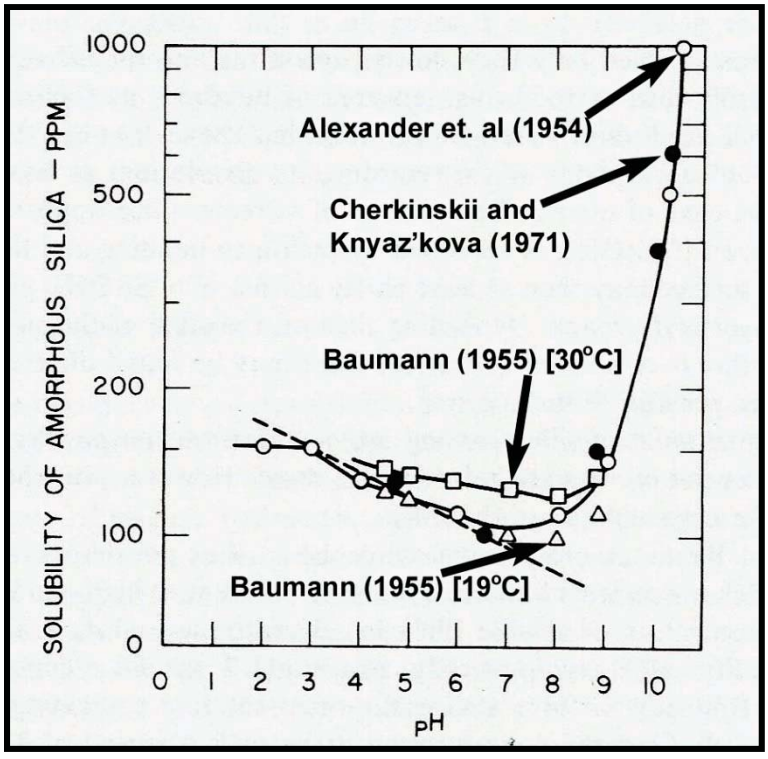

Figure E-33. Four plots of amorphous silica solubility vs. pH in aqueous systems (Iler 1979:42, Figure 1.6).

several hundred m^2 g^{-1} to very low values in those cases where the porosity has collapsed until the **pores** no longer admit the nitrogen used for the measurement.' (Iler 1979:29).

"[The] reported [particle] solubility values for amorphous silicas range from 70 to more than 150 ppm at 25ºC. **Such variations are apparently due to differences in particle size, state of internal hydration, and the presence of traces of impurities in the silica or absorbed onto its surface.**

"Based on data for smaller particles, an extrapolation of Alexander's [...1957] data indicates the solubility of massive amorphous silica to be 90 ppm for silica from pure sodium silicate, and 60-70 pm for silica from commercial water glass, which probably contains traces of impurities that reduce solubility." (ibid. 40).

"Equilibrium is established only very slowly, unless the amorphous silica is so finely divided or microporous as to furnish an area of hundreds or thousands of square meters of surface per liter of water.... Stöber... [1967] has shown that $Si(OH)_4$ is adsorbed on the surface of amorphous silica, **retardin**g its dissolution....

"According to Baumann... [1955] when amorphous silica powder.., is placed in water at 25ºC, the approach to equilibrium is different at high and low pH. Below pH 7, the concentration of soluble silica increases for several days and approaches the final solubility value asymptotically. **Above pH 7, the silica concentration rises rapidly in the first day to form a supersaturated solution** containing, for instance, 155 ppm at pH 9. Then the concentration drops over a period of 3-4 days to the solubility characteristic of the pH and type of silica, such as 125 ppm." (Iler 1979:41)

"Baumann [ibid.] proposes that the initial rate of dissolution at this pH is greater than the rate of deposition, thus leading to temporary supersaturation... "(ibid 41-42)

"...Spychalski...[1938] reported that solubility decreased with increasing hydration. He gave the following tentative 'solubilities' of hydrated silicas at various stages of dehydration...

However, there is no indication that solubility equilibrium had been reached. Nevertheless, there is a consistent relation in that the **solubility... was inversely proportional to the state of hydration**.

'solubility' as ppm in

Composition	Water at 18-22ºC
SiO_2•2.5H_2O	**18**
SiO_2•2.0H_2O	**44**
SiO_2•1.5H_2O	**58**
SiO_2•1.0H_2O	**61**
SiO_2•0.5H_2O	**120**

"... **from pH 9 to 10.7, there is an apparent increase in the solubility of amorphous silica**, owing to the formation of silicate ion in addition to the monomer which is in equilibrium with the solid phase.... **Above pH 10.7, all the solid phase of amorphous silica dissolves to form soluble silicate**, since at higher pH the concentration of $Si(OH)_4$ is greatly lowered by conversion to ionic species, so that no amorphous solid can remain in equilibrium." (Iler 1979:46-47)

"When very small individual silica particles are brought into the same solution as larger ones, especially at pH 9-10 where hydroxyl ions catalyze dissolution and deposition of silica, the smaller ones dissolve and the larger ones grow." (ibid. 50) [Although this specific comment was made regarding submicron size particles, on some scale it could conceivably apply to other size particles. This phenomenon of the "simultaneous occurrence of silica dissolution and overgrowth during diatom diagenesis" was reported for diatom silica dissolution during work on Deep Sea Drilling Project samples. (Mikkelsen 1974:223)]

Regarding the effect of impurities on solubility,

"Certain impurities such as **aluminum** in minute amounts not only **reduce the rate of dissolution** of silica, but by chemisorption on the surface of silica, even in amounts less than a monomolecular layer, **reduce the solubility of silica at equilibrium**... the amount of aluminum on the silica surface required to reduce the solubility of silica has been measured by Iler... [1973]. When only ...5% of the surface was occupied [with aluminum], the rate of dissolution as well as the equilibrium solubility of the surface were drastically reduced..... The dissolution of silica from glass in water (Bacon and Raggon 1959), from biogenic amorphous silica in seawater (Hurd 1973), and from kaolin, talc, and mica dusts in Ringer's solution of serum (Rahman et. al 1973) were all accelerated by removing metal ions from the surface...." (Iler 1979:56-57)

In a subsequent chapter Iler notes that:

> "Silica deposits in plants occur most commonly in the form of particles of characteristic shapes (phytoliths).... The silica is transported as $Si(OH)_4$, and then concentrated and gelled as water evaporates from the leaves [Peinemann et al 1970]. It is not surprising that the edges of leaves of sorghum wheat and corn are most highly silicified because silica is found most highly concentrated where water is lost most rapidly [Handreck and Jones 1968]. The structure of silica in several plants has been shown to consist of a dense gel with pores 1-10 nm diameter full of water; the silica is completely amorphous [Schwab and Wahl 1968]." (Iler 1979: 741)

Considering the previous Iler information, look at the bulliform images in Figures E-24A, O, and Q which all appear to exhibit preferential dissolution from the particle centers. The table reproduced from Iler suggests that the least hydrated portion of the phytolith would be where amorphous silica is the most soluble. Thus, unless other factors trump [pH, competing ions, etc.] this statement seems to indicate that for these bulliform cells, the centers may have been most silicified—that for some reason the centers had the lowest water content of the particle and preferentially dissolved more quickly when exposed to soil water. As an alternative explanation, the center of these bulliform cells could have possessed a much higher density of open pores in the amorphous silica matrix and thus a larger exposed surface area which enhanced solution contact and dissolution. It is also possible that these bulliform cells were only partially formed and the central regions were incomplete. Clearly, more research is needed in this area to elucidate the active mechanisms—and to learn their significance and interpretive potential. Perhaps prescient of this complicated area are several quotes cited by Iler: the "unusual nature of

the silica-water system" and that "some properties of water and silica are so similar that the transition between hydrated silicic acids and the aqueous matrix is a gradual one" (1979:4, 3).

The well-established phytolith particle density range is from 1.5-2.3 g/cm^3 (Piperno 2006:15) with a median of about 2.10 (Jones and Beavers 1963:376). This particle range is primarily attributable to the difference in water content as well as impurities (Iler 1979:40). However, full understanding of the water issue is compounded as multiple forms of water can be present. Phytoliths can be partially hydrated (ibid. 40), and water can also be retained in pores (ibid. 40, 741). Apparently, adsorbed water can be either physically bonded or hydrogen bonded to the surface. Also there are bound silanol groups that can be easily misidentified as water during measurement—these silanol groups can be removed via oven drying (ibid. 629-630).

What of the other illustrated bulliform phytoliths? The process causing bulliform cells to show dissolution along one edge (Figures E-24C, E, J, V, X, Y, and possibly U) could be explained if they were located on a ped surface with only one portion of the phytolith exposed to migrating alkaline water. The particles that are pitted and essentially show evidence of dissolution all over (Figures E-24D, K, N, S, T, W, and possible G, H, and L) could have been uniformly dry throughout (i.e., same degree of matrix hydration) and uniformly exposed to the soil pore water with the particle surface exposed to local concentration differences in adjacent soil constituents.

The dissolution ratio in the prior table seems counterintuitive. One would likely assume that the "wettest" particles would dissolve first whereas the less hydrated particles would dissolve more gradually—apparently that is not the case based on decades of amorphous silica chemical research. Many short cell phytolith morphologies are small, relatively thin, and have a high surface to volume ratio; also, being at the functional location in the plant where transpiration occurs they are presumably fairly dry. If that is the case, the smaller short cell phytoliths would be expected to dissolve first before more water-rich particles and before those with a lower surface to volume ratio regardless of water status. In the calcareous soil matrix at 41TV2161, this is a plausible explanation for the near absence of small short cell phytoliths [fine delicate diatom frustules were also absent]—that they were preferentially dissolved whereas the larger crenates and even more massive bulliform cells remained (although they also sometimes show evidence of partial dissolution).

The final point in this discussion is regarding metals which can protect the phytolith surface; aluminum in particular has been singled out in this regard (ibid. 56, 75, 193). In 2007 it was proposed that high charcoal concentrations in the soil could potentially contribute to selective absorption and removal of protective metals from phytoliths [which are in equilibrium via pore water]—such as aluminum—thereby enhancing the rate of phytolith dissolution in basic pH soils. Following several pages of discussion, the specific comment made was "if the charcoal were to absorb or facilitate absorption of iron and/or aluminum ions from the phytolith surface [via transfer from pore water] and/or the immediate adjacent soil environment, the charcoal could potentially alter the equilibrium concentration of these two metal ions thus negating their protective influence on the phytolith surface." (Sudbury 2007:18). Thus, soil charcoal accelerating phytolith dissolution is a seemingly plausible theory which could apply at 41TV2161.

Also, "'changes in moisture content related to alternating wetting-drying cycle in the soil may influence the silica concentration in solution more readily than other processes.' (Drees et al. 1989:953)" (Sudbury 2007:16). The presence of a relict Onion Creek paleochannel near 41TV2161 (Frederick et al. 2007:32) and the site location on the floodplain implies that frequent past wetting

events may have occurred. Movement of soil pore water would dilute the dissolved silicon; this in turn would shift the equilibrium to dissolve more silicon from amorphous silica particles.

It is hypothesized that the paucity of short cell phytoliths [and diatoms] may at least in part be due to the presence of abundant charcoal in the high carbonate content soil at 41TV2161—in a soil environment (i.e., basic pH, and possibly frequent soil pore water turnover) already conducive to poor phytolith preservation.

A reviewer discounted the 2007 "charcoal affecting dissolution" proposal without consulting the chemical literature as the concept was deemed too radical and not previously proposed by leading phytolith researchers. Thus, the pertinent literature consulted when originally presenting the charcoal/dissolution proposal (Sudbury 2007) is included in this current report making it available for further consideration, discussion, and evaluation by others.

Although the preliminary assessment was that phytolith preservation at 41TV2161 was adequate to merit additional study (Bozarth 2007), the reality is that variation in particle size and hydration—and likely also potentially protective surface ions in the alkaline environment and the presence of charcoal—may have impacted individual phytolith stability, dissolution rate, and survival. It seems possible that most of the smaller high surface to volume ratio particles (i.e., most short cells excluding the larger crenate form [which did survive in this calcareous soil matrix])—as well as the diatoms, preferentially dissolved in these samples leaving behind a pitted bulliform signature along with some crenates that implied a degree of phytolith survival noted during the preliminary 2007 phytolith survey. Although most of the spicules reported in this current study were of normal morphology (Figures E-26 and E-27), some specimens show more erosion which resulted in a larger diameter axial canal (Figure E-28). In spicule morphology case, this could indicate different soil environmental conditions between samples and/or that one sponge species had a different water content in their spicule which made it more readily soluble.

The Big Hole Site (41TV2161) is deficit in short cell phytoliths as was the Sewright Site (39FA1603) (Sudbury 2007:12-18). Another similar instance of phytolith loss was encountered at Dempsey Divide where particle dissolution issues were noted in the upper levels, and no phytoliths at all recovered below 25 cm. (Sudbury 2011b:112-115) Abundant charcoal flecks were present in the soils and the silt fractions from all three of these sites. The 41TV2161 evidence further supports the postulated charcoal enhanced phytolith dissolution correlation in alkaline soil environments.

E.10 DATA - DISCUSSION-SURFACE CONTROL SAMPLES

The two surface samples--one from the floodplain, and one from a hilltop--were dissimilar. The floodplain sample was more comprehensive, whereas the hilltop sample was lower in relative phytolith load. It is presumed that partial erosional deflation mixed the hilltop A-horizon with buried strata producing a hybrid sample rather than true control surface sample. Thus, the floodplain sample (PNUM 2451) was used as the sole surface control sample for the site.

When evaluating various sites, a means of comparing of phytolith assemblages based on their chloridoid cells was devised (Sudbury 2011b:172-179). The various chloridoid species all have the same general cell morphology—referred to as "saddle" form due to their geometry—but the specific cell metrics and assemblages vary by species. Dividing the chloridoid short cells into two groups based on their general morphology—those that were "tall" (taller than wide) and those that were "squat" (wider than tall)—provided interesting results (ibid.).

Figure E-34 was recently presented (Sudbury 2014a) and has been updated here to include the PNUM 2451 data from the Big Hole Site (data from Table E-3). The Lizard Site cluster is from a 100+ mile long meandering drainage, whereas the Caddo Canyon Site cluster is from a short steep gradient riparian setting less than 2 miles long. The Big Hole Site surface sample is intermediate between these site's two oval clusters indicating the expected riparian setting. Interesting, the "saddle" signature at the Big Hole Site is similar even though the Carnegie Canyon and Lizard settings are 500-700 km to the north and northeast. Equally interesting is that four of the data points from Bull Creek also fall in this riparian area--perhaps indicating a stream was active in the Bull Creek area in the first half of the Holocene.

Beyond the surface control sample data, most of the other sample isolates from the Big Hole site showed degradation of the phytolith signature. The bulliform cells ranged from slightly to severely weathered (Figure E-24), elongates were also weathered, and short cells were in poor condition and low abundance—when present at all. Only the cucurbit cells appeared to be relatively resistant to chemical degradation and weathering (Figure E-25).

Other unidentified phytoliths were also encountered during this study. The larger platy forms in Figure E-35 are all from the surface control sample PNUM 2451; several other specimens are in Figure E-36:Z-BB. A few similar specimens to Figure E-35B-I were also noted in PNUM 2450 (not illustrated). The specimen in Figure E-35A is very odd as well as distinctive; it is shown at two focal depths and consists of thick biogenic silica pieces which are roughly hexagonal. These may be the polyhedral cells described by Piperno, but the 4TV2161 specimens are much more uniform than those Piperno illustrated (Piperno 2006:42, 199 Fig. 2.18a). Specimens 35B-D are examples of the so-called jigsaw-puzzle pieces which are plant epidermal cells (ibid. Fig. 2.18b). The botanical origin or cell type of the Big Hole Site specimens in 35F-I is uncertain.

The phytoliths in Figure E-36A-H and J-K are generally thought to be tree phytoliths, species uncertain. The specimen in 36C is discolored from being lightly burned, and the specimens in 36E-G show evidence of light weathering or dissolution. Of particular interest is the specimen in Figure 3E-6I; particles of this general appearance were fairly common in these samples. It is suspected that this was a tree phytolith that was heated high enough to have at least partially melted in a fire at the site; this specimen appears to have been more susceptible to chemical weathering/dissolution. This fragment shows more chemical weathering than the companion specimens that were not melted. The heating which caused partial melting may have lowered the water content making the particle more susceptible to chemical weathering.

Although larger than normally encountered, the specimen in 36N could be calcium oxalate crystals (from cacti). Specimens 36P and T are also crystalline as opposed to amorphous; their identity is not known, but they could be soil minerals rather than of botanical origin. The other biogenic specimens in Figure E-36 are unidentified.

Additional miscellaneous particles are also shown in Figure E-37. Figure E-37J shows some crystallinity and may be fossiliferous. The specimen in Figure E-36Q is likely tracheid element from a tree (part of the vascular system), and 37T could be the same. The other specimens are various unidentified particles.

On a technical laboratory aside, the spicules in Figures E-26 through E-28 that were recovered from the silt fraction are much larger than 50 micron silt particles as are some of the large platy and unidentified biogenic specimens (Figures E-35 through E-38). This is due to protocol changes in laboratory sample processing procedures developed at the JSE laboratory to keep more of the

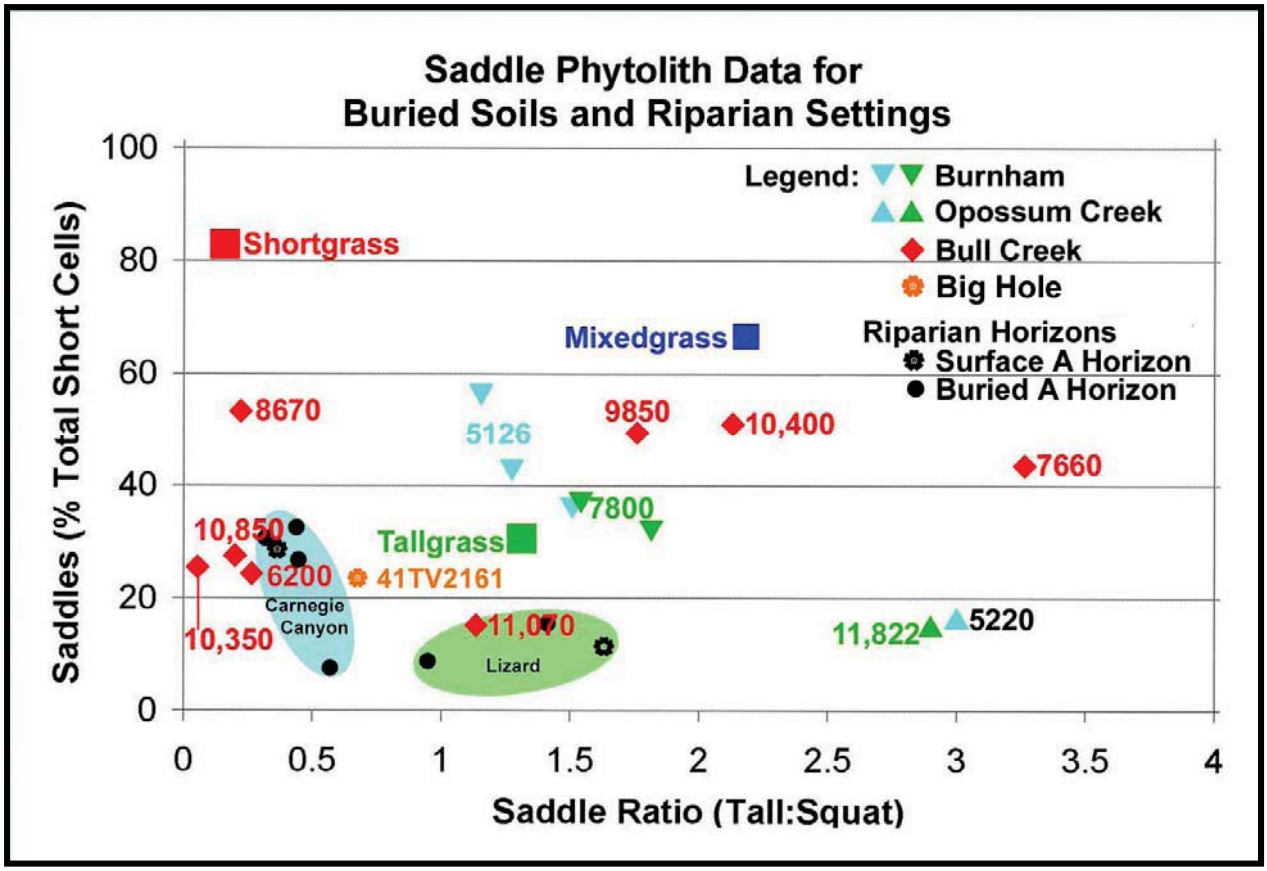

Figure E-34. Chloridoid ("saddle") phytolith plot of dimensional ratio vs. concentration with the 41TV2161 surface control data soil point added (PNUM 2451). The three squares denote upland prairie control surface samples located in Oklahoma. The red diamonds are dates for buried soils at the Bull Creek site (34BV176) (Bement et al. 2007), the downward pointing diamonds are from buried soils at the Burnham site (34WO69), and the upward pointing triangles are from the Opossum Creek site (34NW132) (Sudbury 2011c). The two large color ovals highlight two riparian settings in Oklahoma with more recent buried soils (black circles) and surface A horizons (black flower) data plotted [Carnegie Canyon site (34CD76), Lizard site (34WN107)]. The surface data point for 41TV2161 is in burnt orange.

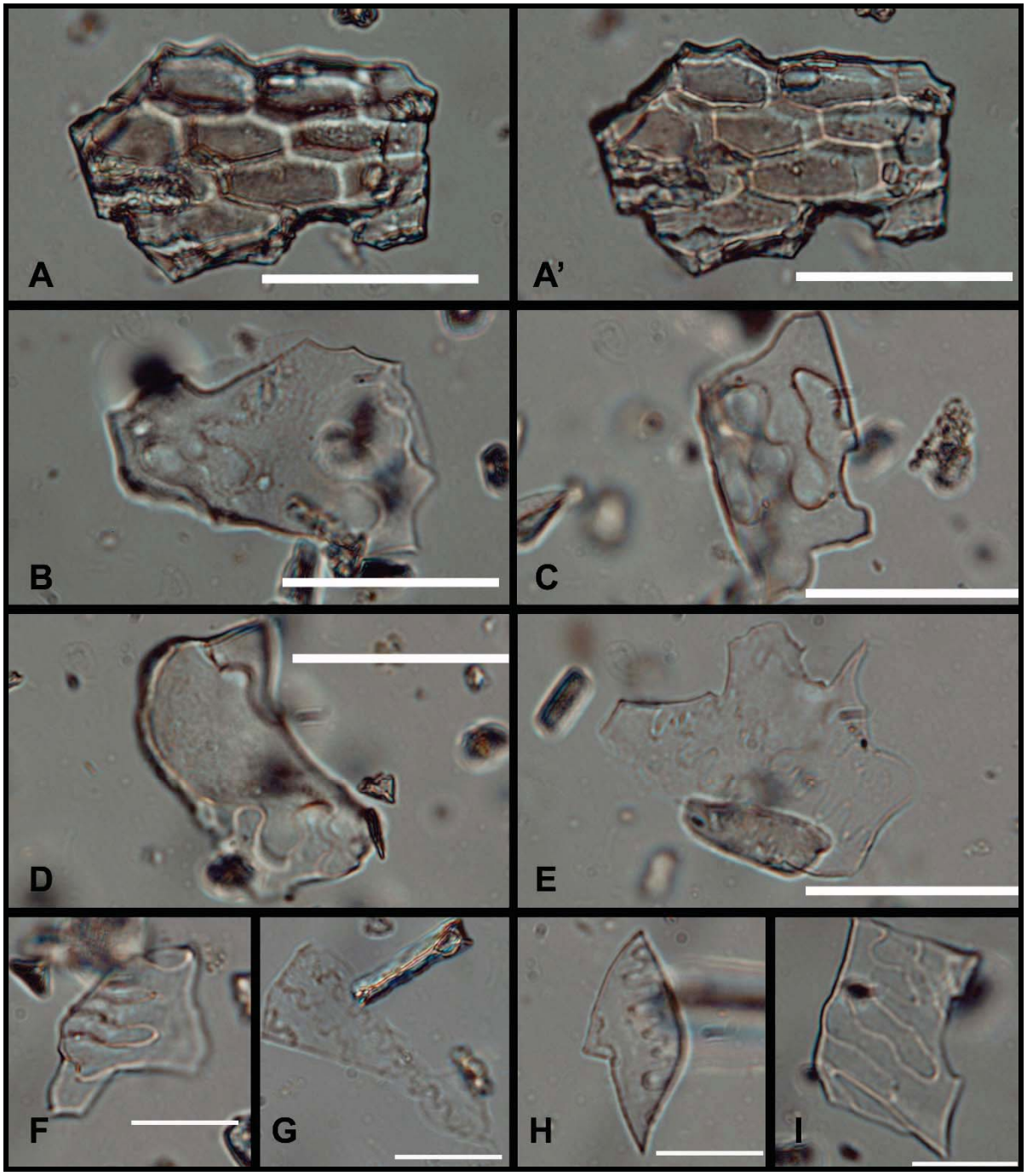

Figure E-35. Unidentified large platy phytoliths (PNUM 2451). Scale bars 50 microns (A-E) and 25 microns (F-I).

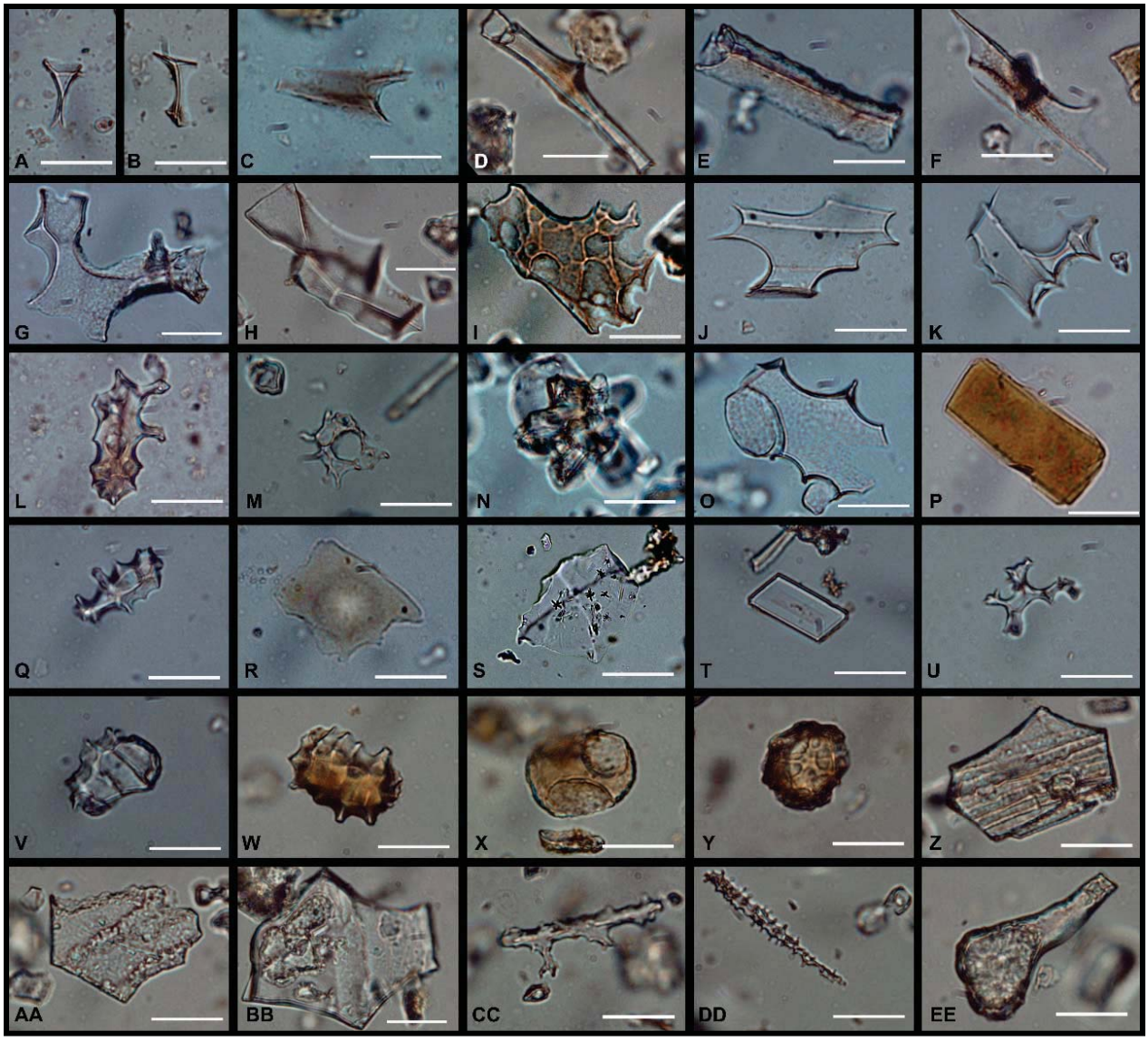

Figure E-36. Miscellaneous phytoliths and particles (1). A-B: PNUM 2407; C: PNUM 2406; D-F: PNUM 2176; G, O: PNUM 2060; H-I, P: PNUM 2179; J, Q: PNUM 2239; K: PNUM 2044; L: PNUM 2092; M-N: PNUM 2146; R-S: PNUM 2280; T-V: PNUM 2275; W-X: PNUM 2450; Y-EE: PNUM 2451. Bar scales are 25 microns.

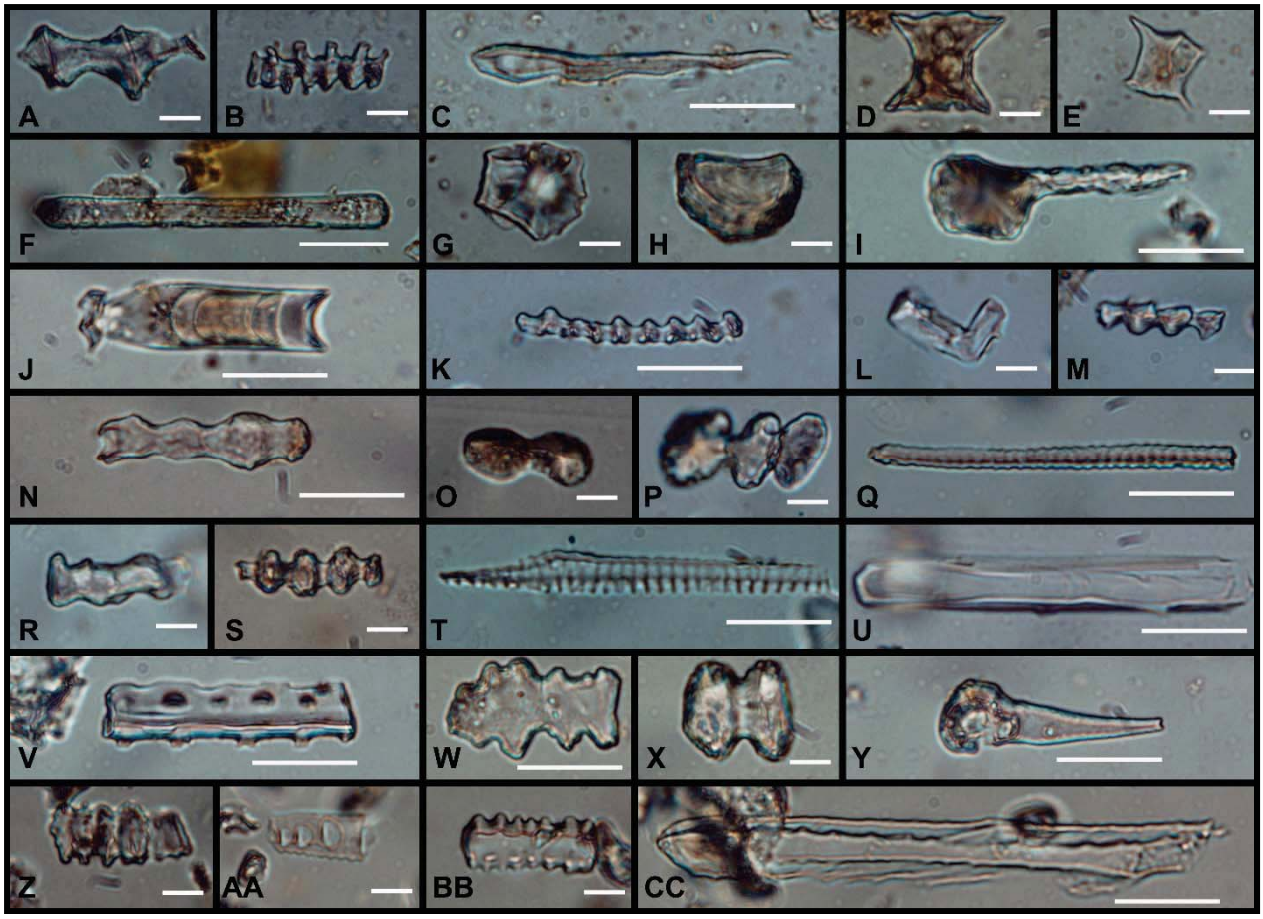

Figure E-37. Miscellaneous phytoliths and particles (2). A-B: PNUM 2110; C: PNUM 2424; D: PNUM 2092; E: PNUM 2246; F-G: PNUM 2367; H-I: PNUM 2146; J: PNUM 2176; K-M: PNUM 2060; N-P: PNUM 2179; Q-S: PNUM 2280; T: PNUM 2044; U: PNUM 2275; V-Z: PNUM 2450; AA-CC: PNUM 2451. Bar scales are 10 and 25 microns.

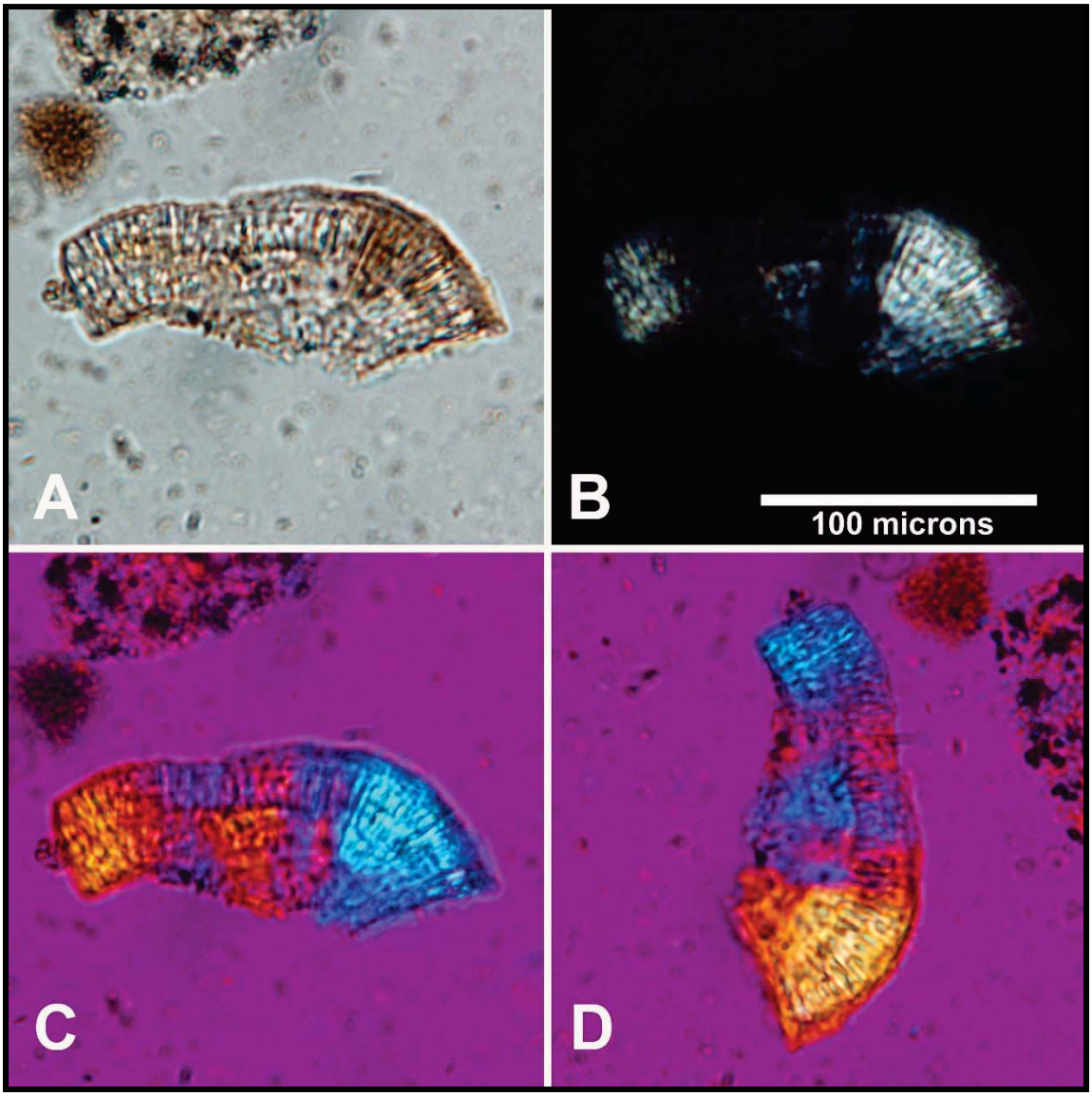

Figure E-38. Calcium carbonate nodule fragment (PNUM 2407). Four images of the same specimen. A: Specimen illuminated with plane polarized light at 500x; B: same as A with crossed polars; C. crossed polars with a full wave plate in place; and D. same as C with stage rotated 90 degrees to evaluate the change in birefringence.

biogenic material together in the silt fraction rather than spreading it across the sand and silt fractions. These changes cut total analysis time, customer cost, and also ensure more complete data recovery. This technique has been developed over the past five years and has effectively preserved and yielded what was previously unrecovered data of significant value. Two other sponge spicule samples have been previously reported using this protocol (Sudbury 2011c, 2014b). Recovery of snail shells is another major benefit of this new protocol.

Thin slivers and fragments of presumed calcium carbonate nodules, what the USDA soil OSD described as "common strongly cemented calcium carbonate concretions about 2 to 5 mm in diameter; calcareous" for Lewisville soil, were observed in several phytolith isolates. Although of higher particle density than the heavy liquid flotation solvent, the thin planar morphology of some carbonate concretion fragments allowed some particles to be recovered in the biogenic fraction. Even after the silt fraction underwent multiple acid neutralization treatments and there was thought to be cessation of effervescence—a few fragments of these nodules remained in the silt fractions. The example in Figure E-38, photographed by polarized light microscopy (PLM), is from PNUM 2407 and consists of a section of the outer crust or rind (top and upper right edge in 38A-C). The crystals radiating toward the center of the former intact nodule are readily visible.

E.11 CONCLUSIONS

Phytolith preservation at the site ranged from moderate to poor depending on cell type. The calcareous soil matrix set the stage for the biogenic preservation issues.

There are numerous indicators in this 41TV2161 data set that the soil environment in this apparent riparian setting was alkaline at the time of deposition and has remained so since that time:

- Very abundant carbonate fragments including some which formed around roots (sand fraction data).
- Abundant calcareous spicules which would not have survived in an acidic aqueous or soil environment (sand fraction data).
- Abundant snail shells which survived in the soils (sand fraction data).
- Calcareous Charophytes which need neutral to slightly alkaline water, and grow in still or slow moving water (sand fraction data).
- Chrysophycean algae which prefer neutral to slightly alkaline water [early specimens—if present—were not preserved].
- The vigorous effervescence encountered when acidifying the isolated silt fractions.

The geology of the site area is rich in limestone bedrock and calcareous alluvial deposits. Modern-day Onion Creek has a basic pH. Recent water quality data from station 12436 on Onion Creek is summarized in Table E-6[2].

The alkaline environmental conditions appear to have adversely affected phytolith survival in soil which resulted in recovering a partial (skewed) phytolith assemblage signature.

Some bulliform cells were in good condition but many exhibited extensive partial localized or general weathering and dissolution. The smaller short cell phytoliths in particular seemed present at unexpectedly low concentrations in all of the

[2] https://www.tceq.texas.gov/assets/public/waterquality/tmdl/31base/31-1427onioncreekfinalreport-pchem.pdf (accessed 3-11-15).

Table E-6. Onion Creek Water Quality Parameters (n=14).

Parameter	Mean	SD	Maximum	Minimum
pH	7.85	0.21	8.20	7.45
Conductivity	492.36	74.18	595	327
Dissolved Oxygen	9.69	1.8	13.29	6.94
Alkalinity	182.72	35.63	227.44	124
TSS	2.0	1.73	4	< 1

profile and feature samples. The likely cause of the dearth of small short cell phytoliths was selective dissolution of particles with specific physical properties (density and/or volume to surface area ratio), possibly exacerbated by the postulated effect of charcoal in the soil affecting phytolith surface and cation concentrations in the soil environment. The silica, soil, and chemical high points explaining this interpretation of phytolith preservation are presented in the preceding discussion. Experimentation can and should be performed to confirm or refute this suggestion, but that study is beyond the scope of the current project.

The flood plain surface sample provided a good phytolith particle count distribution. Comparison of the surface sample's chloridoid morphology ratio to total concentration places it squarely in the riparian portion of the chart. Interestingly, the base chart is derived from Oklahoma sites; thus the 41TV2161 result implies that the water provided by a stream trumps most other local climatic/botanical issues across a much broader geographical area.

The occurrence of burned phytoliths was noted--in short cells, cucurbit, and tree origin phytoliths. Although short cell phytoliths were under-represented in these samples, the high % of burned panicoid phytoliths in Features 26 and 29 (PNUM 2110 and 2424) suggests use of either Panicoid biomass for fuel, or harvesting and processing Panicoid for other purposes. Mature Panicoids harvested for food or other processing would likely occur in the fall, whereas dry Panicoid biomass used for fuel could have been anytime from fall to spring.

The spicule count in Feature 16 (PNUM 2110) was more than three times higher than any other sample—most likely implying extensive water usage. One interpretation of this feature would use for cooking via boiling water.

Cucurbit phytoliths were present in multiple samples, and seem resistant to the soil chemical weathering processes. The presence of these wild gourd phytoliths in roughly one-third of the feature samples and none of the stratigraphic samples suggests that the plants likely were actively gathered and used by site occupants. The gourds would have ripened in late summer and fall, but may have been curated.

A variety of unidentified phytoliths are illustrated so future researchers will be able to contribute additional information to this data base. Statospores—suggestive of occasional drying episodes—were present in the surface samples, but likely dissolved from the strata related to site occupations if they were originally present.

The soil textural information—especially for the Block C profile samples—showed considerable variability in sand content suggestive of stream flow variations with peak flow occurring in the 300-320 cmbs interval (PNUMs 2405, 2406, and 2407). This is the same zone where Charophytes were more numerous. The other profile samples all had a fairly constant soil textural value suggesting relatively stable environmental conditions.

The sand fractions of the samples contained numerous well-preserved snails--at least in part due

to the alkaline soil conditions. Not only were they abundant, but there was also a wide variety of species. Follow-up study to identify the species and their preferred environmental niche would potentially provide insights into the site's paleoenvironment. Some of the snail fragments have been burned—a possible indicator of anthropogenic activity.

Charcoal fragments were also noted in the sand fractions. Distinctive patterned charcoal fragments were noted in PNUM 2060, but remain unidentified. Bone and burned bone was also noted, as well as a few micro flakes. Oogonia of Charophytes were noted in some sand fractions suggesting neutral to alkaline still or slow-moving water. A number of microfossils were present which originated from the area's geological outcrops, including abundant carbonate spicules and foraminifera.

Although no species-identifiable siliceous freshwater sponge spicules were recovered, there was an abundant spicule sample at the site which was generally better preserved than the other forms of biogenic silica (except for the cucurbits). The spicule concentration peak in the soil column at PNUM 2406 indicates wetter conditions which may correlate with an attractive environment for site occupation. The spicules and the snail data could potentially help correlate the soil profile with the extremely variable strata encountered across the site. Spicule concentrations may also potentially be helpful in determining feature function and/or length of use.

E.12 Acknowledgements

Deep appreciation is expressed to Barbara Winsborough, Henry Reiswig, Chad Yost, Leslie Bush, Richard Drass, Phil Winsborough, and Mike Quigg for their assistance in various technical aspects of this project.

E.13 REFERENCES

Alexander, G. B.
1957 The Effect of Particle Size on the Solubility of Amorphous Silica in Water. *Journal of Physical Chemistry* 61(11):1563-1564.

Alexander, G. B., W. M. Heston, and R. K. Iler.
1954. The Solubility of Amorphous Silica in Water. J. Phys. Chem. 58(6):453-455.

Anderson, C., F. Moreno, and J. Meech.
2005. A field demonstration of gold phytoextraction technology. *Mineral Engineering* 18(4):385-392.

Bacon, F. R., and F. C. Raggon.
1959 Promotion of Attack on Glass and Silica by Citrate and Other Anions in Neutral Solution. *Journal of the American Ceramic Society* 42(5):199-205.

Baumann, H.
1955. Solubility of silica in water. *Beitr. Silikose-Forsch*. 37:45-71.

Bement, L. C., B. J. Carter, R. A. Varney, L. S. Cummings, and J. B. Sudbury.
2007 Paleoenvironmental reconstruction and bio-stratigraphy, Oklahoma Panhandle, USA. *Quaternary International* 169-170:39–50.

Bozarth, S. R.
2007 Appendix E. Phytolith Analysis from Soil Samples. In *Data Recovery at 41TV2161 Travis County, Texas: Interim Report*, by Quigg, J. M., P. M. Matchen, C. D. Frederick, and E. Schroeder, pp 165-167. Texas Department of Transportation Environmental Affairs Division, Archeological Studies Program, Interim Report No. 51831. Austin, Texas.

Carsey, D. O.
1926 Foraminifera of the Cretaceous of central Texas. *UT Bulletin* 2612.

Cheatum, E. P., and J. P. Harris, Jr.
1953 Ecological observations upon the fresh-water sponges in Dallas County, Texas. *Field Lab*. 23:97-103.

Cherkinskii, Y. S., and I .S. Knyaz'kova.
1971 *Dokl. Akad. Nauk. USSR* 198:358.

Drees, R., L. P. Wilding., N. E. Smeck, and A. L. Senkayi.
1989 "Chapter 19. Silica in Soils: Quartz and Disordered Silica Polymorphs. In *Minerals in Soil Environments Second Edition*, Dixon, J. B. and S. B Weed (Eds.), pages 913-974. Soil Science Society of America. Madison, Wisconsin.

Duff, K. E., B. A. Zeeb, and J. P. Smol.
1995 *Atlas of Chrysophycean Cysts*. Kluwer Academic Publishers, Dordrecht. 189 p.

Eshleman, S. K.
1950 A key to Florida's fresh-water sponges, with descriptive notes. *Quart. J. Florida Acad. Sci*. 12:35-44.

Frederick, C., E. Schroeder, and J. M. Quigg.
2007 Geoarcheological Evaluations. In *Data Recovery at 41TV2161 Travis County, Texas: Interim Report*, by Quigg, J. M., P.M. Matchen, C. D. Frederick, and E. Schroeder, pages 24-32. Texas Department of Transportation Environmental Affairs Division, Archeological Studies Program, Interim Report No. 51831. Austin, Texas.

Handreck, K. A., and L. H. P. Jones.
1968 Studies of silica in the oat plant. *Plant and Soil* 29(3):449-459.

Harrison, F. W.
1974 Sponges (Porifera:Spongillidae). In *Pollution Ecology of Freshwater Invertebrates*, pp. 29-66. Hart, C.W., Jr. and S.L.H. Fuller (Eds.) Academic Press, New York.

Hoff, C. C.
1943 Some records of sponges, branchiobdellids, and molluscs from the Reelfoot Lake region. *J. Tennessee Acad. Sci.* 18:223-227.

Hurd, D. C.
1973 Interactions of biogenic opal, sediment and seawater in the Central Equatorial Pacific. *Geochimica Et. Cosmochimica Acta*. 37(10):2257-2282.

Iler, R. K.
1973. Effect of adsorbed alumina on the solubility of amorphous silica in water. *Journal of Colloid and Interface Science* 43(2):399-408.

1979. *The Chemistry of Silica*. John Wiley & Sons: New York. 866 p.

Jewell, M. E.
1939 An ecological study of the fresh-water sponges of Wisconsin, II. The influence of calcium. *Ecology* 20:11-28.

Jones, R. L., and A. H. Beavers.
1963 Some Mineralogical and Chemical Properties of Plant Opal). *Soil Science* 96:375-379.

Mikkelsen, N.
1977 Silica dissolution and overgrowth of fossil diatoms. *Micropaleontology* 23(2):223-226.

Moore, W. G.
1953 Louisiana fresh-water sponges, with ecological observations on certain sponges of the New Orleans area. *Trans. Amer. Microsc. Soc.* 32:24-32.

Neidhoefer, J. R.
1940 The fresh-water sponges of Wisconsin. *Trans. Wisconsin Acad. Sci. Arts Lett.* 32:177-197.

Neumann, D.
2003 "Silicon in Plants." In *Silicon Biomineralization Biology--Biochemistry--Molecular Biology--Biotechnology*, pp. 149-160. W. E. G. Müller (Ed.). Progress in Molecular and Subcellular Biology, Vol. 33. Springer-Verlag: Berlin.

Old, M. C.
1932a. Environmental selection of the fresh-water sponges (Spongillidae) of Michigan. *Trans. Amer. Microsc. Soc.* 51:129-136.

1932b. Taxonomy and distribution of the fresh-water sponges (Spongillidae) of Michigan. *Papers Michigan Acad. Sci. Arts Lett.* 15:439-476.

Pearsall, D. M.
2000. *Paleoethnobotany: A Handbook of Procedures.* 2nd Ed. Academic Press, San Diego. 700 p.

Peinemann, N., M. Tshapek, and R. Grassi.
1970 Properties of phytoliths. *Zeitschrift für Pflanzenemährung und Bodendurde* 127(2):126-133.

Penney, J. T., and Racek, A. A.
1968 Comprehensive revision of a worldwide collection of fresh-water sponges (Porifera: Spongillidae). *U. S. Nat. Mus. Bull*. 272:1-184.

Piperno, D. R.
1988 *Phytolith Analysis: An Archaeological and* Geo*logical Perspective.* Academic Press, San Diego. 280 p.
2006 *Phytoliths A Comprehensive Guide for Archaeologists and Paleoecologists.* AltaMira Press, New York. 237 p.

Poirrier, M. A.
1969 Louisiana fresh-water sponges: Taxonomy, ecology, and distribution. PhD. Thesis, Louisiana State Univ. [Univ. Microfilms Inc., Ann Arbor, Michigan, Number 70-9083]).

Potts, E.
1887 Contributions toward a synopsis of the American forms of fresh-water sponges with descriptions of those named by other authors and from all parts of the world. *Proc. Acad. Natur. Sci. Philadelphia* 39:158-179.

Quigg, J. M., P. M. Matchen, C. D. Frederick, and E. Schroeder
2007 *Data Recovery at 41TV2161 Travis County, Texas: Interim Report*. Texas Department of Transportation Environmental Affairs Division, Archeological Studies Program, Interim Report No. 51831. Austin, Texas.

Rahman, Q., M. U. Beg, P. N. Viswanatham, and S. H. Zaidi.
1973 *Environ. Physiol. Biochem. India* 3(6):286.

Reiswig, H. M., T. M. Frost, and A. Ricciardi.
2010 Porifera. In *Ecology and Classification of North American Freshwater Invertebrates*, pp. 91-123. Thorp, J.H., and A. P. Covich (Eds.) Academic Press, New York.

Schwab, G. M., and B. Wahl
1956 Beiträge zur Strukter der organismichen Kieselsäure. *Naturwissenschaften* 43:513.

Smith, F.
1921 Distribution of fresh-water sponges of North America.*State Ill. Dept. Registration Educ. Div. Nat. History Survey 1*4:9-22.

Stephens, J.
1912 Clare Island survey. Freshwater Porifera. *Proc. Roy. Irish Acad.* 31:1-15.

Stöber, W.
1967 Formation of silicic acid in aqueous suspensions of different silica modification. In Gould R. F. (Ed.), *Equilibrium concepts in natural water systems. Adv. Chem. Ser.* 67:161-172.

Spychalski, R.
1938 Zur Stabilität von Kieseloxydhydraten definierter Zusammensetzung. *Zeitschrift Fur Anorganische Und Aligemeine Chemie* 239(3):317-320.

Strömberg, C. A. E.
2009 Methodological concerns for analysis of phytolith assemblages: Does count size matter? *Perspectives on Phytolith Research: 6th International Meeting on Phytolith Research. Quaternary International* 193:124-140.

Sudbury, J. B.
IP "Phytolith and Biogenic Silica Assessment of Select Sediment Samples from 41BL278." (MS Submitted 8-6-14)

2014a "Phytolith Insights into the mid-Holocene Calf Creek Paleoenvironment." Presentation at the SAA Annual meeting, Austin (April 26).

2014b Appendix F: Environmental Biosilica Data from 41LM50 and 41LM51, Early Archaic through Late Prehistoric Periods. In *Eligibility Testing at Three Prehistoric Sites at Lynch Creek, Lampasas County, Texas,* by Quigg, J. M., P. M. Matchen, R. A. Ricklis, S. Gray, and C. D. Frederick, pp. 303-348. Texas Department of Transportation, Environmental Affairs Division, Archeological Studies Program, Report No. 161, Austin, Texas.

2013 Appendix B: 41RB112 Sediment Sample Phytolith Analysis. In *Long View (41RB112): Data Recovery of Two Plains Village Period Components in Roberts County, Texas Volume II*, by Quigg, J. M., P. M. Matchen, C. D. Frederick, and R. A. Ricklis, pp. 707-766. Texas Department of Transportation Environmental Affairs Division, Archeological Studies Program, Report No. 147. Austin, Texas.

2011b *Quantitative Phytolith Analysis—A Working Example from Modern Prairie Soils and Buried Holocene A Horizons.* Phytolith Press, Ponca City, Oklahoma. 288 p.

2011c *Biogenic Silica from an Opossum Creek Soil* Phytolith Press, Ponca City, Oklahoma. 107 p.

2011d "Sponge Spicules in the Opossum Creek Soil Profile, Nowata County, Northeastern Oklahoma". *Biogenic Silica from an Opossum Creek Soil Profile, Nowata County, Oklahoma USA*, pp. 75-101. Sudbury, J.B. Phytolith Press, Ponca City, Oklahoma. 107 pp.

2007 Sewright Site (39FA1603) Phytolith Analysis. J. S. Enterprises Project Report 2007-2. Manuscript in possession of the author.

Wetzel, R. G.
1983 *Limnology*. Saunders College Publishing; Philadelphia.

Wikipedia
2014 "Charophyta." http://en.wikipedia.org/wiki/Charophyta [accessed 5-30-14]

Wilkinson, A. N., B. A. Zeeb, and J. P. Smol.
2001 *Atlas of Chrysophycean Cysts II.* Kluwer Academic Publishers, Dordrecht. 169 p.

Wilson-Corral, V., C. Anderson, M. Rodriguez-Lopez, M. A. Vargas, and J. Lopez-Perez
2011 Phytoextraction of gold and copper from mine tailings with *Helianthus annuus* L. and *Kalanchoe serrata* L. *Minerals Engineering* 24(13):1488-1494.

Winsborough, B. M.
2015 Diatom Paleoenvironmental Analysis of Sediments from Archaeological Site 41TV2161, Travis County, Texas. (MS submitted May 2014).

Wurtz, C. B.
1950 Fresh-water sponges of Pennsylvania and adjacent states. *Not. Natur. Acad. Natur. Scie. Philadelphia* 228:1-10.

Big Hole (41TV2161): Two Stratigraphically Isolated Middle Holocene Components in Travis County, Texas

Volume I

By:

J. Michael Quigg, Benjamin G. Bury, Robert A. Ricklis, Paul M. Matchen, Shannon Gray, Charles D. Frederick, Tiffany Osburn, and Eric Schroeder

with contributions by

Beta Analytic, Steven Bozarth, Henry and Mary Chigey, Hector Coronado, J. Phil Dering, Jeffrey R. Ferguson, Timothy Figol, Michael D. Glascock, Trisha-Ann Gonzales, Bruce Hardy, Mary Malainey, Linda Perry, Mary Schabel, Steven Shackley, Byron Sudbury, and Barbara Winsborough

Prepared for:

Texas Department of Transportation
Environmental Affairs Division
Archeological Studies Program
Report No. 144 (CSJ: 0440-06-006)
Austin, Texas

Prepared by:

TRC Environmental Corporation
TRC Technical Report
Nos. 51831 (112368), 181822, 208177, 228154
Austin, Texas

J. Michael Quigg, Principal Investigator
Texas Antiquities Committee Permit No. 4064

2016

Printed by:

Document Engine
Round Rock, Texas

July 2016

Jointly published by:

Texas Department of Transportation
Environmental Affairs Division
Archeological Studies Program
Scott Pletka, Ph.D., Supervisor

and

TRC Environmental Corporation
TRC Technical Report Nos. 181822, 184348, 208177, and 228154
Austin, Texas

ISBN #978-1-935545-11-8

EXECUTIVE SUMMARY

During April and May 2006, an archeological team from the Cultural Resources Section of the Planning, Permitting and Licensing Practice of TRC Environmental Corporation's (TRC) Austin office conducted geoarcheological documentation and data recovery excavations at prehistoric site 41TV2161 (CSJ: 0440-06-006). Investigations were restricted to a 70 centimeter (cm) thick target zone between ca. 220 and 290 cm below surface (bs) on the western side of site 41TV2161 – the Big Hole site in eastern Travis County, Texas.

This cultural investigation was necessary under the requirements of Section 106 of the National Historic Preservation Act (NHPA), the implementing regulations of 36CRF Part 800 and the Antiquities Code of Texas (Texas Natural Resource Code, Title 9, Chapter 191 as amended) to recover a sample of the significant cultural materials prior to destruction by planned construction of State Highway 130 (SH 130). The latter by a private construction firm – Lone Star Infrastructure. This necessary data recovery was for Texas Department of Transportation (TxDOT), Environmental (ENV) Affairs Division under a Scientific Services Contract No. 577XXSA003 (Work Authorization No. 57701SA003). Over the years since the original award, multiple work authorizations between TxDOT and TRC were implemented and completed towards specific aspects of the analyses and reporting. The final analyses and report were conducted under contract 57-3XXSA004 (Work Authorization 57-311SA004). All work was under Texas Antiquities Committee Permit No. 4064 issued by the Texas Historical Commission (THC) to J. Michael Quigg.

Initially, an archeological crew from Hicks & Company encountered site 41TV2161 during an intensive cultural resource inventory conducted south of Pearce Lane along the planned construction zone of SH 130 in the fall of 2005. Following the initial site discovery, archeologists expanded their investigations to the west across the SH 130 right-of-way, and completed excavation of 10 backhoe trenches, 13 shovel tests, and 11 test units at site 41TV2161. The investigations encountered at least seven buried cultural features and 1,034 artifacts, some in relatively good context. The survey and testing report to TxDOT presented their findings and recommendations (Campbell et al. 2006). The ENV Affairs Division of TxDOT and the THC reviewed the initial findings and recommendations, and determined site 41TV2161 was eligible for listing on the National Register of Historic Places and as State Antiquities Landmark as the proposed roadway development was to directly impact this important site and further excavations were required.

Subsequently, TRC archeologists led by Paul Matchen (Project Archeologist) and J. Michael Quigg (Principal Investigator) initiated data recovery excavations through the mechanical-removal of between 220 and 250 cm of sediment from a 30-by-40 meter (m) block area (roughly 3,000 m^3). This was conducted to allow hand-excavations to start just above the deeply buried, roughly 70 cm thick targeted zone of cultural material. Mechanical stripping by Lone Star Infrastructure staff created a large hole with an irregular bottom that varied between 220 and 260 cmbs. To locate specific areas to initiate hand-excavations within the mechanically stripped area, a geophysical survey that employed ground penetrating radar (GPR) was conducted by Tiffany Osburn then with Geo-Marine in Plano, Texas. Over a dozen electronic anomalies were detected through the GPR investigation. Following processing, data filtering, and assessment, Osburn identified and ranked the anomalies for investigation. The highest ranked anomalies (1 through 8) were thought to have the greatest potential to represent cultural features. Anomalies 1 through 6 were selected and targeted through

hand-excavations of 1-by-1 m units that formed continuous excavation blocks of various sizes. Blocks were designated A, B, C, D, E, and F. The type, nature, quantity, and context of encountered cultural materials in each block led the direction and expansion of each excavation block as needed. In total, TRC archeologists hand-excavated 38.5 m^3 (150 m^2) from a vertically narrow target zone within this deep, multicomponent and stratified prehistoric site.

Hand-excavation in the two largest Blocks, B and D (51 m^2 and 62 m^2 respectively), revealed two vertically separate cultural components between roughly 220 and 290 cmbs. The younger component was restricted to Block B and yielded a Bell/Andice point and point base, plus a complete Big Sandy point. These points were associated with at least eight small burned rock features, one cluster of ground stone tools, limited quantities of lithic debitage, few formal chipped and ground stone tools, and a rare vertebrate faunal assemblage. Roughly 20 to 25 cm below the Bell/Andice component in Block B and across Block D was a component identified by a single corner-notched Martindale dart point. This point was associated with a scattered burned rocks, three charcoal stained hearth features, scattered animal, bird, and fish bones, mussel shells, and less than a dozen formal chipped and ground stone tools.

Both identified components contained cultural materials in good stratigraphic context with high spatial integrity. Significant, both were radiocarbon dated by multiple charcoal samples to a narrow 200-year period between 5250 and 5450 B.P. during the middle Holocene. With exception of the well-preserved faunal assemblages, perishable materials were poorly preserved in the moist silty clay loam. Charcoal lacked structure and was reduced to dark stains. Microfossils (e.g., phytoliths and starch gains) were present, although in very limited numbers and deteriorated conditions.

The four much smaller Blocks (A, C, E, and F) yielded various quantities of cultural material and features, but these blocks also lacked sufficient charcoal dates and diagnostic artifacts Those artifacts and samples were left unassigned and analyzed separately from the Bell/Andice and Martindale components. The two well-defined components in Blocks B and D are the focus of this technical report. The components provide very significant data towards understanding rare and poorly understood hunter-gatherer populations during late stages of the Altithermal climate period.

This final report builds upon the interim report submitted to TxDOT (Quigg et al. 2007) that briefly described the methods, excavations, preliminary findings, initial results from six feasibility studies, and proposed an initial research design for data analyses. Context and integrity of the cultural materials in the two identified components was excellent. This rare circumstance combined with detailed artifact analyses, solid documentation of their ages through multiple radiocarbon dates, and multidisciplinary approach to analyses, allowed significant insights and contributions concerning the two populations involved. Results provide a greater understanding of human behaviors during a rarely identified time in Texas Prehistory.

The cultural materials and various collected samples were temporarily curated at TRC's Austin laboratory. Following completion of analyses and acceptance of this final report, the artifacts, paper records, photographs, and electronic database were permanently curated at the Center for Archaeological Studies (CAS) at Texas State University in San Marcos.

TABLE OF CONTENTS

LIST OF APPENDICIES